Institut für Luft- und Raumfahrt
der Technischen Universität München

Ground-Operational Assessment of Novel Aircraft Cabin Configurations

Michael Schmidt

Vollständiger Abdruck der von der Fakultät für Maschinenwesen der Technischen Universität München zur Erlangung des akademischen Grades eines

Doktor-Ingenieurs

genehmigten Dissertation.

Vorsitzender:	Univ.-Prof. Dr. rer. nat. Dr. h.c. Ulrich Walter
Prüfer der Dissertation:	1. Univ.-Prof. Dr.-Ing. Mirko Hornung
	2. Univ.-Prof. Dr. phil. Klaus Bengler

Die Dissertation wurde am 21.09.2017 bei der Technischen Universität München eingereicht und durch die Fakultät für Maschinenwesen am 22.02.2018 angenommen.

Für

Lieken und Horst

Acknowledgments

This work was mostly created during my time as a Munich Aerospace scholarship holder based at Bauhaus Luftfahrt. The excellent working environment contributed significantly to the success of this work. I would like to thank my supervisor, Prof. Dr.-Ing. Mirko Hornung, for the opportunity and support during this time. I would also like to thank Prof. Dr. phil. Klaus Bengler for kind acceptance of the second assessment of this work. Furthermore, I would like to thank Prof. Dr. rer. nat. Dr. h.c. Ulrich Walter for his friendly chairmanship.

I would like to thank the staff of Bauhaus Luftfahrt for the exceptionally working atmosphere and the numerous inspiring discussions from which the motivation for this work emerged. I would like to thank Philipp, Patrick, Uli, Sascha and Clément from the Visionary Aircraft Concept team in particular as well as Anne for their competent advice I have often sought and whose professional and friendly support have contributed greatly to the success of this work. My special thanks go to Kay, who devoted a lot of time to me as a mentor and central supporter of my scientific work over the years. I am grateful to all the students I have worked with in their research projects and in particular Marc for his support during the development of PAXelerate. Furthermore, I would like to thank my Munich Aerospace scholarship sparring partner Christoph for all the fruitful discussions.

Last but not least, I would like to thank my long-standing friends for their motivating support. However, my greatest thanks go to my parents, who, with their constant support and unconditional backing, have made a significant contribution to the successful completion of this work.

Michael Schmidt

Munich, March 2018

Abstract

This thesis focuses on the turnaround as the connecting element between airport and aircraft. A review of current research showed that only a few concepts for improved ground operational and passenger processes have been thoroughly analyzed. Since current models and frameworks are by the majority, not accessible and neither extendable, the development of a holistic assessment framework for advanced ground operational concepts was undertaken.

The framework presented comprises: cabin design heuristics, agent-based passenger flow simulation, turnaround modeling and operational cost assessment. Mission performance analyses are integrated with sensitivity analysis produced with state-of-the-art aircraft design tools. The core of this research is dedicated to the development of the agent-based passenger flow simulation which has been made available for the community[1].

The framework application covered the assessment of single- and twin-aisle configurations with passenger numbers ranging from 180 to 300. The analyzed sensitivities comprise passenger characteristics and the impact of changes to the cabin layout. Furthermore, several individual concepts were combined into two case studies aiming to capture cascading effects.

The overall goal of novel cabin concepts is to allow for a seamless passenger egress and ingress through the avoidance of queues caused by aisle and row interferences. Especially, the stowing and retrieving of hand luggage items increased the average boarding time by up to 68 %. Doors should be placed near the center of the fuselage to allow for a split of the passenger stream resulting in up to 48 % shorter boarding times. The comparison of single- and twin-aisle determined an advantage of 40 % of the twin-aisle over the single-aisle. The implementation of foldable seats provided a backward compatible solution to increase the boarding efficiency of up to 30 %. The afore identified boarding time reduction resulted in shorter turnarounds, since the passenger processes were on the critical path.

The integrated studies showed significant passenger process time savings, however those savings came with penalties in terms of higher fuel burn and maintenance cost, which almost outweigh the savings on direct operating cost level. A 1 % direct operating cost improvement was identified on the 500 nm distance, where the benefit decreases for longer missions close to the design range. The findings demand further concept improvements in terms of weight, maintenance effort and the integration into current aircraft configurations.

[1] The source code of the agent-based passenger flow simulation "PAXelerate" and any accompanying materials can be obtained from http://www.paxelerate.com [1].

Contents

List of Tables

List of Figures

Abbreviations

AAVP Advanced Air Vehicle Program.

ABS agent-based simulation.

ACARE Advisory Council for Aviation Research and Innovation in Europe.

AEA Association of European Airlines.

AHM Airport Handling Manual.

AOC additional operation cost.

APD Aircraft Preliminary Design.

API application programming interface.

APU auxiliary power unit.

ASEP asymmetric simple exclusion process.

ASK available seat kilometers.

ASP air service provider.

ATA Air Transport Association of America.

ATAG Air Transport Action Group.

ATLR aircraft top level requirements.

ATM air traffic management.

BWB blended wing body.

CA cellular automaton.

CO_2 carbon dioxide.

COC cash operating cost.

COO cost of ownership.

CPM critical path method.

CS Certification Specification.

CTLR cabin top level requirements.

DEL Delhi Airport.

DES discrete event simulation.

DMC direct maintenance cost.

DOC direct operating cost.

EC Expected Contribution.

EIS entry into service.

EMF Eclipse Modeling Framework.

EMOF Essential Meta-Object Facility.

ETS Emission Trading Scheme.

EWR Newark Liberty International Airport.

FAR Federal Aviation Regulations.

FRA Frankfurt Airport.

FSC full service carrier.

GDS global distribution system.

GPU ground power unit.

GSE ground support equipment.

HL hand luggage.

IATA International Air Transport Association.

IGOM IATA Ground Operations Manual.

IMC Indirect maintenance cost.

IOC indirect operating cost.

JFK John F. Kennedy International Airport.

LCC low cost carrier.

LF load factor.

LHR London Heathrow Airport.

LSP lifting seat pan.

LTH Luftfahrttechnische Handbuch.

MCT minimum connecting time.

MDO multi-disciplinary design optimization.

MEX Mexico City Airport.

MTOW maximum take-off weight.

NO_x nitrogen oxides.

OEM original equipment manufacturer.

OFAT one-factor-at-a-time.

OMG Object Management Group.

OR Operation Research.

OWE operating weight empty.

PCA pre-conditioned air.

PEK Beijing Airport.

PIC Productivity Index for Commercial Aircraft.

RG Research Goal.

RI Research Issue.

SA single-aisle.

SFS sideways foldable seat.

SLA service level agreement.

TA twin-aisle.

TLRs top level requirements.

TOC total operating cost.

TOFL take-off field length.

ULD unit load devices.

UML Unified Modeling Language.

USD US-Dollars.

WHO World Health Organization.

Nomenclature

List of Symbols

α	Value for the resistance of the fuel tank
A	Area (m^2)
C	Cost (USD)
CV	Coefficient of variation (%)
c	Individual assigned cost/specific unit cost
d	Diameter (m)
E	Set of edges
f	Final path cost
g	Movement cost
G	Directed graph
γ	Smallest path weight
h	Heuristic
h	Height (m)
k	Factor
l	Length (m)
m	Decision boundary
μ	Median
n	Number (of entities)
p	Pressure (Pa)/Path
r	Rate ($\frac{1}{s}$)
σ	Standard deviation

t	Time (s)
v	Vertex/Specific volume ($\frac{1}{PAX}$)
V	Volume (m^3)/set of vertices
w	Width (m)/weight of an edge/confidence interval width
W	Weight (kg)
t	Wall thickness (m)

List of Subscripts and Superscripts

ab	Seat abreast
act	Process activity
ap	Airport
aisle	Aisle
bag	Passenger bags
bulk	Bulk cargo
cabin	Cabin
cargo	Cargo
cat	Catering
clean	Cleaning/cleaner
cone	Aircraft tailcone
crew	Crew
crit	Critical
dep	Depreciation
door	Cabin door
equip	Equipment
ex	Execution
exit	Cabin exits
flight	Flight
fuel	Fuel/refueling

furn	Furnishing
fuse	Fuselage
gal	Galley
good	Good/material
in	In (flow)
ins	Insurance
int	Interest
labor	Labor
lav	Lavatory
mon	Cabin monument
mov	Movement
neck	Aircraft fuselage necking
noise	Noise
nose	Aircraft nose
out	Out (flow)
pax	Passenger
pb	Aircraft pushback
proc	Process
pos	Position
power	Power
pw	Door passway
real	Real
rect	Rectangular
req	Required
rem	Removal
repos	Repositioning
res	Resource
seat	Seat

sp	Seat pitch
splice	Partial element
sup	Supplies
sur	Surface
trol	Galley trolley
ta	Turnaround
vac	Vacuum
waste	Waste water
water	Potable water
zf	Zero fuel

1. Introduction

The aviation industry will be challenged by an annual 4.4-4.7 % growth in passenger traffic in the next 20 years [2, 3]. It is imperative that advancements in all aspects of current aircraft operations are developed to deal with increasing congestion at major hub airports. Current research majorly focuses on aircraft efficiency in terms of reduced carbon dioxide (CO_2), nitrogen oxides (NO_x) and noise emissions. This trend is due to ambitious goals promoted by national and international regulators, such as Advanced Air Vehicle Program (AAVP), Air Transport Action Group (ATAG) or Advisory Council for Aviation Research and Innovation in Europe (ACARE) [4–6]. However, the implementation of current research in fulfillment of the goals proposed by these regulators would require significant operational efficiency improvements, a topic which is often not addressed. The ACARE work group demands a reduction of turnaround times by 40 % in 2050 using novel handling concepts as well as actual arrival and departure times to be within one minute of scheduled times [7, 8].

Especially, regional and short-to-medium haul flights are of concern, since delays can hardly be compensated during the flights. Figure 1.1 illustrates that approximately 79 % of the world-wide flown flight distances in 2016 are under 1,000 nm (1,852 km) for short-to-medium haul aircraft [9]. This results in an increased number of performed legs and turnarounds per day. Hence, an efficient aircraft turnaround is an essential component of airline success serving those routes. The current ground operational procedures are highly optimized for available infrastructure and aircraft types. Further improvements are targeted by refining process execution, providing better predictability for each step improving

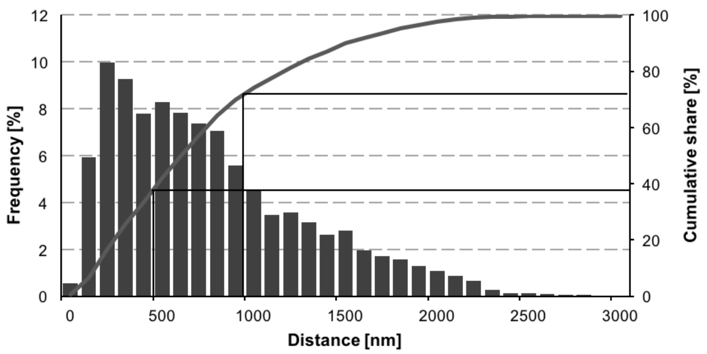

Figure 1.1.: World-wide utilization spectrum for short-to-medium haul aircraft in 2016 (A320 and B737 family) [9].

on-time performance and by reducing additional planned buffer times. In short-haul operations, passenger egress and ingress together with refueling, cleaning or catering are on the critical path which determines the total turnaround time [10]. Reducing passenger boarding and disembarking time would simultaneously shorten turnaround time and free up airport capacity. Turnaround time and punctuality are not on the same level of criticality for long-haul operations, since delays can be absorbed during the longer flight time and airport curfew hours may determine to envisaged scheduled and departure times.

1.1. Problem description and motivation

Airports are the origin and destination of all commercial passenger flights. They allow aircraft to take-off and land while providing necessary facilities to service the aircraft. Figure 1.2 provides an overview of a generic airport. Airport operations are divided into landside where passengers arrive, drop off their luggage and go through security and airside processes. The latter cover the take-off and landing of aircraft as well as taxiing procedures [11]. The focus here is on the turnaround, the connecting element between the airport and the aircraft. This special role of the turnaround results in various influences, like airport capacity constraints, aircraft type diversity, schedule disruptions as well as airline cost reduction pressure. In the following, each of the predominant factors of influence is categorized as Research Issue (RI) of this thesis and are further elaborated.

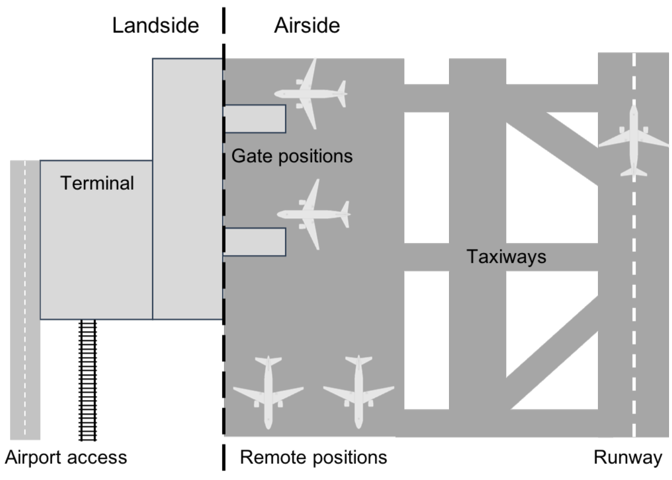

Figure 1.2.: Generic airport with landside and airside elements (based on [11]).

Research Issue 1: Increasing passenger numbers result in prolonged egress and ingress time

The use of larger aircraft is one solution to cope with an increase in air traffic, other than increasing the flight frequency. Since the 1960’s, the average number of installed seats per aircraft on short-haul segments has increased from 110 to 160 [12]. This is caused by the trend towards denser aircraft cabins, which was driven by low cost carrier (LCC) and by the choice of larger single-aisle aircraft types, such as the A321 or B737-900.

Recent aircraft type upgrades for the A320 and B737 family manage to accommodate an increased passenger number while keeping the overall dimensions constant [13, 14]. Denser aircraft cabins are an effective development direction, since 10 % more passengers in current short-to-medium haul aircraft reduce the fuel burn per passenger nautical mile by 6 % [15]. Unfortunately, passengers have to face a reduced level of comfort due to shrinking legroom, reduced catering and a reduced number of lavatories.

The passenger boarding process has been an issue over the past 40 years, where the average boarding velocity dropped from around 20 passengers per minute to nearly nine passengers per minute [16]. This decline is a result of increased carry-on luggage, airline service strategies and passenger demographics. Further contributing factors to prolong passenger egress and ingress times are continuously increasing passenger load factors from 67 % in 1995 up to 84 % in 2015 [17] together with a trend towards an excessive amount of cabin luggage. This results in longer gate occupation times and could lead to schedule disruptions due to the unpredictable passenger behavior.

Research Issue 2: Capacity constraints at major hub airports

A study for European airports revealed that especially large hub airports, such as London Heathrow Airport (LHR) and Frankfurt Airport (FRA) airport, handling 15 % of the total European passengers, are congested and already operate at their capacity limit [18]. These airports are constrained by existing infrastructure and are unable to expand due to local and political conditions, lack of available areas and high investments needed. The remaining 90 % of the airports in this study are mainly characterized by moderate to low capacity utilization. The same trend is recognizable around the globe where a multiplicity of hub airports operate close to their maximum capacity and exhibit increasing average delays. It is expected that the challenges for a capacity increase of the airport system in certain regions of the world will not change substantially in the near future [18, 19].

Research Issue 3: Schedule disruptions cause a significant impairment of airport operations

During peak hours, congested hub airports often operate at their maximum runway capacity, taxiway and gate utilization. Each schedule disruption due to a late arrival of aircraft or unreliable and inefficient ground operation processes could result in significant delays opening the potential for significant airport operation impairment. The average taxi-out times at airports are an indicator of the congestion level in terms of aircraft queue lengths. It exceeds the unimpeded taxi times at large international airports [20]. The taxi-out time averaged between 10 and 20 minutes in European airports in 2013, with most large hub airports ranging closer to the upper end of this average. For some of the busiest international airports, such as Beijing Airport (PEK), Delhi Airport (DEL) and Mexico City Airport (MEX), taxi-out times average more than 20 minutes and in the case of New York (John

F. Kennedy International Airport (JFK), Newark Liberty International Airport (EWR)) up to an average of 40 minutes [21].

High ground congestion levels can lead to schedule disruptions and network delays. Around 45 % of the European delays in 2013 were reactionary delays caused by late arrival of aircraft or crew from another flight. A considerable amount of 17 % was caused by ground operation disruptions including aircraft and ramp handling, passenger and baggage handling, aircraft damage, flight operation and crewing, as illustrated in Figure 1.3. Technical aircraft failure, weather, authorities and air traffic flow cause the remaining 38 % [21]. The punctuality performance is important to maintain the linkage and stability of aircraft rotations [22] and furthermore represent also costs to airlines, which is influenced by the choice behavior of passengers in terms of bad reputation and unsatisfied passenger [23, 24]. In general, delays can be partly compensated by means of improved ground process efficiency and scheduled buffer time between two flights. They can be completely absorbed when the aircraft goes off rotation or they can be absorbed during long-haul trips [25].

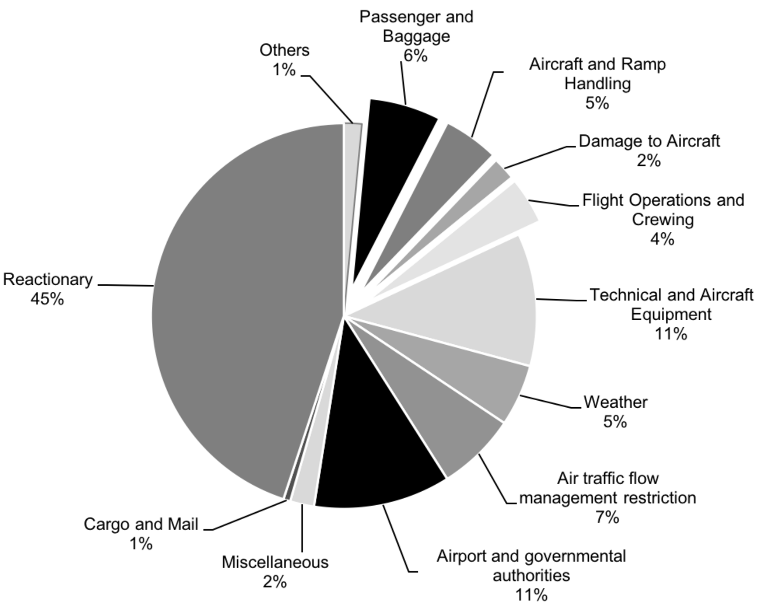

Figure 1.3.: Flight delay cause in 2013 at European airports [21].

Research Issue 4: Extended ground times reduce aircraft utilization

Aircraft utilization measures operational efficiencies as a function of aircraft specifications, aircraft availability, trip distances and ground time. An improved aircraft utilization allows for the spread of fixed cost of ownership (COO), which account for around 20 % of the DOC for current short-to-medium haul aircraft [26], across more trips and passengers resulting in lower cost per available seat mile. For regional and short-haul operation with shorter trips this increases the number of annual trips as well as executed aircraft turnaround events. A reduction from 40 to 30 minute turnaround could increase the number of annual trips by 8 % on a 500 nm (926 km) trip [27]. Current LCC try to maximize the airtime of their aircraft through faster ground processes, which notably worked for the airline Southwest, who achieved a minimum of a 15 minute turnaround time [28]. A faster turnaround improves not only the aircraft utilization but also all factors of production such as gates, ground equipment and labor. These essential operational efficiencies result in lower cost which stem from reduced process complexity.

Research Issue 5: Increasing cost pressure for aviation stakeholders

Even if the global airline industry continues to grow rapidly, the ability to deliver cost efficiencies and productivity improvements remain crucial for aviation stakeholders and airlines. Most of the players in the value chain turn a respectable profit, such as providers of global distribution system (GDS), aircraft manufacturer or leasing companies, whereas airlines struggle to break even [29].

The emergence and rapid growth of LCC since the 1960's has increased competition within the airline industry and poses significant competitive challenges to network airlines. A sharp rise in jet fuel prices between 2003 and 2008 increased the urgency for overall cost reductions. In 2004, a 36 % cost gap in terms of operating costs per available seat kilometers (ASK) existed for the three largest US network airlines versus LCC. In Europe, the gap between network airlines and LCC was even higher with 40-60 % and in Asia and Latin America, up to 60-70 %. Part of the cost gap reflects the premium service offered by network airlines and their network structure. Other main cost efficiency contributors are product, distribution and overhead, increased seat density, used infrastructure, aircraft, fuel and labor. In matters of ground operation, efficiency gains are envisaged through the identification of personnel shortage, lack of communication, inefficient use of infrastructure, a standardization of service level agreement (SLA) as well as increased crew involvement for cleaning and loading procedures [30]. These gains are available to network airlines and in many cases are already implemented by LCC [31].

A significant degree of regulation and the vulnerability to exogenous events, such as security concerns, volcanic eruptions and infectious diseases, underlines the idea of a worldwide aviation cycle. The resulting price pressure has led to a consistent decline in airline yields since the 1950's [32]. In this time, the inflation-adjusted yields have also fallen at an annual rate of 3 %. Based on productivity improvements in aircraft and operation, airlines were able to lower fares in an effort to remain competitive. The industry is highly cyclical but even in profitable times does not generate exceptional returns [29].

Research Issue 6: Missing quantitative capabilities to assess novel ground operation processes

Novel aircraft operational approaches are driven by the investigation of aircraft configurations in combination with integrated innovative sub-systems. Recent research projects and conceptual studies target time efficiency improvements, increased predictability as well as reduced disruptions with the main focus on passenger processes, airport infrastructure and ground handling procedures [33–36]. From an aircraft perspective, optimized cabin layouts featuring foldable seats [37, 38], hand luggage stowing [12] and door positions [12, 37, 38] could contribute to further reduce the process times. However, these disruptive conceptual ideas demand advanced quantitative assessment capabilities.

During the early stages of the conceptual aircraft design phase, ground operational requirements are traditionally not foregrounded. Aircraft performance characteristics and payload capabilities are considered as major design drivers and the compatibility with current airport infrastructure and processes is ensured [39]. Most studies of the air transportation system assume the related processes to be of constant length or do not even consider ground operations [19]. Hence, the development of assessment capabilities for ground operational performance is backwardly compared to other areas. Additionally, a lack of public accessibility and their inapplicability for advanced concepts [40] increases the demand for new solutions.

1.2. Research objectives

The interaction between aircraft en-route operations and airport infrastructure is exposed to manifold influences where for aviation stakeholder it remains crucial to deliver cost efficiencies and productivity improvements. A range of concepts targets to increase the current performance, however quantitative assessment capabilities enabling a coherent and holistic selection of the most promising novel and disruptive ground operation concepts are non-existing thus far.

Outlined below are the proposed goals of this thesis, comprised of three conceptual objectives and one methodical objective addressing the aforementioned identified research issues.

Research Goal 1: More time efficient passenger egress and ingress processes

One main contribution of this research is to develop compatible conceptual aircraft cabin layouts to reduce the time of the passenger egress and ingress processes. Efficiency gains in these procedures, based on its importance and vulnerability, would simultaneously shorten aircraft ground times contributing to address RI 4 (extended ground times reduce aircraft utilization) and lower the aircraft operator cost (RI 5 - increasing cost pressure for aviation stakeholders). The design scope is narrowed down to the short-to-medium haul segment addressing RI 1 (increasing passenger numbers result in prolonged egress and ingress time).

Research Goal 2: Development of robust and reliable turnaround processes with enhanced performance

The developed aircraft cabin layouts should be embedded within novel ground operational concepts which target an enhanced turnaround process from a holistic point of view. Specifically, this means, turnaround processes should be competitive in terms of required time and resources as well as compatible with current airport infrastructure and aircraft types. This could free up additional capacities at airports (addressing RI 2 - capacity constraints at major hub airports) and increase aircraft utilization (RI 4 - extended ground times reduce aircraft utilization). The attainment of defined process target times should be developed through a simplification, shortening, parallelization or abolishment of current procedures. In this context, the robustness and reliability towards external events, such as schedule disruptions (RI 3) and particularly passenger processes (RI 1), should be increased.

Research Goal 3: Identify cost competitive concepts

For all aviation stakeholder, such as airlines, airports and manufactures, it remains crucial to operate in a cost efficient way. This demands for an assessment of operational economics of the novel concepts to identify cost neutral or benefitting solutions as a response to RI 5 (increasing cost pressure for aviation stakeholders).

Research Goal 4: Develop assessment capabilities for novel and disruptive ground operation processes

The realization of the previous conceptual goals requires a demonstration based on a holistic evaluation and assessment. A detailed analysis of passenger flows in novel cabin concepts necessitates a precise understanding and modeling of the passenger processes. The obtained results should be included into the selection of best performing candidates in terms of ground operation taking into account aircraft service procedures, such as refueling, cargo loading and cabin service. The demonstrator should be flexible, adaptable and extendable for disruptive conceptual ideas. Furthermore, an integration of the results into the early stages of the conceptual aircraft design should be feasible as well as the availability within the research community to enable a reuse of the developed methods for future research. This goal addresses RI 6 (missing quantitative capabilities to assess novel ground operation processes).

1.3. Structure of the thesis

This thesis aims to develop a holistic assessment framework for advanced ground operational concepts. The research issues presented in this chapter provide the motivation for this work. Chapter 2 aims to support the assumptions and research goals presented in the introduction. After a general description of aircraft operation from an operator perspective (Section 2.1), an overview of current ground handling operations is given. Section 2.2 covers, besides the turnaround process, also the aircraft cabin layout as well as regulations and guidelines in place. A review of related research projects and conceptual studies is presented in Section 2.3 covering aircraft handling and aircraft design implications driven by cabin designs. The current state-of-the-art in aircraft turnaround modeling and passenger flow simulations is covered afterward (Section 2.4). Previous research efforts are structured in the conclusion of Chapter 2, aiming to define Expected Contributions in the context of research gaps in existing research.

Chapter 3 introduces the methodical approach undertaken to enable a holistic assessment of advanced ground operational concepts. The framework combines cabin design heuristics, passenger flow simulation, turnaround modeling, operational cost assessment and an interface with state-of-the-art aircraft design tools. For each module, the core method functionalities are highlighted as well as their interfacing. The validation of developed framework for state-of-the-art single- and twin-aisle aircraft is presented in Chapter 4.

The application to selected case studies is outlined in the following, starting with an overview of the sensitivities to be investigated for each framework module. The analyzed sensitivities comprised passenger characteristics and the impact of changes to the cabin layout. A combination of design driving parameters is combined to form two integrated studies which are further examined on aircraft, turnaround and operating cost level. Chapter 5 concludes with a recapitulation of the study results and a discussion about the concept integration into current operations and aircraft design programs. An overall discussion of the research contributions, critical assessment of the applied methods and potential future work is presented in Chapter 6.

2. Review of research on aircraft ground operation

Airports have been repeatedly challenged by new aircraft programs throughout the history of aviation, even if current aircraft processes on the ground seem archaic. Some of those aircraft were revolutionary for their time, such as the Boeing 747 (B747) in 1970 and recently in 2007 the Airbus A380. Before the B747 entered service, a thorough understanding of the terminal-related functions, ground handling characteristics and operational economics was necessary for the determination of aircraft servicing so it would not be limited by facilities [41]. The B747 revolutionized the cargo handling in terms of speed, through the introduction of further automation with unit load devices (ULD). Prior to the entry into service (EIS) of the A380, the stakeholders involved analyzed their current airport systems to identify shortcomings and requirements for improvement [42]. Consequently, airports had to expand their runways, taxiways and gate positions to accommodate this new aircraft type. Applying modified processes in conjunction with adapted GSE allowed new aircraft types to be successfully operated at existing airports and partly improve the operation of existing aircraft types. The next generation of aircraft featuring more-electric systems, hybrid-electric propulsion or non-drop-in fuels will again challenge the airports [43].

After an introduction to different aircraft operator business models, this chapter provides an overview of aircraft ground operations for contemporary single-aisle (SA) and twin-aisle (TA) single-deck aircraft. The aircraft characteristics related to ground operation are reviewed first and subsequently the procedures of an aircraft turnaround as well as of the passenger ingress are outlined. A summary of regulations and guidelines concerning aircraft design and ground operation in place is given in Section 2.2.4. In the second part of this chapter, a summary of studies which focus on the aircraft turnaround process is provided and pathways for process improvements are explored (see Section 2.3). Furthermore, a review of existing aircraft turnaround modeling approaches as well as simulations for passenger egress and ingress is conducted aiming to find solutions which allow a holistic performance assessment during the early stages of a conceptual aircraft design project. This chapter concludes with a recapitulation of the findings enabling a sharpening of the pursued research goals and the definition of expected contributions of this work.

2.1. Aircraft operator perspective

Airlines provide air transport services for passengers and freight using owned or leased aircraft. Aircraft operators have incorporated diverse business models which can be divided into the full service carrier (FSC), also referred to as network or legacy carrier, and the LCC known as no-frills, budget or low-fare airlines which emerged during the 1970's [44]. Furthermore, regional carriers operate in an effort to provide connections to communities with reduced demand while charter carriers lease their entire aircraft without a specific flight schedule. However, this distinct differentiation is blurring, since carriers in each classification are adopting the best features from others [45, 46].

The FSC are characterized by the traditional hub-and-spoke network serving from large cities and using a mixed fleet. The passenger is usually provided with a high level of service on ground and in-flight. There is no standard business model or definition for an LCC. The term itself incorporates a wide range of airlines with significant differences in the type of routes and the level of passenger service offered [31]. The LCC business model still remains competitive due to the economic principle of density which targets to maximize the flying time as a result of reduced ground time [47]. The airport infrastructure should allow quick turnarounds with simple terminal layouts, fast check-in facilities, good passenger facilities and accessibility [48]. This improves the operational efficiency of the airline by increasing its aircraft utilization [49]. LCC service their point-to-point network from secondary airports or former military bases in order to reduce infrastructure costs and airport charges. These uncongested airports enable reduced taxiing and holding leading to a higher punctuality rate [28, 50]. However, recently a shift towards larger airports and the offering of connecting flights was identified [46]. As the majority of them does not sell connecting flights on their websites, a shorter turnaround time means higher aircraft utilization. This is accompanied by reduced catering and almost non-existent belly-cargo loading [51]. Typically, the cabin layout is in one-class configuration with roughly 18 % more seats than FSC. The service level on-board is reduced and the selling of food and beverages in-flight generates additional revenues in addition to that generated by the sale of preselected seats. All this contributes to the streamlining of tasks and processes leading to significant cost advantages [28, 48, 52, 53].

2.2. Overview of current ground handling operations

Aircraft ground handling, or also referred to turnaround, is a fundamental part of commercial aircraft operations and describes all operations for preparing an aircraft for the next flight. The turnaround process starts when the aircraft reaches the parking position after landing and the chocks are set (on-block time). The parking position can be either located at the terminal referred to as gate position or on the apron, known as remote position (see Figure 1.2 on page 2). The process ends when the aircraft is ready to leave and the chocks are removed (off-block time). Commercial aircraft depend on vehicles and systems known as GSE to perform the required processes. The turnaround time depends on the business model of the aircraft operator which influences the aircraft type, the number of passengers, amount of loaded and unloaded cargo. In addition, the parking location of the aircraft, the level of cabin services and the passenger boarding sequence is affected by the aircraft operator. The aircraft turnaround consists of various processes which are provided by more than one service provider. The course of activities follows a strict chronological order, however some processes can be executed concurrently, while others only sequentially.

2.2.1. Aircraft characteristics related to ground operation

Aircraft are equipped with multiple interfaces, such as doors and hatches, to exchange goods, passengers or liquids during the ground service. The position of these interfaces may vary, if the aircraft features wing-mounted or aft-fuselage-mounted engines, or if it is a low-wing or high-wing aircraft. A cluster analysis of regional and SA aircraft in and out of production [54] revealed a trend shifting towards communality, such as for the potable and waste water connector at the aft fuselage (see Figure 2.1a and 2.1b). Also, the electrical power interfaces are in general located in the forward section of the fuselage, as illustrated in Figure 2.1c while the fuel connector is located on the outer side from the engine. Figure 2.1d depicts that in general passenger doors are located at each end of the passenger cabin enabling an uninterrupted passenger cabin and allowing a freely adjustable seating layout in terms of seat pitch and class configuration. Galleys and lavatories are situated in the entrance area enabling an easy trolley exchange through the opposite service door during the aircraft turnaround. Larger SA aircraft feature additional quarter doors (L2) in front of the wing due to their higher passenger capacity which allow for passenger egress and ingress. Due to the spatial separation of passenger boarding and cargo operations, cargo doors are, in general, located on the right side. High-wing configurations with turboprop engines allow boarding and disembarking as well as loading and unloading operations to be easily performed without the requirement of external airstairs due to the lower sill height [54].

The seating layout inside the fuselage is driven by the number of passengers transported, door positions and the operator's business model. The latter determines the number of cabin classes, the targeted aircraft operation in terms of average flight distance and the seat pitch. The existence of premium cabin classes requires a higher ratio of lavatories and galleys per passenger compared to SA layouts with only economy seats. This applies also for long-haul operations. Overhead bins for luggage storage are mounted on the ceiling on both sides along the aisles. For SA aircraft above 50 passengers, a common seat abreast varies between 4 - 6 and for TA aircraft it ranges from 7-10. The resulting fuselage width should be compatible to fit current ULD types into the cargo compartment.

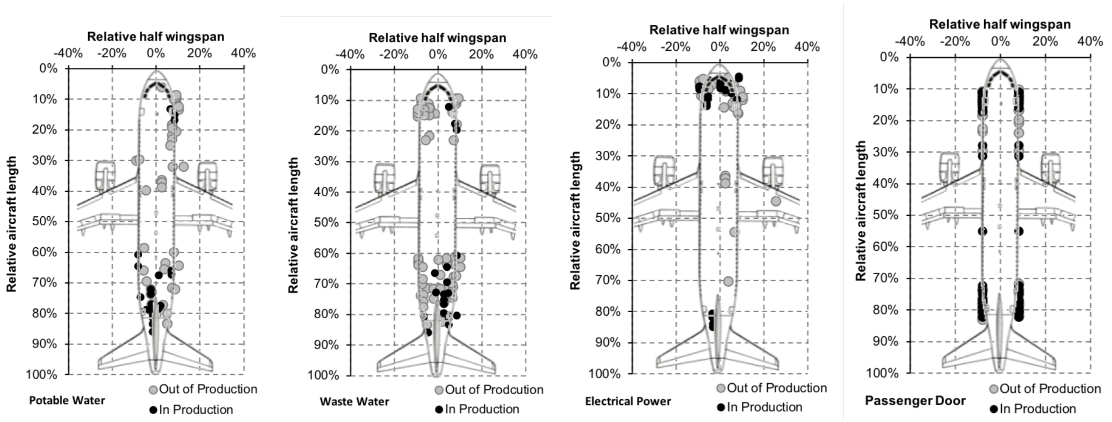

(a) Potable water (b) Waste water (c) Electrical power (d) Passenger door

Figure 2.1.: Aircraft interface locations for short-to-medium haul aircraft (adapted from [54]).

2.2.2. Aircraft turnaround processes

The ground power supply is connected after the chocks are placed before the wheels. This allows the engines and auxiliary power unit (APU) to be turned off. If the climate conditions require, the pre-conditioned air (PCA) unit is connected. A passenger jetbridge typically docks at the front left side door (L1) at the terminal parking positions (see Figure 2.2a). At remote apron positions, passenger stairs or aircraft-integrated stairs are used on the forward (L1) and aft left side door (L4). As soon as the doors are opened, passenger disembarking begins and simultaneously cargo and baggage are unloaded. Also at this time, the potable water is replenished. Hygienic standards prescribe this service to be completed before waste water servicing may commence (see Airport Handling Manual (AHM) 440 [55]). The equipment may be repositioned, since certain aircraft feature more than one waste tank. An aircraft is refueled after the last passenger has left the aircraft, according to requirements stated in EU-OPS 1.305 (FAR 121.570) [56, 57]. In the meantime, the flight crew can begin preparation for the next flight, check the airworthiness of the aircraft with a walk around, set up the flight computers and execute system checks. The cabin crew examines the general cabin condition and cabin emergency equipment [58]. Inside the aircraft cabin, the catering provider exchanges the trolleys and the cabin interior is cleaned and prepared for the next flight. These operations are usually performed in the absence of passengers because of noise and comfort issues. Once the cargo and baggage unloading is complete, the loading for the next flight can commence. After the fuel has been completely replenished, the passenger ingress is initiated and a final head count is performed before leaving the parking position. Electrical power switches from the ground power supply to the APU. The chocks are removed and if the aircraft is parked at nose-in position, a pushback is required [59].

Figure 2.2a depicts a typical top view of the ramp layout at the gate position for a short-to-medium haul aircraft. The left side doors are used for the passenger egress and ingress and

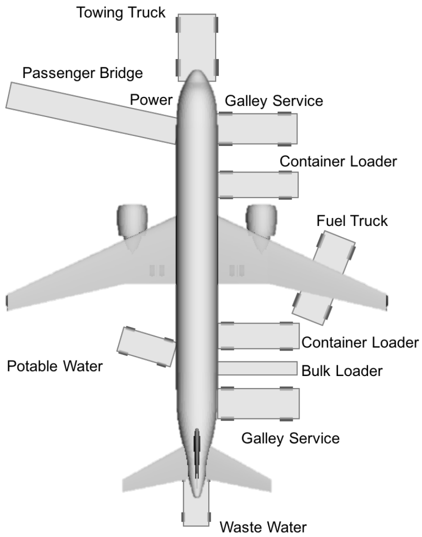

(a) Ramp layout at gate position

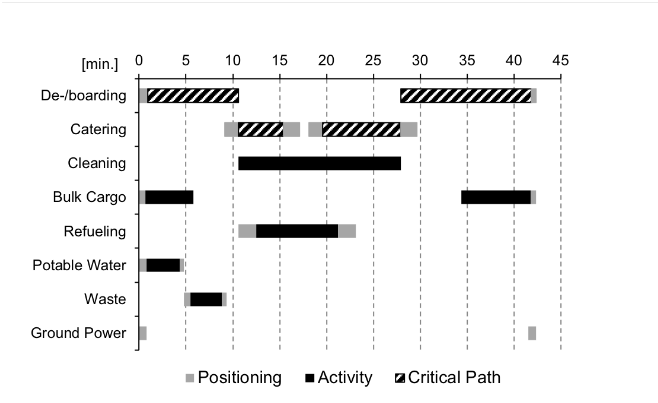

(b) Gantt chart

Figure 2.2.: Airport turnaround operation (adapted from [59]).

the right doors are utilized for catering and cargo handling. Commonly, the position of the service vehicles is predefined due to the interface locations of the aircraft. The corresponding Gantt-chart (see Figure 2.2b) presents the duration of individual handling operations in a sequence. The logical chain, regulations and restrictions due to limited space around the aircraft lead to a strict chronological order for certain handling operations. These operations mark the critical path of the turnaround process, since the minimum necessary turnaround time depends on these. In most instances, the critical path consists of the passenger and aircraft cabin activities, however in several circumstances the fueling operation may become the critical path. Other activities, such as unloading, loading and aircraft servicing, can normally be performed without impact on or from the critical path activities (AHM 021) [55]. Analysis for handling processes of short-haul flights by Fricke et al. [60] underline that, besides passenger processes, catering and refueling also have a major impact on the overall turnaround time. Thus, reducing time devoted to these processes would shorten turnaround time, which un turn directly influences the gate utilization and the number of flights that an aircraft can perform per day.

In the SA aircraft segment between 100 and 200 passengers, the turnaround time averages 35 minutes with a maximum of 51 minutes, as illustrated in Figure 2.3. The required time averages around 17 minutes for regional aircraft and 61 minutes for TA aircraft. However, the actual turnaround time of an aircraft is of a stochastic nature [61], since passenger numbers, replenished fuel and cargo loads vary from flight to flight. Airlines try to handle this variance through the incorporation of buffer times which leads to a large variation of scheduled on-block times compared to the original equipment manufacturer (OEM) guidelines.

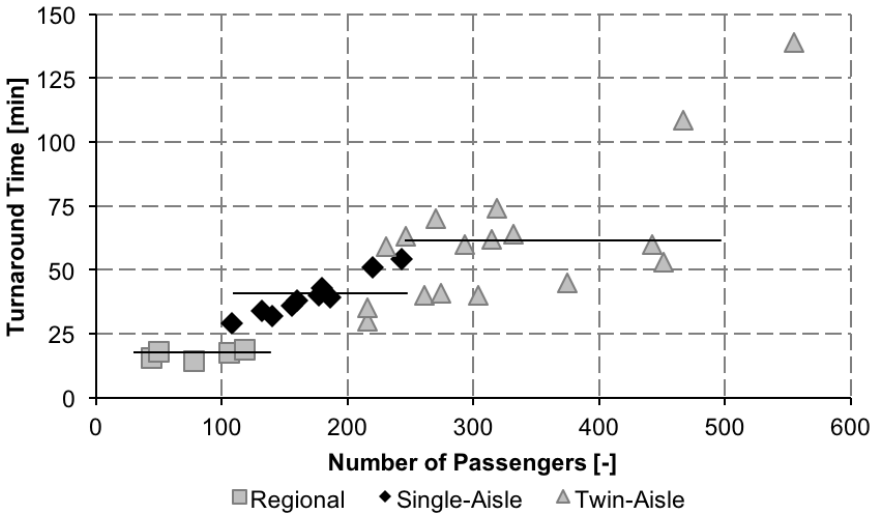

Figure 2.3.: Turnaround time correlation with the number of passengers for regional, single-aisle and twin-aisle aircraft (horizontal lines represent median values, based on manufacturer data) [40].

2.2.3. Passenger egress and ingress

As stated by Marelli et al. [16], passenger aircraft boarding process has been an issue since the late 1970's. The decline of the average boarding velocity is a result of increased hand luggage, airline service strategies and passenger demographics. Other factors which influence the process include aircraft configuration, cabin layout, boarding schemes, passenger properties and airport environment. One contributing aspect that cannot be influenced by the aviation stakeholders are the passengers themselves. The passenger demographics and therefore the travel behavior changes. The passenger ratio of male and female air travelers' shifts [62] as well as their anthropometrics in terms of average weight and body size [63–65]. This results in a demand for more space to experience the same level of comfort as before.

Common pre-boarding practices sequence families with small children and passengers with restricted mobility to board the aircraft first. Second, passengers booked in premium travel classes or with frequent flyer status are allowed to board the aircraft and finally all other remaining passengers. After passengers have entered the aircraft, their initial goal is to search for their assigned seat. They are limited in their movements due to the constricted aisle layout. Prior to taking a seat, the outerwear is taken off and HL is stowed under the seat or in the overhead bins. If a passenger blocks the aisle during this time, the stowing task, it is referred to as aisle interference, as illustrated in Figure 2.4. A row interference occurs when a passenger must wait for another passenger in their row to sit down before they can enter the row, this often also results in an aisle interference.

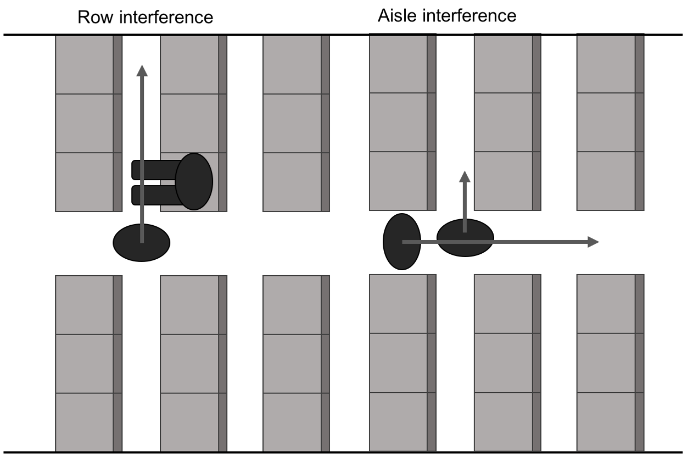

Figure 2.4.: Row and aisle interference (based on [66]).

Passengers disembarking behavior, although not organized or planned, often follows a distinct pattern; passengers will wait for other passengers in the rows before them to leave before leaving themselves. This causes a queuing of passengers in the back rows. In most cases, passengers in the same row will leave from aisle seat to window seat eliminating the row interferences. The passenger's behavior in an aircraft is comparable to a crowd behavior where everyone tries to get to the same destination first [67].

In general, methods for a shorter overall boarding times offer a reduced ingress time for each individual passenger [68]. Hence, a smooth boarding procedure would benefit passengers and airlines in the same way, since the boarding procedure is the last process to complete the turnaround [69].

2.2.4. Regulations and guidelines in place

The regulatory framework for turnaround operations examines the procedures from an aircraft design point of view in the Certification Specification (CS) for Large Airplanes CS-25 [56] and Federal Aviation Regulations (FAR) Part 25 - Airworthiness Standards: Transport Category Airplanes [57]. From an operation perspective, guidelines can be found in the International Air Transport Association (IATA) AHM, IATA Ground Operations Manual (IGOM) [55], as well as the European Commission Regulations [70].

The cabin layout should be designed to allow evacuation being accomplished within 90 seconds (CS/FAR 25.803) through a distinct amount and size of emergency exits depending on the number of passenger seats (CS/FAR 25.807 (g)). They should be distributed uniformly along the fuselage (e), preferable in the proximity of the flight deck (j) and near the end of the cabin on each side (f). The exits can show a certain asymmetry (d) and should be located where persons using them will not be endangered by the propellers (CS/FAR 25.809). Cabin attendant seats should be placed next to the emergency exists to provide a direct view of the cabin area (CS/FAR 25.785 (h)). The minimum aisle width for passenger aircraft is defined as 0.38 m (15 in) on the floor and 0.51 m (20 in) at 0.64 m (25 in) above the floor level and should be connected with the emergency exits through a passageway with least 0.91 m (36 in) width for larger exits (CS/FAR 25.813). For SA configurations, no more than three seats may be placed on each side of the aisle in any row (CS/FAR 25.817) and if the passenger seats are tilted towards the aircraft centerline, an additional safety belt is required to prevent head injuries (CS/FAR 25.785 (d)). Stowage compartments, such as the overhead bins, must be completely enclosed to avoid the items to be moving around (CS/FAR 25.787).

To ensure safe operation, the aircraft should be staffed with one cabin crew member for every 50 passenger seats installed (EU-OPS 1.990) also in the case of passengers are onboard during ground operation (EU-OPS 1.311). While passengers board or disembark, the aircraft should not be refueled. Otherwise necessary precautions must be taken to initiate a required evacuation of the aircraft (EU-OPS 1.305, AHM 175, AHM 630). Before the departure, all hand baggage which is taken into the passenger cabin should be adequately and securely stowed (EU-OPS 1.270).

The IATA AHM [55] covers process specifications for passenger, baggage and cargo handling, and moreover serves as a guideline for aircraft loading and airside safety management. All aircraft operators should determine a ground time which is designed to meet operational requirements but should not compromise safety (AHM 021). In general, the potable water servicing should comply with the World Health Organization (WHO) standards and the connectors shall be kept at certain distance away from the waste storage or treatment and toilet servicing equipment (AHM 440/441). The IGOM delivers step-by-step procedures for each necessary handling task. Cabin baggage cannot be accepted, if it is unsuitable due to its weight, nature, or does not fit under the seat or in the overhead compartments. Baggage is characterized as bulky or oversized, if its weight exceeds 32 kg (70 lb). Also, the incident reporting duty is highlighted, since aircraft damage can endanger passengers and employees, and the resulting disruptions could negatively impact safe airline operations [55].

2.3. Related research projects and conceptual studies

Recent research projects and conceptual studies are targeting an evolution of the ground operation processes towards improved time efficiency, increased predictability and reduced disruptions. The targeted time frame spans from short-term concepts (<10 years) to long-term disruptive solutions (>30 years). This section first summarizes studies which focus on the aircraft turnaround event before pathways for improved passenger processes are explored.

2.3.1. Aircraft ground operation concepts and studies

A review of research projects and conceptual studies covers ground operational concepts in terms of airport infrastructure, passenger and turnaround processes and aircraft conceptual changes. An overview of the investigated projects is summarized in Table 2.1. From an airport point of view, modifications of current boarding bridges are investigated to speed up passenger processes using multiple doors [33]. An additional underground supply system for electrical power, potable and waste water and PCA, besides the existing fuel pipe system, could minimize the number of GSE and apron traffic [34–36]. A relocation of the aircraft interfaces for fuel, potable and waste water, ground power and PCA becomes feasible in this context. Process times are unaffected by the changes, however the number of required vehicles can be dramatically reduced as well as required manpower and complexity of the ground servicing procedures. The aircraft itself would need additional ducts and pipes, if traditional locations of sub-systems are not changed [54]. The application to existing airports is limited for most of these concepts, since infrastructural modifications would disrupt the operation heavily and require huge investments. Furthermore, backwards compatibility with current aircraft in-service hast to ensured.

Table 2.1.: Overview of analyzed European research projects [33–36, 71–75].

		Scope			Results		
Project	Duration	Landside	Ground handling	Aircraft	Concepts	Software	Process
E-CAB	2006-2009			X	X		X
ALOHA	2007-2011		X	X	X		
ASSET	2008-2011	X			X		X
TITAN	2009-2013		X			X	X
The 2050+ Airport	2011-2014	X			X		X
FANTASSY	2012-2014			X	X		
INTERACTION	2013-2016		X		X		X

Automated de-icing and GSE docking could be accomplished in the short term aiming towards a higher automation in apron services. A combination of machine vision algorithms and targets on the aircraft fuselage enables the automated docking of passenger boarding bridges or cargo loaders [33]. A further step would be fully autonomous moving ground vehicles with remote monitoring and control. In this context, robots are used to transfer baggage, consumables and equipment [33–36]. These concepts could minimize the GSE docking and maneuvering time while simultaneously avoiding potential collisions. Mature technologies would also be required to provide security against hacking of the control system and in case of incidents, liability issues need to be addressed.

In the past, studies have investigated aircraft which are equipped with all tools and equipment required for an autarkic turnaround [34–36, 71]. Novel aircraft configurations that integrate innovative subsystems optimized for ground handling activities increase the independence from airport resources and reduce the number of required GSE. A quantitative assessment of a high-wing aircraft with tail-mounted engines, integrated stairs, foldable seats and conveyor belts inside the compartment revealed around 4 % higher DOC per seat-mile compared to a state-of-the-art reference aircraft. The gained benefit of the increased utilization could not outweigh the drawback of a higher maximum take-off weight (MTOW) due to the embedded systems [71].

The so-called SkyGate vehicle [76–78], which is designed with a minimal number of interfaces between aircraft and ground could reduce turnaround time through the realization of passenger egress and ingress during taxiing operations. The vehicle combines the functions of a towing truck, a shuttle bus and a jetbridge into a single multi-functional vehicle driven by electric motors and controlled autonomously. The main idea behind this concept is to let passengers disembark the aircraft directly into the new vehicle as soon as it was docked to the aircraft directly after the latter has vacated the runway upon arrival. While the disembarking is in progress, SkyGate tows the aircraft to its parking position, allowing the aircraft engines to be switched off for fuel-saving and noise-reduction purposes. After completing the disembarking process and separating from the aircraft at its parking position, the vehicle continues its journey to the terminal, where passengers can disembark. A first assessment shows an improvement potential of 8 % in reduced fuel consumptions per flight and increased annual aircraft utilization by 11 % on a 616 nm (1,141 km) mission based on time ground time savings of 15 minutes per trip. However, regulatory barriers concerning the passenger movement during taxiing still exist [76–78].

2.3.2. Studies and concepts to improve passenger processes

Current research shows six general development directions for improved passenger processes and advanced aircraft cabins: boarding schemes, aisle, door, seats, hand luggage storage and general layout modifications [38]. An overview of the associated concepts is listed in Table 2.2 and key aspects are highlighted in the following.

Boarding strategies

Airlines seek alternative strategies to increase boarding process efficiency. They have applied various boarding strategies that call for a predefined sequence of passengers entering the cabin depending on their allocated seat. Nyquist [79] and recently Jaehn and Neumann [80] provide an overview of Operation Research (OR) in this field covering methods such as back-to-front, zone boarding or random seating. Steffen and Hotchkiss [81, 82] conducted an experimental comparison of different aircraft boarding methods and found a significant reduction in the boarding times when using improved methods. Methods which call for parallel boarding processes showed more efficient use of the aisle. If more passengers stow

Table 2.2.: Overview of cabin modifications. *Benefits are measured against random boarding (based on [38]).

Modification	Concept	Benefit	Method	Reference
Boarding Strategy	Steffen and Hotchkiss	25%*	simulation	[81, 82]
	Milne and Kelly	28%*	simulation	[83]
	Zeineddine	24%*	simulation	[84]
Aisle	Aisle width (0.2m)	5-7%	simulation	[12]
	Multi-aisle (two)	50%	simulation	[12]
Door	Quarter door	3-24%	simulation	[12, 69]
	Door size	-	-	-
	Number of doors (two)	30-47%	simulation	[12]
Seat	Sideways foldable seat (SFS)	60%	simulation	[92]
	Lifting seat pan (LSP)	37%	simulation	[90, 91]
Luggage Storage	Larger overhead bins	-	simulation	[12]
	Center luggage storage	-	-	
Layout	Increased seat pitch	-	-	-
	Multi-deck	-	-	[76, 77, 97]

their luggage simultaneously, the number of aisle interferences is reduced which leads to increased speed in passenger ingress by almost 25 %. Building upon these findings, Milne and Kelly [83] presented a modified method in which passengers are individually assigned seats based on the amount of luggage they carry with the goal of distributing them evenly throughout the aircraft. The results show efficiency gains of up to 28 %. However, most of the strategies tested are not practical in regular flight operation as passengers must be grouped in a predefined way, which can split some groups. To avoid that, Zeineddine [84] proposed a dynamically optimized boarding strategy where passengers are sequenced in a boarding queue based on their seats' positions, associated groups, and the possibility of interferences, immediately after the last check-in. The results of this strategy show similar performance as compared to the Steffen strategy [81].

Only a few studies have investigated disembarking methods. The results show that the commonly used random strategy is competitive, but could be enhanced by a reverse window-to-aisle strategy where passengers seated on the aisle leave the aircraft first [67, 85, 86]. In this case, the applicability in regular operation is questionable due to the intrinsic passenger urge to leave the aircraft.

Aisle

A widening of the aisle results in a reduced seat width, seat abreast or in an increased aircraft cross-section diameter. The latter requires new aircraft design programs which manufactures try to avoid due to high development and certification expenses. The minimum aisle width for passenger aircraft is defined as 0.38 m (15 in) on the floor and 0.51 m (20 in) at 0.64 m (25 in) above the floor level (CS/FAR 25.815) [56, 57] (see Section 2.2.4). In current SA configurations, the aisle width is between 0.48 and 0.64 m (19 in to 25 in) [59, 87]. First studies of an aisle widening of 0.20 m (8 in) show a boarding time reduction potential for common SA aircraft, of 5-7 %, depending on the cabin size and number of passengers. This results from fewer aisle interferences due to an increased number of overtaking possibilities [12].

Switching from a SA layout to a TA configuration allows for the separation of passenger flow into two different streams. This shortens the queue lengths and number of aisle interferences. However, traditional SA configurations are superior in drag, weight and fuel burn from an aircraft design point of view [88]. Fuchte [12] investigated SA and TA cabin layouts in the range from 150 to 340 seats. A patent from Boeing [89] shows a concept for around 200 passengers in a TA configuration, preferably, with a seven-abreast configuration. A seven-abreast TA out-performs a six-abreast SA with 180 seats in terms of boarding time by 50 % with HL taken into account. This results from fewer seat interferences, slightly reduced walking distances and added overhead volume due to a larger cross-section.

Door

Changes to the door positions from the cabin ends to the middle allow for the division of the passenger flow into two separate streams. For SA aircraft above 180 seats, a so-called quarter door could achieve a 3-24 % boarding time reduction [12]. The results, correlated with the fuselage length, show larger potentials for higher passenger numbers due to the separation of the doors along the fuselage. For smaller aircraft, the limited fuselage length does not grant a sufficient margin between quarter and forward doors. This concept, however, has a substantial aircraft weight penalty below 220 seats, since then no full-size emergency exits are required [12]. Similar gains of 26 % have been shown by Schultz et al. [69] of an A320 with 174 seats. Airbus and Boeing have presented in their recent derivatives of the A320 and B737 family that it is possible to implement minor modifications to doors and emergency exits enabling larger seating capacity and improved cabin layouts [13, 14]. Thus, an enhanced aircraft could be offered to airlines without engaging in the extensive certification process when modifications to the cross-section are performed.

Significant improvements could be made using the forward (L1) and the rear door (L4) simultaneously for passenger processes. Fuchte [12] showed a 33 % boarding time reduction for this scenario. A further option is to install larger doors that allow two passengers to enter the cabin simultaneously. This would split the passengers into two streams within the jetbridge.

Seat

The concept of a lifting seat pan (LSP), also referred to as cinema seats, was introduced by AIDA Development [90] and initially assessed by Hertl [91]. The aim is to increase the moving space of passengers in the row and enhance their access to the overhead bins. The foldable seat pan allows passengers to step into the row, if the aisle seat is not yet occupied, and to stow their hand luggage in the overhead bin without blocking the aisle. If passengers try to get to their window or middle seat when the aisle seat is occupied, the aisle passengers can stand up while remaining within the row, reducing the duration of aisle interferences. First studies of Hertl estimate a 60 % boarding time reduction [91]. A similar concept called sideways foldable seat (SFS) allows the aisle seat to slide over the middle seat, as proposed by Molon [92], or under the middle seat, as introduced by Isikveren et al. [93, 94]. This enables a three-fold increase of the aisle width allowing passengers seamlessly to pass other passengers who stow their hand luggage in the overhead bins. Molon estimates a 37 % boarding time reduction [92].

Hand luggage storage

The HL is usually stowed in the overhead bins and under the seats. Since the storage volume is often at its capacity limits, an increase of the overall volume or an increase of the efficiency to stow large HL items is favored [12, 95, 96]. A concept from the German Aerospace Industry Association shows a central luggage storage concept where passenger can drop off their bags close to the entrance door [97].

Cabin layout

Although beneficial for passenger comfort, an increased seat pitch is disadvantageous for airlines as it reduces the cabin's capacity. For boarding and disembarking procedures, a sufficient seat pitch would enable passengers to get to their seat without the need of other passengers to stand up, thereby eliminating row interferences. Furthermore, passengers could stow their luggage in the overhead bins without blocking the aisle, significantly reducing aisle interferences.

An alternative proposal is the arrangement of passengers on two decks which could increase the number of seats considerably. A design study, based on a typical narrow-body aircraft, accommodates several passengers in the under-floor space, which is used today for cargo [76, 77, 97]. This change would only require a slight enlargement of the fuselage diameter. Rearranging the aircraft doors would enable parallel passenger boarding on the lower and upper deck, as well as, on both fuselage sides. First estimations show that current egress and ingress time could be retained despite a 20 % increase in number of passengers [76].

2.4. Existing methodical approaches

The review of ground operation research projects and conceptual studies showed a large diversity when it comes to their impact on current processes. To claim the required resources for a further development in terms of their top level requirements (TLRs), a holistic performance assessment is aspired during the early stages of a conceptual aircraft design project. This section provides an overview of existing aircraft turnaround modeling approaches as well as simulations for passenger egress and ingress. The focus is on their application to assess the performance of the previously highlighted concepts.

2.4.1. Aircraft turnaround modeling

Various approaches exist to model airport ground operations in general. Most existing frameworks follow the critical path method (CPM) which identifies time constraint aircraft turnaround activities. These models usually do not capture the uncertainties of schedule punctuality or the operational uncertainties of aircraft turnaround operations [98, 99]. The applied modeling techniques cover stochastic probability functions based on historic data, discrete event simulation (DES) and agent-based simulation (ABS) approaches. A summary of the reviewed frameworks is compiled in Table 2.3.

Focusing on a more detailed perspective, microscopic models are more flexible and represent the entities found in the real system with their individual attributes and behavior. One approach applied to microscopic system modeling are ABS models. These are characterized by common actions of autonomously deciding agents [100]. The system behavior in ABS is modeled as a collection of autonomous decision-making agents, although each agent individually assesses its situation and makes decisions based on a defined set of rules. The modeling from the involved agents' point of view is referred to as individual perspective. The resulting interactions are heterogeneous and can generate network effects [101]. The behavior of the overall system is based on the interactions of the entities as macro phenomenon. This view also characterizes other modeling styles such as individual-based, object-oriented or DES [100].

Ip et al. [102] proposed an ABS model to support the decision making in GSE allocation in an effort to minimize the chance of delays and operating cost. The considered GSE and aircraft are performance-wise identical and all process times are assumed to be determinable and known in advance. An approach using Petri nets[1] is pursued by Vidosavljević, and Tosić [103] encompassing taxi-in, turnaround and taxi-out procedures. Based on traffic data from Belgrade airport, the number or required GSE could be determined. Voulgarellis et al. [104] proposed an airport ground handling simulation using Matlab that aimed to estimate the number of required GSE to serve a specific flight plan. Using model blocks for each operation, the airport operation dynamics can be simulated

[1] Petri nets are a graphical and mathematical modeling technique which consists of places, transitions and arcs.

Table 2.3.: Overview of existing turnaround modeling approaches (n.a. = not accessible or currently not available for purchase).

Name	Year	Method/Tools	Purpose	Availability	Reference
Voulgarellis et al.	2005	Matlab	Flight plan	n.a. / commercial	[104]
Ioannidis et al.	2005	Simulink	Flight plan	n.a. / commercial	[105]
Ip et al.	2010	ABS	GSE allocation	n.a.	[102]
Vidosavljevic and Tosic	2016	Petri nets	GSE allocation	n.a.	[103]
Norin et al.	2012	DES/Arena	Turnaround	n.a. / commercial	[109, 110]
Andersson et al.	2000	Integer programming model	Turnaround	n.a.	[19, 106]
Tian et al.	2013	Virtual simulation	Turnaround	n.a.	[111]
Mota et al.	2015	DES	Turnaround	n.a.	[108]
Wu and Caves	2004-08	Markovian	Turnaround uncertainties	n.a.	[22, 61, 107]
Fricke et al.	2008-10	Statistical density functions	Turnaround uncertainties	n.a.	[10, 60, 117]
Schlegel	2010	Stochastic functions	Turnaround uncertainties	n.a.	[118]
Bevilacqua et al.	2015	Stochastic functions/ProSim, WITNESS	Turnaround	n.a. / commercial	[114-116]
Crönertz	2008	CPM	Turnaround	n.a.	[112]
CAST Ground Handling	2009	ABS	Turnaround	n.a. (commercial)	[113]
Sanchez	2009	Stochastic functions	Turnaround	n.a.	[119]

and time delays can be predicted. The turnaround itself is not modeled in detail and is assumed to last for a fixed time period. Following a similar approach, Ioannidis et al. [105] built a model using Simulink. Andersson et al. [19, 106] proposed an integer programming model[2] to capture the dynamics of the aircraft turnaround based on available ground operational data. Their goal was to simulate airline operational decisions about pushback times under resource constraints. Wu and Caves [22, 61, 107] published various studies on the modeling and simulation of aircraft turnaround operations focusing on operational uncertainties. They used a Markovian[3] type simulation model [107] combined with Monte Carlo techniques[4] in order to capture the stochastic effects of flight punctuality and operational uncertainties. With this method, the stochastic transition behavior between major aircraft turnaround activities and potential disruption activities from passengers and aircraft ground services can be modeled. A second approach [22] applied an analytical model to simulate the efficiency of aircraft turnaround operations at airports targeted at minimizing the aviation system costs by balancing trade-offs between schedule punctuality and aircraft utilization.

Focusing more on the individual ground handling processes, a detailed DES model of the turnaround operations at Lelystad airport was developed by Mota et al. [108]. The modular model covers a detailed airport layout representation and performed each ground handling task using fixed process time values. The focus of the work from Norin et al. [109] is on the de-icing services at Stockholm Arlanda airport. The compiled model covers all procedures from the touch down and taxiing into the stand, the turnaround process itself and ends with taxiing out to the runway and taking off. To model each process, the commercial DES package ARENA [110] is used. The turnaround model includes some simplifications in terms of process dependencies. A sophisticated virtual simulation-based approach was presented by Tian et al. [111] to evaluate the handling of advanced aircraft concepts with unconventional configurations, such as blended wing body (BWB) and joined wing. This framework requires a three-dimensional aircraft model as input and determines the vehicle movement paths during the simulation. Crönertz [112] developed a detailed activity-based turnaround model focusing on the turnaround cost. The necessary equipment and labor is assigned to each process allowing to capture detailed sensitivities. The commercial software Comprehensive Airport Simulation Tool (CAST) Ground Handling [113] developed by the Airport Research Center (ARC) comprises ABS ground handling simulation, three-dimensional visualization and collision detection. It provides a chronological ground handling simulation considering rules and delays, compatibility analysis and detailed movement animation. Bevilacqua et al. [114] applied the commercial simulation software ProSim [115] and WITNESS [116] to model ground handling opera-

[2] An integer programming model is a mathematical optimization where some or all of the variables are restricted to of datatype integer.

[3] A Markov model is a part of probability theory used in stochastic modelling to model randomly changing systems where it is assumed that future states depend only on the current state not on the events that occurred before it.

[4] A Monte Carlo approach relies on repeated random sampling to obtain numerical results.

tions. The time for the sub-processes was determined with stochastic functions based on triangular and lognormal distributions using historical data.

Based on an extensive dataset of recorded real turnaround events, Fricke et al. [10, 60, 117] produced statistical density functions for each sub-process of a turnaround event. However, no distinction of the aircraft type or operation was conducted. Schlegel [118] pursued a similar approach modeling stochastic functions for the turnaround processes based on recorded flight data. He combined the determined functions to a simulation model analyzing impacts of operational impairments. Sanchez [119] created statistical equations based on real turnaround observations for each individual process of a turnaround. The process times are calculated using a specific flow rate per minute for the exchanged good, such as containers or passengers.

2.4.2. Passenger egress and ingress simulation

Different approaches to model passenger ingress and egress processes have been proposed in literature, but distinguishing between these concepts is not straightforward. Table 2.4 provides an overview of existing microscopic passenger flow model approaches focusing on aircraft and terminal applications.

Macroscopic models use a system of differential equations describing associations between variables at the overall system level. A survey showed diverse macroscopic approaches ranging from a physical-mathematical point of view using Lorentzian space-time geometry and a CPM [120, 121], a non-linear assignment model with quadratic and cubic terms [66, 122] to mixed integer linear programs [123] in combination with genetic algorithms[5] [124].

Dealing primarily with boarding strategies, Van Landeghem and Beuselinck [125] applied the commercial software Arena [110] to investigate boarding strategies. Ferrari and Nagel [126] conducted a computer simulation similar to the latter using a simplified cell-based simulation architecture. An ABS approach was pursued by Livermore [127] and Audenaert et al. [128] to investigate the applicability of boarding strategies. Cimler et al. [85, 129] used an ABS model based on NetLogo[6] [130] to compare aircraft boarding and disembarking methods. The model enabled the experimentation of various scenarios and parameters settings, such as the number of passengers, the ratio of passengers carrying luggage and the size of the aircraft. Also focusing on boarding strategies, Qiang et al. [131] used a cellular automaton (CA) model based on the Nagel-Schreckenberg model, which is a theoretical model for the simulation of freeway traffic, to test the behavior of boarding strategies under different conditions considering seat and aisle interferences.

[5] A genetic algorithm is an evolutionary algorithm which is inspired by the process of natural selection.

[6] NetLogo is an open-source programmable modeling environment well suited for modeling complex systems developing over time. It is available under the terms of the GNU General Public License (GPL). Further information can be obtained from https://ccl.northwestern.edu/netlogo/

Table 2.4.: Overview of existing passenger flow simulations (n.a. = not accessible or currently not available for purchase).

Name	Year	Method/Tools	Purpose	Availability	Reference
Landeghem and Beuselinck	2002	DES/Arena	Boarding strategies	n.a. / commercial	[110, 125]
Ferrari and Nagel	2005	CA	Boarding strategies	n.a.	[126]
Livermore et al.	2008	ABS	Boarding strategies	open-source	[127]
Audenaert et al.	2009	ABS	Boarding strategies	n.a.	[128]
Steiner and Philipp	2009	DES	Boarding strategies	n.a.	[133]
Cimler et al.	2013	DES/NetLogo	Boarding strategies	n.a. / open-source	[85, 129, 130]
Qiang et al.	2014	CA	Boarding strategies	n.a.	[131]
Schultz	2010	CA	Airport terminal	n.a.	[132]
TOMICS - DLR	2011	DES	Airport terminal, aircraft de-/boarding	n.a.	[68, 135]
PEDS - Boeing	1998	DES	Aircraft de-/boarding	n.a.	[16]
MASim - Richter	2007	ABS	Aircraft de-/boarding	n.a.	[137]
CAST Cabin - Airport Research Center	-	ABS	Aircraft de-/boarding	commercial	[136]
Boeing	2013	CA	Aircraft de-/boarding	n.a.	[138]
Schultz et al.	2013	ABS	Aircraft de-/boarding	n.a.	[69]
Fuchte	2014	ABS	Aircraft de-/boarding	n.a.	[34]
airExodus - Fire SafetyEngineering Group	2015	ABS	Aircraft evacuation	commercial	[134]

A wider range of applications was targeted by the approach of Schultz [132] who developed a stochastic model for passenger movement behavior in airport terminal facilities representing the extension of a spatially discrete microscopic model based on CA. The Airplane Boarding Simulator by Steiner and Philipp [133] is a DES to study the influence of differencing factors on the boarding time. AirExodus [134] is a comprehensive ABS framework especially designed for aircraft evacuation certification which is commercially available. It has the ability to represent agent interaction with signage and smoke, and allows the simulation of thousands of agents without performance penalties.

Focusing on the application to aircraft cabins, Boeing's [16] approach uses DES to combine the effects of mathematical queuing theory with an analysis of random behavior. This simulation features various interior configurations, passenger mixes, and boarding scenarios. Passengers can be assigned certain attributes, such as walking speed, type of carry-on luggage, luggage put-away time, and relationship with other passengers. Schultz et al. [69] proposed a microscopic approach of modeling the passenger flow using an asymmetric simple exclusion process (ASEP) where the passenger is defined as a one dimensional, stochastic time and space discrete transition process. Based on a grid with a rather limited resolution, luggage stowing and seat interferences can be simulated. Other potential disturbances, such as congested overhead bins, missed rows or overtaking passengers are not taken into account. Their analysis focused on the application of boarding strategies in conventional cabins. TOMICS by the German Aerospace Center [68, 135] is a DES built for analyzing passenger flows within airport facilities, such as terminal areas and security checks, as well as boarding and disembarking processes. The simulation features a comprehensive path-finding algorithm and cabin procedures, like luggage stowing, however the adaption capabilities to deal with advanced cabin concepts are unknown.

The commercial CAST Cabin framework [136] is based on an ABS approach and provides a promising implementation to model passenger boarding processes. A similar approach is pursued by Richter [137] featuring a variety of agent properties as well as executable subtasks, such as luggage stowing. Unfortunately, this framework suffers from performance issues with an increasing number of agents. The approach of Fuchte [12] is based on the latter model and eliminates performance issues. The simulation includes an overhead bin model considering the actual remaining luggage capacity. The implemented path finding algorithm disregards other agents which leads to queuing of passengers and during the simulation no dynamic change of the path is possible. A patent from Boeing [138] describes a three-dimensional ABS boarding and disembarking tool. Passenger characteristics are described with walking speed and amount of hand luggage, and their interferences are modeled with a predefined waiting time.

2.5. Recapitulation

The ground operational processes are the connecting element between aircraft en-route operations and airport infrastructure. Aircraft operators are challenged by prolonged passenger process times, airport capacity constraints, schedule disruptions, reduced aircraft utilization and the increasing cost pressure. Therefore, industry and research organizations are looking for solutions to enable competitive aircraft operations for all involved stakeholders. Based on the outline in this chapter, general observations are given and reference is made to the research issues depicted in the problem description in Section 1.2. Finally, the research goals are refined to justify and detail the further method development in this thesis.

Current ground handling operations

The current diverse market of airline types ranging from FSC to LCC demand for contradictary requirements for future aircraft. Requirements differ for offered range capabilities, in-flight amenities and turnaround performance resulting from the distinct operational schemes, such as hub-and-spoke or point-to-point connections.

Especially, the aircraft ground handling is a highly competitive market with multiple stakeholders. Unfortunately, this process often causes delays and disruptions which stem from aircraft and ramp handling, passenger and baggage handling, the resulting damages to aircraft and flight operation as well as crewing. This leads to substantial impairments to airport operations. The regulated-driven sequential order of passenger and cabin processes, and refueling often constitutes the critical path. Thus, a further parallelization or shortening of these processes would reduce the overall turnaround, which could increase the aircraft utilization.

Focusing on the passenger processes as the most time critical procedure of the turnaround, a decrease in the boarding velocity was observed due to increasing load factors and an excessive amount of HL. Not only airlines would profit from faster boarding procedures, since it is the last process before the departure, also each passenger would benefit from shorter queue length. However, the scientific driven analyses of the boarding process often disregard operational facts, such as HL distribution or seat load factors.

Related research projects and conceptual studies

The review of conducted studies and developed concepts showed opportunities to free up airport capacity through an optimized use of airport infrastructure (RI 2 and 3). The reduction of additional buffers should allow faster door-to-door travel for passengers which could generate higher revenues for airlines (RI 4 and 5). Promising approaches try to reduce apron traffic through underground supply of liquids or parallelize passenger processes and taxiing. A further parallelization or shortening of processes on the critical path would reduce the overall turnaround time increasing the aircraft utilization. However, this could push other resources to their limits, such as gate positions and taxiways, and so far unconstrained processes might become constraining, including aircraft brake cooling times or cockpit procedures.

One aspect which cannot be influenced by the stakeholders are the passengers and their behavioral patterns. Besides the application of boarding strategies, novel cabin layouts focusing on aisle, door, seat, luggage storage and general layout modifications are another way to increase the boarding efficiency (RI 1). Alternative door positions and adaptable seats show large efficiency potentials with a comparatively low market entry barrier. A combination of suitable concepts could implicate cascade effects which further increase the expected benefits. However, the operational applicability including the economics of the concepts' integration still has to be shown, since they have not been seriously considered by the aviation community.

Existing methodological approaches

The assessment of novel ground operational concepts relies on the modeling and simulation of the processes during the early stages of the product development (RI 6). The variety of models and frameworks dealing with the aircraft turnaround cover resource allocation, operational uncertainties as well as the detailed modeling of each sub-process. Using recorded data allows to follow stochastic approaches of modeling turnaround procedures, however they do not permit to assess novel concepts with modified operations. Sophisticated simulation frameworks built on three-dimensional aircraft models which require a high availability of design-specific data and a detailed ground handling process definition to assess each step in detail. Unfortunately, these data are often not available in the early stages of the conceptual aircraft design. A compromise based on both approaches could offer the necessary depth for critical processes, such as the passenger egress and ingress, and a high-level model for the remaining processes.

In the field of passenger process simulations inside of the cabin, a variety of macroscopic and microscopic models exist. Especially DES and ABS approaches allow to model the individual behavior of each passenger during the boarding and disembarking process. Unfortunately, most of the reviewed frameworks are only published partly in form of research papers and do not allow the access of the model foundation which is required for a deeper understanding and for model extensions. Hence, the developed methods and tools should be built upon open-source frameworks and ideally are made available to the community.

Expected contributions

This thesis focuses on the improvement of the passenger egress and ingress (Research Goal (RG) 1) through the development of robust and reliable turnaround processes (RG 2). Based on a methodical review conducted in this chapter, assessment capabilities need to be developed which allow a holistic concept evaluation (RG 4), since current approaches are commonly not accessible nor extendable. The evaluation is done based on DOC to identify cost competitive concepts (RI 5). These research issues and goals can be translated into the following contributions which are expected in the scope of this thesis:

Expected Contribution 1: The research of this thesis aims to develop a holistic assessment framework for advanced ground operational concepts. The framework comprises: (1) aircraft design heuristics, (2) passenger flow simulation, (3) turnaround modeling and (4) operational cost assessment. Each module should be flexible and customizable for a variety of application cases. The data exchange should be accomplished using defined interfaces and, where applicable, a central meta model containing the data structure and representation.

Expected Contribution 2: Through the usage of a consistent data representation with a central meta model, an integration into existing conceptual aircraft design frameworks becomes feasible. Insights from the ground operation performance are directly linked to the overall aircraft design assessment which enables the developed framework to be embedded in multi-disciplinary design optimization (MDO) environments.

Expected Contribution 3: A coherent down-selection of promising candidate solutions is facilitated through the application of the developed framework to identify concepts with enhanced performance.

Expected Contribution 4: The obtained insights of the concept evaluation enable the identification of design criteria for the next generation of commercial transport aircraft, addressing any exposed research issues. These criteria form the basis for strategy planning of the involved stakeholders.

3. Methodical approach for a ground operational assessment framework

A holistic assessment of aircraft ground operations during the conceptual design phase is imperative in addressing the challenges of current ground operations. As illustrated in Figure 3.1, a framework is proposed which comprises: (1) cabin design heuristics, (2) passenger flow simulation, (3) turnaround simulation and (4) direct operating cost assessment. Furthermore, an interface with state-of-the-art aircraft design tools is required to investigate the in-flight performance (5). Each module was developed to be flexible and customizable for the application to manifold concepts.

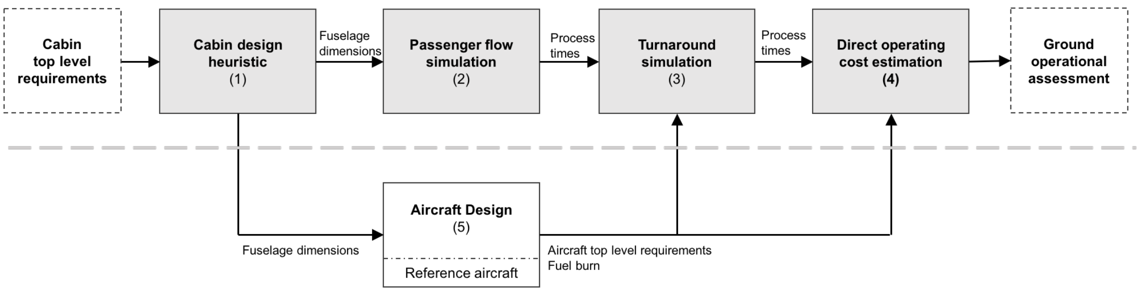

Figure 3.1.: Overview of the ground operational assessment framework modules and their interaction.

The payload specification, operator business model and targeted aircraft category form the input for the initial aircraft cabin layout generation. Design heuristics (1), covering current regulations and empirical values, derive the overall fuselage dimensions. Furthermore, they form the basis for a detailed cabin layout generation and the integration of novel concepts. An in-depth analysis of the layout candidates is accomplished using agent-based passenger flow simulations (2) which elucidates the best performing solutions. The use of contemporary aircraft design tools (5) enables the derivation of trade factors for geometry and OWE changes compared to reference configurations. This enables the evaluation of in-flight performance of the investigated candidates. Changes to the cabin configuration mainly influence the turnaround operations, which can be assessed using an activity-based turnaround model (3). Finally a DOC analysis (4) is conducted to holistically assess the results on a time and fuel burn basis. In the following, the structure and incorporated methods of each framework module are highlighted.

3.1. Cabin design heuristics

The aircraft design process starts from a cabin design point of view with the definition of the payload, in terms of passengers and cargo, and their integration into the fuselage. This produces basic fuselage dimensions, such as the diameter and length, which are crucial for the subsequent design steps. Regulations according to CS/FAR [56, 57] have to be ensured during the initial cabin design (see Section 2.2.4). The number of passengers and basic seat dimensions are required as input to determine the overall fuselage dimensions. Based on the operator business model, cabin class and the targeted aircraft operation, the seat pitch is defined. These parameters are referred to as cabin top level requirements (CTLR).

Fuselage width

The necessary fuselage width w_{fuse} depends mainly on the interior cabin width w_{cabin} and the fuselage wall thickness t_{fuse}, as illustrated in Figure 3.2. If the latter is unknown, the empirical Equation (3.2) by Fuchte [12] can be used instead to determine the fuselage width.

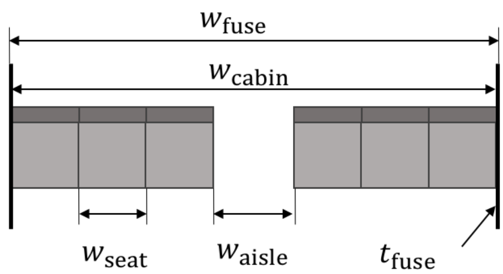

Figure 3.2.: Cabin parameters and dimensions associated with the fuselage width.

$$w_{fuse} = w_{cabin} + 2 \cdot t_{fuse} \tag{3.1}$$

$$w_{fuse} = 1.045 \cdot w_{cabin} + 0.084 \tag{3.2}$$

The required cabin width w_{cabin} is the sum of the seat width w_{seat} of each seat in a row and the aisle widths w_{aisle} (Equation 3.3). Usually, SA aircraft above 50 passengers have a seat abreast between 4 and 6, and for TA aircraft it ranges from 7 to 10. This results from the regulation that no more than three seats may be placed on each side of the aisle (CS/FAR 25.817). The minimum aisle width is defined as 0.51 m (20 in) at 0.64 m (25 in) above the floor (CS/FAR 25.813) [56, 57] (see Section 2.2.4).

$$w_{cabin} = \sum_{i=1}^{k} w_{seat,i} + n_{aisle} \cdot w_{aisle} \tag{3.3}$$

Fuselage length

Figure 3.3 illustrates the cabin parameters and dimensions associated with the fuselage length. The length of the fuselage l_{fuse} is mainly driven by the cabin length l_{cabin}. The required space for the tail cone l_{cone} and flight deck l_{nose} can be estimated with Equation 3.5 [12]. The cabin length is the sum of the required length to place all seats l_{seat}, the emergency exits l_{exit} and the cabin monuments l_{mon}, such as lavatories or galleys. The cabin floor area is of non-rectangular shape, since the fuselage is tapered in the forward and aft areas. Therefore, a fuselage necking factor k_{neck} is applied to account for deviations from the rectangular shape.

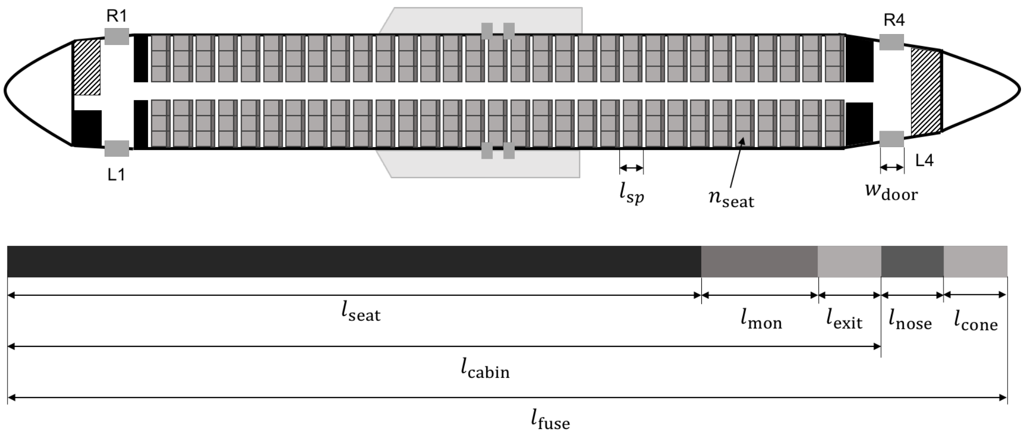

Figure 3.3.: Cabin parameters and dimensions associated with the fuselage length.

$$l_{fuse} = l_{cabin} + l_{nose} + l_{cone} \tag{3.4}$$

$$l_{nose;cone} = 1.6 \cdot w_{fuse} \tag{3.5}$$

$$l_{cabin} = \frac{l_{seat} + l_{exit} + l_{mon}}{k_{neck}} \tag{3.6}$$

The required fuselage lengths for the seats l_{seat} (Equation 3.7) is based on the number of rows, which in turn depends on the seat abreast n_{ab}, the number of seats n_{seat}, and the seat pitch l_{sp}. The seat pitch is defined as the distance from any point on one seat to the same point on the following seat. For economy class seating, the seat pitch varies between 29 in (0.74 m) for short-haul and 32 in (0.81 m) for long-haul aircraft [139]. Currently, no CS/FAR regulation specifies a minimum seat pitch.

$$l_{seat} = \frac{n_{seat}}{n_{ab}} \cdot l_{sp} \tag{3.7}$$

The number and type of emergency exits must allow evacuation to be accomplished within 90 seconds (CS/FAR 25.803). These dimensions are specified in CS/FAR 25.807 (g), however each aisle connected to a floor-level exit requires a passageway of at least 0.91 m (36 in) (CS/FAR 25.813) [56, 57]. The required additional fuselage length for emergency exits l_{exit} results from the minimal passageway width w_{pw} or the individual door width w_{door}.

$$l_{exit} = \sum_{i=1}^{k} max(w_{pw,i}; w_{door,i}) \tag{3.8}$$

Usually, cabin monuments, such as galleys and lavatories, are placed at exits and are often grouped to generate cabin sections. The equivalent fuselage length l_{mon} (Equation 3.9) is determined based on the required monument areas $A_{gal,req}$ and $A_{lav,req}$.

$$l_{mon} = \frac{A_{gal,req} + A_{lav,req}}{\sum_{i=1}^{k} w_{seat,i}} \tag{3.9}$$

The required monument areas $A_{gal,req}$ and $A_{lav,req}$ are derived from the number of passengers n_{pax} and a specific monument space requirement for each passenger $k_{gal;lav}$. The values are empirically determined based on OEM data. For galleys in economy class the k-factor results to $k_{gal,sa} = 0.011\frac{m^2}{PAX}$ for short-haul SA aircraft and $k_{gal,ta} = 0.019\frac{m^2}{PAX}$ for long-haul TA aircraft. For lavatories the values are $k_{lav,sa} = 0.014\frac{m^2}{PAX}$ and $k_{lav,ta} = 0.02\frac{m^2}{PAX}$.

$$A_{gal;lav,req} = n_{seat} \cdot k_{gal;lav} \tag{3.10}$$

The fuselage necking factor k_{neck} results from the ratio of the ideal rectangular cabin area A_{rect} and the real area A_{real} with the tapered forward and aft fuselage sections. These values are empiricall determined based on OEM data. The fuselage necking factor amounts to $k_{neck} = 0.92$ for SA and $k_{neck} = 0.79$ for TA configurations.

$$k_{neck} = \frac{A_{fuse,rect}}{A_{fuse,real}} \tag{3.11}$$

3.2. Passenger egress and ingress simulation

The passenger flow simulation [40] is based on a microscopic approach applying agent-based modeling techniques as it has been pursued earlier by Richter [137] and Fuchte [12]. Each passenger is represented as an agent with individual properties such as body dimensions, walking speed, target seat or type of carry-on luggage. This allows agent interactions to be modeled and to capture the resulting complex system behavior. Due to the unavailability of precise data during the conceptual aircraft design phase, the simulation environment uses the generated cabin parameters of the previously introduced design heuristics to generate a simplified two-dimensional representation of the cabin layout (see Figure 3.4). Detailed cabin layouts are created allowing for advanced concepts modifications covering aisle, door, luggage storing, seat and general layout. A special focus is set on modeling of the HL process, since this is currently one of the major bottlenecks during boarding and it is often disregarded in most scientifically driven analyses (see Section 2.4.2). As a result, the simulation module produces detailed cabin designs and process times.

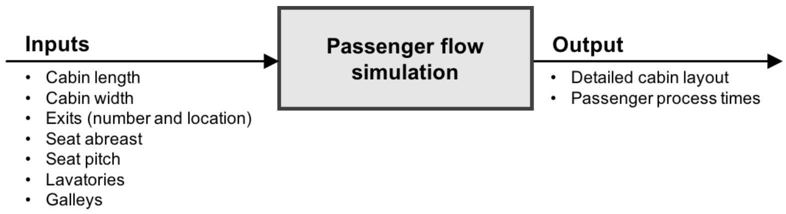

Figure 3.4.: Input and output of the passenger flow simulation module.

After a general introduction into agent-based simulation, the modeling of each element (cabin layout, agents and their behavior) is further elaborated in detail. Concluding, remarks about the framework architecture and the simulation execution are given.

3.2.1. Structure of agent-based passenger flow simulation

Agent-based modeling and simulation is an approach to model systems comprised of individual, autonomous and interacting agents. The system behavior is a result of the collection of autonomous decision-making agents, although each agent individually assesses its situation and makes decisions on the basis of a set of rules. The interactions are heterogeneous and can generate network effects [101, 140]. In general, an ABS consists of three elements:

- Environment, where agents act and interact
- Agents with their attributes
- Agent behavior and methods of interaction

3.2.1.1. Environment - cabin layout

The representation of the cabin environment is first introduced on a meta model basis covering cabin elements and then the underlying mathematical counterpart is highlighted, which includes the mapping of the model elements to a grid-based structure.

Meta model

The specification of model elements allows for the build up of diverse environments where agents move and interact. The meta model specification used to build up the underlying data model structure follows the Essential Meta-Object Facility (EMOF) [141] standard model-driven engineering provided by Object Management Group (OMG). In this definition, four model levels ranging from M0 to M3 represent different layers of abstraction. As illustrated in Figure 3.5, M0 contains the objects of reality which are real aircraft cabin parts in this context. These elements are represented in M1 as objects using the cabin meta model syntax developed in M2. The definition of the M2 simulation meta model follows the modeling syntax of the M3 Eclipse Modeling Framework (EMF) [142] Ecore meta model which is a reference implementation of EMOF [143]. This enables the model exchange with other frameworks following the EMOF specification.

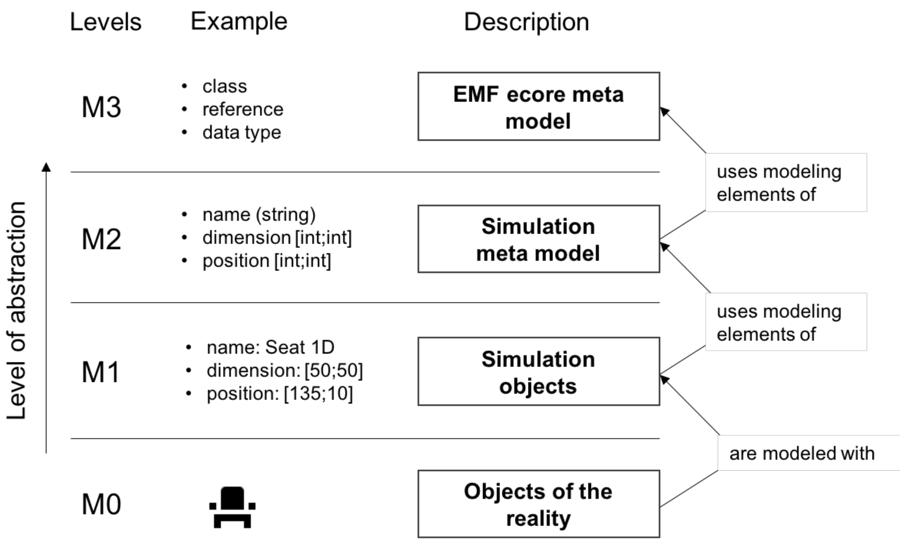

Figure 3.5.: Four-level modeling language stack of passenger flow simulation according to EMOF [141].

The simplified structure of the M2 simulation meta model is depicted in Figure 3.6 using Unified Modeling Language (UML). The *Cabin* class is the root element with references to the cabin monuments and doors, and attributes defining the overall cabin dimensions. The cabin monuments classes, such as *Lavatory*, *Galley* or *LuggageStorage*, inherit from *PhysicalObject* the basic attributes, such as dimensions of the rectangular shaped object and the position inside of the cabin. Also derived from *PhysicalObject*, the *Seats* are grouped in *Rows* with a distinct seat abreast and assigned a *SeatingClass*, such as economy or business. For each *Seat*, a reference to one *Passenger* can be established. The *LuggageStorage* objects are assigned to a certain area in the aircraft cabin and can either be mounted to the ceiling or the ground. Their net volume is determined by the amount of HL which can be stowed. The *Doors* define the location where passengers can enter and exit the cabin. Their basic attributes cover position and dimensions.

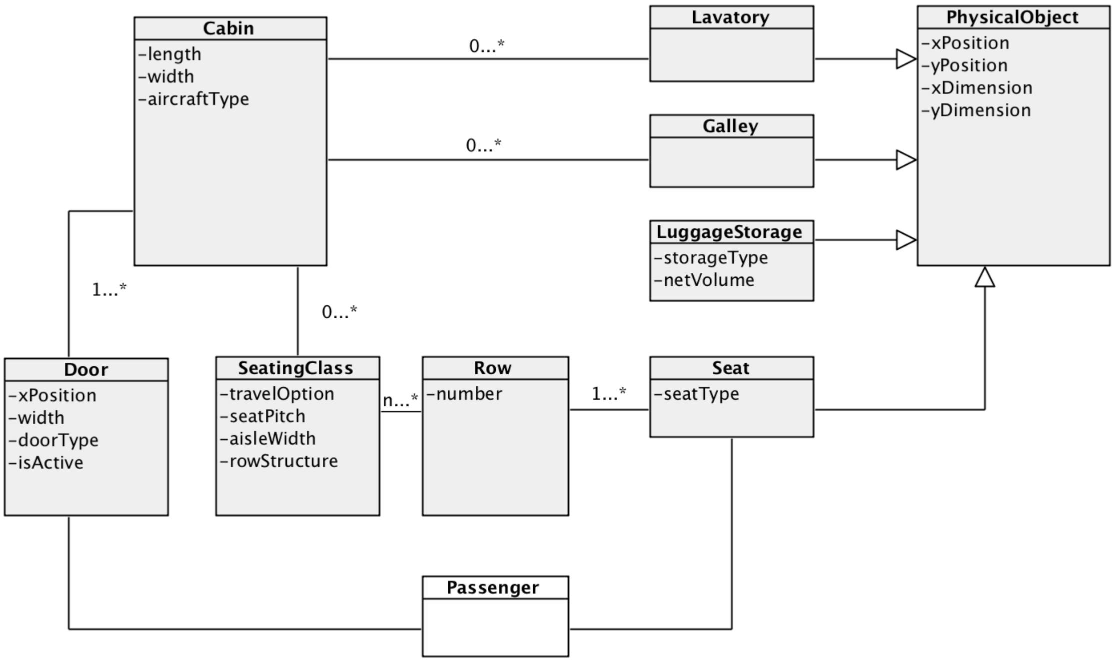

Figure 3.6.: Simplified UML meta model used for cabin layouts.

This meta model (M2) allows for the build up of various cabin layouts based on instanced objects (M1). These cabin models comprise multiple object instances of seats, monuments and doors with their pre-described attributes. The values for each attribute are assigned during the object instantiation process. This data provides the basis for the model transformation into a form suited for the simulation environments.

Mathematical representation

The cabin dimensions, in terms of length and width, are translated into a rectangular grid of vertices. The advantage of a grid is that the axes are orthogonal and for the determination of a position of a point, node or vertex $v[x, y]$, Cartesian coordinates can be used. The grid itself is a representation of a directed graph $G = (V, E)$, where V is a set of vertices and E is a set of edges from each vertex in the graph. An excerpt of a grid is exemplarily depicted in Figure 3.7. Each vertex $v[x, y] \in V$ is a zero dimensional point. An edge $(v_0, v_k) \in E$ is a mathematical representation of a one-dimensional line segment ending at two vertices v_0 and v_k respectively. A weight function $w(v_0, v_k)$ of an edge (v_0, v_k) describes the sum of distance between the vertices v_0 and v_k and the assigned cost of the target vertex v_k [144]. The cost of each vertex allows to represent different objects on the grid.

The grid of vertices provides in total eight movement directions which are captured through the identification of the neighbor vertices, as illustrated in Figure 3.8. Their position is referred to with cardinal directions. The vertical and horizontal distances between the vertices are referred to as grid scale allowing to specify the accuracy level of the layout

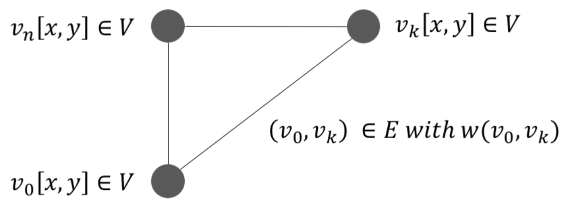

Figure 3.7.: Basic graph theory terminology (based on [144]).

representation. The vertices themselves comprise information about their location, type and associated cost. The vertex type can be either *void*, *obstacle*, *agent*, *start* or *goal*. During initialization all vertices are set to type *void*. The cabin monuments, except the ceiling-mounted *LuggageStorage* objects, are mapped to the grid as obstacles based on their position and dimension. The doors are translated into starting locations for passengers. The resulting grid with its vertices and edges describes the general cabin layout with blocked and unblocked areas.

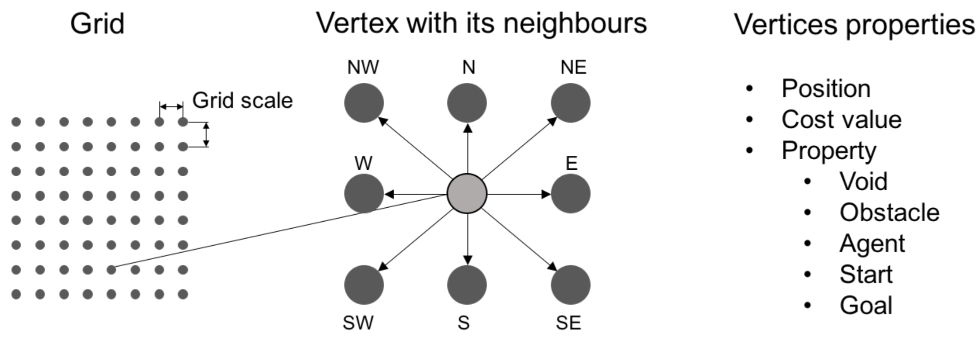

Figure 3.8.: Grip composition and its properties.

To illustrate three-dimensional effects, such as lower ceilings or general preferred walking paths, the default vertex cost can be adjusted. Around vertices of the type *obstacle* a gradient of higher vertex cost is applied as well as below overhead bins. A lower value is assigned to the vertices in the middle of the door entrance as well as the middle of the aisle.

3.2.1.2. Agents - passenger

The representation of agents is also specified in the structure of the meta model at M2 level, as highlighted in the previous section. The agents are characterized by anthropometric attributes of waist width, body depth [145] and walking speed in the *Passenger* class (see Figure 3.9). The selection of attributes is based on the findings of Liu et al. [146], who showed that especially the waist width has a large impact on egress times beside the walking speed. The walking speed is derived using a correlation in dependence of gender and age [147]. The values for anthropometric attributes can be adapted to represent passengers with different demographics. Furthermore, each agent is assigned to one door and one seat, which acts as starting point and goal for the pathfinding. Assigning the seats in a predefined order to the agents allows to mimic group behavior as well as to illustrate boarding sequences.

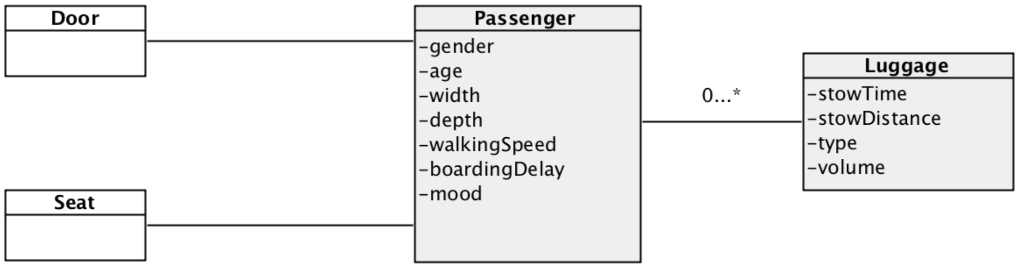

Figure 3.9.: UML of *Passenger* and *Luggage*.

The modeling of the *Luggage* is implemented with a high level of detail, since current bottlenecks in daily operation result from a higher amount of carried HL. Each agent can be assigned multiple luggage items where the number and type influence the walking speed. Based on three different luggage types (small, medium and large bag) with associated volumes, the required stowing time and distance from the seat where the luggage is stowed is chosen. See Appendix A.1 for the used empirical data.

The two-dimensional oval agent body shape is approximated with a rectangular shape and transferred to the grid of vertices, as depicted in Figure 3.10. The type of the affected vertices is set to *agent* which also acts as a temporary obstacle to other agents. The vertices around the body show higher cost to mimic the agents personal space. The structure of the grid allows the agent to rotate in 45-degree steps. The associated luggage items are not represented on the grid.

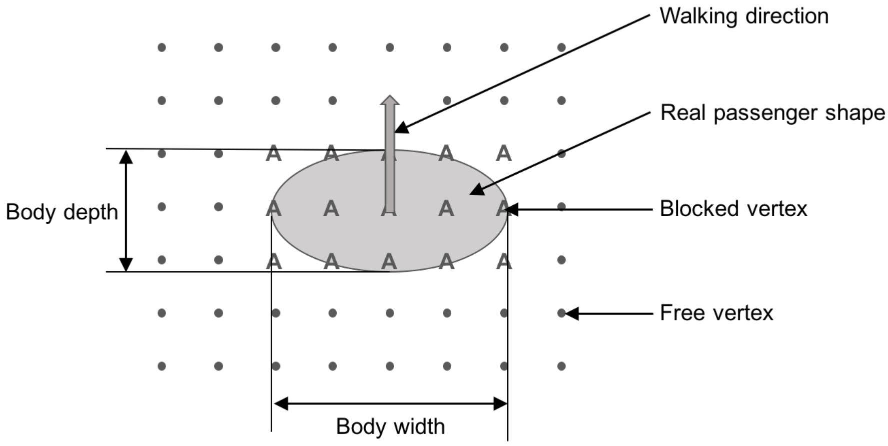

Figure 3.10.: Grid based representation of *Passenger*.

3.2.1.3. Behavior

The behavior of the acting agents summarizes all actions or tasks which can be executed during the time until the final target is reached and more precisely how each situation is handled. The decision which behavior is adopted in a certain situation is done during simulation runtime. The modeling of the agent behavior distinguishes between the following options, with this set being extendible:

- Step forward
- Collision
    - Wait
    - Pass
- Wait for row clearance
- Stow luggage

From a cabin layout perspective, the collisions and luggage stowing are a representation of aisle interferences and row interference is modeled by *wait for row clearance*.

The default behavior of the agent is to follow a certain path until its seat is reached. To determine the path, more precisely the optimal shortest path, a pathfinding algorithm is required. According to Cormen et al. [144], a pathfinding algorithm uses a general weighted directed graph $G = (V, E)$ with a weight function $w(v_0, v_k)$ by starting the search at one vertex and exploring adjacent vertices until the goal vertex is reached. This is provided by the mathematical cabin representation consisting of the grid of vertices, their distances and associated cost values. The weight $w(p)$ of the path $p = \langle v_0, v_1, \ldots, v_k \rangle$ is the sum of the weights of its constituent edges:

$$w(p) = \sum_{i=1}^{k} w(v_{i-1}, v_i) \tag{3.12}$$

and the smallest path weight $\delta(v_0, v_k)$ from v_0 to v_k is defined by:

$$\delta(v_0, v_k) = \begin{cases} min\{w(p) : v_0 \rightsquigarrow v_k\} & \text{if there is a path from } v_0 \text{ to } v_k \\ \infty & \text{otherwise} \end{cases} \tag{3.13}$$

The shortest path from vertex v_0 to v_k is then defined as any path p with the weight $w(p) = \delta(v_0, v_k)$.

In literature, various pathfinding algorithms are documented [144, 148, 149], such as the Breadth First Search, Dijkstra's algorithm and A* algorithm, which differ in their performance and ability to find the optimal shortest path. As depicted in Figure 3.11a, the Breadth First Search explores the graph equally. Dijkstra's algorithm instead favors lower cost paths instead of exploring all possible paths equally and is guaranteed to find a shortest path from the starting point to the goal (see Figure 3.11b). From a starting point, the algorithm repeatedly examines the closest not-yet-examined vertex, adding its vertices to the set of vertices to be examined. It expands outwards from the starting point until it reaches the target. The A* algorithm is a modification of Dijkstra's algorithm that is optimized for a single destination, where the Dijkstra's algorithm can find paths to all locations, the A* algorithm finds paths to one location (see Figure 3.11c). Furthermore, it prioritizes paths that seem to be leading closer to the target. Dijkstra's and A* strategically eliminate paths to achieve lower time complexities [144, 149]. Since the A* algorithm is well-documented in literature, widespread in game development and shows performance advantages compared to other algorithms, it is applied for the simulation framework here.

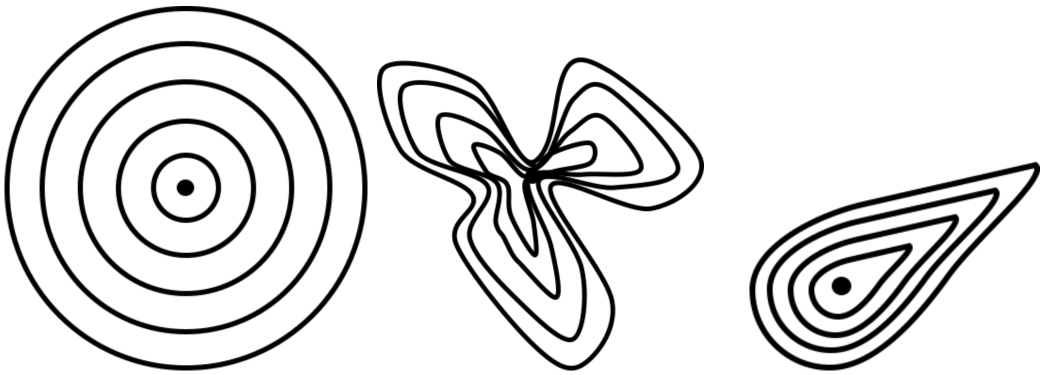

(a) Breadth First Search (b) Dijkstra's algorithm (c) A* algorithm

Figure 3.11.: Pathfinding algorithms (based on [149]).

The A* algorithm [150] uses both the actual distance from the start and the estimated distance to the target employing heuristics to guide its search resulting in better performance. If the algorithm plans the next step, all neighbor vertices are assessed except for the vertices which are already part of the current path, as depicted in Figure 3.12. All paths identified from the neighbor vertices that lead to the target are built up and each partial path is ranked in consideration of Equation 3.14:

$$f(v_0, v_k) = g(v_0, v_n) + h(v_n, v_k) + c(v_n) \tag{3.14}$$

where $g(v_0, v_n)$ are the known movement cost to traverse from v_0 to v_n, $h(v_n, v_k)$ is the estimate of remaining distance to the target from the neighbor vertex v_n following a certain heuristic, $c(v_n)$ are individual additional costs assigned to the vertex v_n, and $f(v_0, v_k)$ is the estimated final cost of path from the start v_0 to the current position v_m through v_n to the target v_k. The assessment of the final path cost $f(v_0, v_k)$ is repeated for all relevant neighbor vertices until the neighbor vortex $v_{n,i}$ with lowest path cost $f(v_0, v_k)$ is chosen as part of the path (see Figure 3.12). This procedure is repeated until the target vertex (v_k) is reached. Revising the steps from the goal (v_k) to the start (v_0) produces the optimal shortest path p with the weight $w(p) = \delta(v_0, v_k)$.

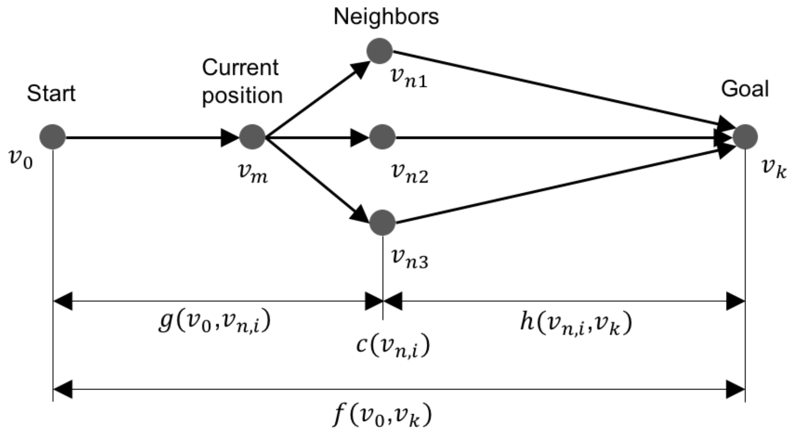

Figure 3.12.: A* algorithm.

As proven by Hart et al. [150], the A* is guaranteed to find a path from the start to the goal, if a path exists. Furthermore, the algorithm makes the most efficient use of the heuristic, which means that there is no search algorithm that needs fewer vertices to find the optimal path using the same heuristic function.

Classical heuristics functions[1] $h(v_n, v_k)$ are Manhattan, diagonal, or Euclidean distance calculations, and represent a minimum possible distance between the current vortex v_n and the goal v_k. The Euclidean heuristic function given in Equation 3.15 is used to determine the remaining distance.

$$h(v_n, v_k) = \sqrt{(v_{k,x} - v_{n,x})^2 + (v_{k,y} - v_{n,y})^2} \tag{3.15}$$

Step forward

To allow the agent to step forward, the stored shortest optimal path p with $w(p) = \delta(v_0, v_k)$ is split into partial paths $p(v_m, v_n)$ of the length of a single step, where v_m and v_n denote the starting and ending vertex of this specific step (see Figure 3.13a). The step length is determined based on the current walking speed of the agent (Figure 3.13b). From the ending vertex v_n of the step, the neighbor vertices representing the agent body dimensions as well as the vertices between the current v_m and desired position v_n are checked to see if their type is *void*. Subsequently, the area is blocked by the agent and the previously occupied vertices around the starting vertex v_m are set to type *void* (Figure 3.13c). If one

[1]See [149] for more information about classical heuristics functions.

of the vertices are either of type *obstacle* or *agent* (not being the moving agent itself), the step cannot be conducted. In this case, a collision occurs.

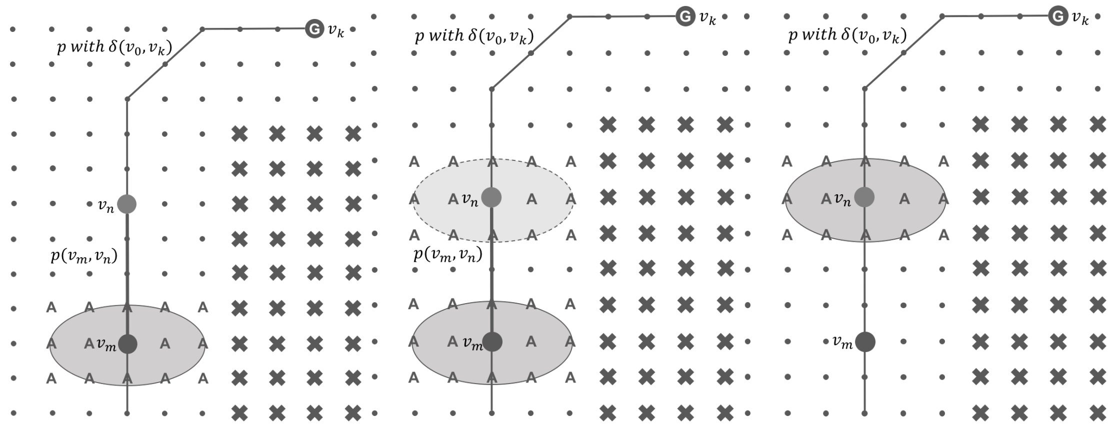

(a) Determines agents step length. (b) Blocks vertices around new position. (c) Removes blocking status of old position.

Figure 3.13.: Agent moves one step forward.

Collision - wait or pass

If during the execution of a next step, one of the required vertices representing the agents body dimensions are either from type *obstacle* or *agent* a collision occurs. Obstacles, such as cabin monuments, are usually objects, which do not move at simulation runtime, while agents occupy specific areas only for a limited amount of time. This can happen in the following cases:

- The preceding agent walks slower than the following agent
- The preceding agent queues up behind another agent
- The preceding agent stows luggage

The agent can distinguish between two behavior patterns in the case of a collision: waiting or passing. The environment of an aircraft cabin has a limited amount of space and so the passing of a preceding agent may not be reasonable in every case, such as if the agent walks slower than the preceding agent or if agents queue behind other agents. Collision-strategies are introduced to model various personalities of agents, which resort to a different basis for decision-making. Based on pre-defined agent characteristics a related collision-strategy can be chosen.

Wait: Even with the decision to wait behind an obstacle or agent, the stored shortest optimal path p is always followed. In very short iterations the vertices related to the next step are checked for their status. This procedure is repeated until the required vertices allowed to perform the next step are reached. Hence, the following of a slower agent through the aisle is feasible with short discontinuities in the average walking speed due to the waiting procedure.

Pass: The second option in the case of a collision is to pass the blocking agent or cabin monument, which requires recalculation of the initial shortest optimal path p. To reduce the required calculation time, a local path repair strategy is applied [149] (see Figure 3.14). Given the current vertex v_m where the collision occurs, the remainder of the path is given by $p(v_m, v_k)$. A new path segment $p_{splice}(v_m, v_n)$ is computed, where v_n is a vertex between the current vertex v_m and the target vertex v_k. From the remainder of the initial path $p(v_m, v_k)$, the path segment $p(v_m, v_n)$ is removed and the new path segment $p_{splice}(v_m, v_n)$ is spliced in. The decision about the fitness of the new path segment $p_{splice}(v_m, v_n)$ is based on the weight comparison of $w_{splice}(p_{splice}(v_m, v_n))$ and $w(p(v_m, v_n))$. Different decision boundaries $m > 1$ can be set for each agent individually.

$$w_{splice} \begin{cases} \leq m \cdot w & \text{pass} \\ > m \cdot w & \text{wait} \end{cases}$$

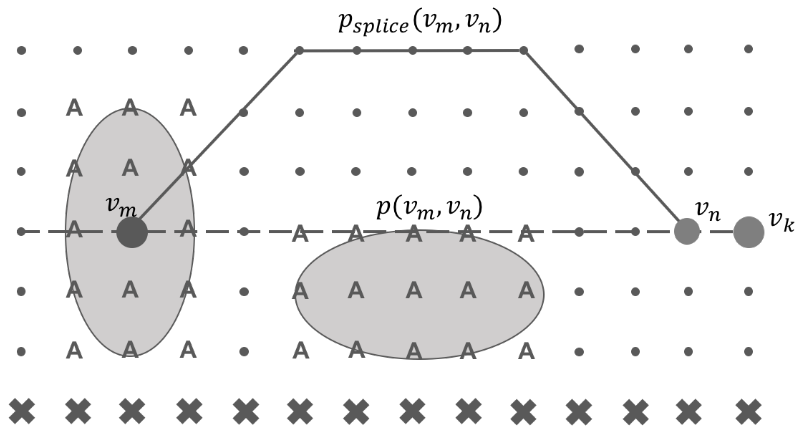

Figure 3.14.: Local path repair strategy during the passing of a waiting agent.

Stow luggage

As soon as the agent approaches the ending vertex v_k of the path p (its assigned seat) optional carried luggage has to be stowed, either in the overhead bins or under the seat. The position of the stowing process is determined by a pre-defined value for the remaining path length $p(v_n, v_k)$, where v_n denotes the current vertex and v_k the final target vertex. At the vertex v_n, available *LuggageStorage* elements are checked for their remaining storage volume. Based on type and volume of the carried luggage items, a suitable storage space is chosen. In the course of the required space calculation, the bulkiness factor of the luggage items is considered. During the stowing process the agent position remains fixed. The time required to stow the items is based on their type and is adjusted based on the current filling degree of the *LuggageStorage* element. If the remaining volume of the available

LuggageStorage elements reaches its limit, the remaining luggage items are stored in any of the storages with available space and the agent's stowing time will be increased by a time penalty. After the stowing process is completed, the remaining path $p(v_n, v_k)$ is followed until the goal seat vertex v_k is reached.

Row interference

In contemporary aircraft cabins, not every seat has direct access to the aisle, hence agents cannot reach their assigned seat with ease in each case, since other already seating agents might block them (see Figure 2.4 in Section 2.2.3). As shown in Figure 3.15, after reaching a vertex v_n with the distance $l_{sp} = d(x) = |v_k - v_n|$ in x direction, the seats which are closer to the aisle are checked for their occupancy status. The distance of the agent in this situation is equivalent to the seat pitch (l_{sp}) which is just before the agent enters the part of the row where its seat is located. Based on the number of identified agents seated closer to the aisle, the required time for clearing the row and seating is determined. The approaching agent blocks the aisle partly during this procedure.

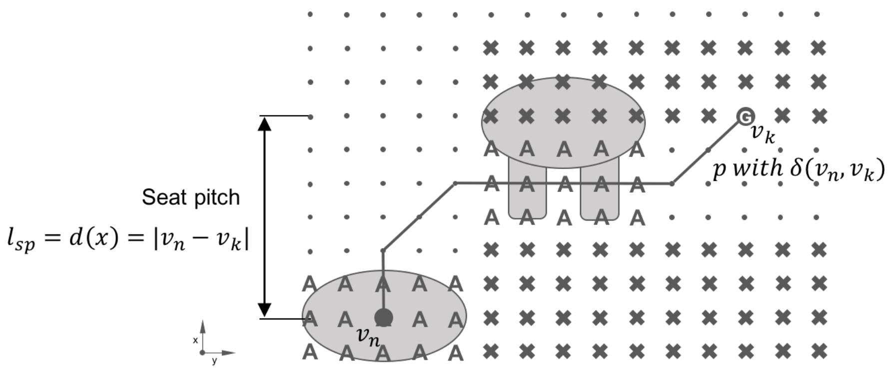

Figure 3.15.: Row interference with one agent detected.

3.2.2. Framework architecture and implementation

The general workflow of the simulation is based on four steps. The detailed cabin layout is generated based on the CTLR and the basic fuselage dimensions using design heuristics. Cabin monuments and seats are positioned and sized under consideration of current rules and regulations. In the second step, the virtual passengers are generated, with their anthropometrics and assigned seat. In order to retrieve results which are not driven by a specific set of agents and their characteristics, functionalities to conduct Monte Carlo experiments are required. Therefore, agent anthropometrics and properties, such as walking speed and body dimensions, can be distributed among the agents using probability functions before each simulation run. Since the input data set for the agent properties only consist of minimum, maximum and mean values, a normal distribution is used to represent real-valued random input variables. After cabin layout and agents are created, the initial pathfinding is conducted to search for the most cost efficient path for each agent. The agents interact with each other and the environment during the simulation. The current path is updated based on their implemented behavior and the simulation terminates after all agents reach their assigned seats.

The set of problems to investigate aircraft cabin layouts with a couple hundred passengers requires the execution of the single path finding algorithm for all agents, which demands a performance driven architecture. The pathfinding between a unique start and goal has to be conducted separately for each agent, even if the environment is equal for each agent. A multi-threading architecture, which is supported by contemporary operating systems and programming languages, allows the processor to execute multiple threads concurrently aiming to increase its utilization. The implementation of software architecture allows the initial pathfinding and each path recalculation concurrently, raising the maximum possible number of simultaneously acting agents. During the execution of the simulation, the multi-threading software architecture underlines the autonomy of each agent following the path to the assigned seat.[2]

3.3. Aircraft level assessment and mission performance

Pre-conceptual aircraft studies produce a set of TLRs which are binding for the forthcoming design phases. In general, the product design process is broken down into conceptual design, preliminary design and detailed design [151–153].

The conceptual design phase is characterized by an iterative procedure to identify the most promising overall aircraft design concept. The objective is to find a design which is technically and economically viable. Furthermore, the technical risks and cost of possible failure are closely examined. Even if only a marginal portion of the life-cycle cost is spent, irrevocable decisions on the aircraft design are taken which makes it difficult and costly to modify later on. Therefore, an understanding of the detailed design, manufacturing process, operation and sensitivity of the design is essential. The applied design tools are semi-empirical and low to medium fidelity methods in trade-off studies and basic optimizations. The preliminary design phase targets to determine subsystem architecture, making component trade-offs and optimizations. During the detailed design phase, the detailed component geometry is specified and the manufacturing process is planned. Subsequently, the actual components will be built, installed and tested [151–153].

To evaluate novel ground operational concepts holistically, an aircraft level assessment covering en-route performance in terms of fuel burn and emission is necessary. Seitz [154] and recently Briggs [155] provide an overview of available aircraft conceptual design frameworks. Here, the Aircraft Preliminary Design (APD) commercial software package by Pacelab [156] is applied. It supports the modeling, sizing, analysis and optimization of new and derivative aircraft in the conceptual and preliminary design phases. The design process is based on handbook methods [151, 152, 157] in an iterative process.

[2] The developed passenger flow simulation module "PAXelerate" [1] builds upon the OpenCDT which is framework for conceptual aircraft design using Java Eclipse.

Therefore, cascading effects are covered and all parts and systems are appropriately sized. A mission analysis tool evaluates mission specific parameters, such as block fuel and time, and determines a flight profile including step climbs, when practical. This can be applied for design as well as off-design missions. Here, the focus is on the methods for the fuselage and cabin interior mass estimation since they are influenced by the reviewed concepts in Section 2.3.

3.3.1. Aircraft fuselage weight estimation

The fuselage mass W_{use} is a deceive factor for the resulting aircraft performance. According to the Luftfahrttechnische Handbuch (LTH) [158], the fuselage mass is calculated with Equation 3.16 using only geometrical parameters, where l_{fuse} is the fuselage length and d_{fuse} is the fuselage diameter.

$$W_{fuse} = 12.7 \cdot (l_{fuse} \cdot d_{fuse})^{1.298} \cdot \left\{ 1 - \left(-0.008 \cdot \left(\frac{l_{fuse}}{d_{fuse}}\right)^2 + 0.1664 \cdot \left(\frac{l_{fuse}}{d_{fuse}}\right) - 0.8501 \right) \right\} \tag{3.16}$$

3.3.2. Cabin furnishing weight estimation

The implemented aircraft design process uses empirical correlation [152] based on the zero fuel weight W_{zf} to determine the cabin furnishing weight W_{furn} covering the seats, wall and floor coverings, cabin monuments and overhead bins. To account for changes in the furnishing weight due to novel concepts, the delta weight (see Equation 3.17) has to be determined which is then translated into OWE changes.

$$W_{furn} = 0.196 \cdot {W_{zf}}^{0.91} \tag{3.17}$$

The baseline weight for doors, seats or storage compartments can be calculated as follows. An assessment of current seat data shows an average seat weight for economy class seats of 9.2 kg (20.3 lb) and for business class seats of 61.7 kg (136.0 lb) [159].

The weight of additional doors W_{door} depends on the maximum operation pressure differential of the relevant fuselage section Δp, the height h_{door} and width w_{door} of the door, and the wetted area of the door A_{door} [152]. For emergency exits no reinforcement of the frames are required.

$$W_{door} = 44.2 \cdot \sqrt{\Delta p} \cdot w_{door} \cdot h_{door} + 22.3 \cdot \sqrt{A_{door}} \tag{3.18}$$

3.3.3. Fuel burn trade factors

The design studies undertaken are derived from a state-of-the-art SA and TA aircraft type. Their aim is to show trade-offs between the cabin layout configurations investigated, instead of providing optimized design studies. Using trade factors for deviations in OWE, fuselage length and width account for changes in the cabin configurations in terms of fuel burn. The trade factors are derived for both design and off-design missions.

3.4. Turnaround simulation

The following section explains the approach undertaken to model the turnaround operations. For each turnaround activity the execution time is calculated separately and dependencies in terms of concurrent or consecutive execution are incorporated in a second step. Therefore, aircraft related input data about the number of interfaces and the amount of goods which have to be exchanged is used as illustrated in Figure 3.16. The structure of the underlying data model follows the EMOF [141] standard model-driven engineering provided by OMG, as highlighted in Section 3.2.1.1. The turnaround module covers passenger boarding and disembarking, cargo loading and unloading, cabin services such as cleaning and catering, replenishment with fuel and water, waste water service and ground power supply. Air conditioning and air starter procedures are not included. The flexibility to simulate further parallelization or shortening processes is ensured, as it is proposed by novel concepts (see Section 2.3.2).

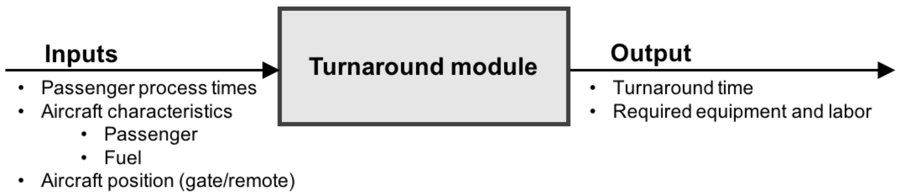

Figure 3.16.: Overview of the in- and output of the turnaround module.

To evaluate the impact of modifications to passenger processes, it is necessary to integrate the gained results into a holistic turnaround assessment. Based on the requirements in terms of resources and process times, an evaluation of aircraft operating cost level becomes feasible.

3.4.1. Input parameters definition

For the turnaround assessment, basic aircraft related input data about the number of interfaces, such as doors or fuel connectors, and the amount of goods which have to be exchanged is required. Using data from the detailed cabin layout generated during the passenger flow assessment allows for the derivation of the number of passenger, lavatories and galley space.

For each passenger, a volume of potable water $v_{water} = 0.34 \frac{l}{PAX}$ [119] has to be replenished and a volume of $v_{waste} = 0.09 \frac{l}{PAX}$ [119] must be disposed. For short-haul operations, the required number of galley trolleys for each passenger is $v_{trol} = 0.05 \frac{trolley}{PAX}$. The number of bags n_{bag} to be unloaded and loaded can be estimated with Equation 3.19, where each bag is assumed to weigh $w_{bag} = 13.6kg$ [119]. The passengers bags are either handled as bulk cargo or are packed into ULD.

$$n_{bag} = 0.4296 \cdot n_{pax} + 19.05 \tag{3.19}$$

3.4.2. Process modeling

The approach to model each turnaround process is based on empirical data of turnaround operations [43, 114, 119]. In general, each process time t_{proc}, such as refueling or catering, consists of a GSE positioning time t_{pos}, the process execution time t_{ex} and the removal time t_{rem} for the GSE. Setup and preparation times are not accounted for, since they are highly dependent on the airport layout. In some cases, an equipment repositioning time t_{repos} must also be accounted for. In the following, each contributing term of Equation 3.20 is examined in more detail.

$$t_{proc} = t_{pos} + t_{ex} + t_{rem} + t_{repos} \tag{3.20}$$

3.4.2.1. Positioning and removal of ground handling equipment

The time required for positioning t_{pos} and removing GSE t_{rem} is dependent on the type of equipment and the position of the interface on the aircraft. Since the exact dimensions and locations of aircraft interfaces are often unknown during the conceptual aircraft design phases, empirical data were consulted [114, 119]. A median value is determined for each positioning and removal process based on empirical data (see Appendix A.2). In case an equipment repositioning becomes necessary, such as to serve a forward and aft galley with one catering truck, a repositioning time t_{repos} covering the removal, vehicle movement[3] and positioning process, will be accounted for.

$$t_{repos} = t_{rem} + t_{mov} + t_{pos} \tag{3.21}$$

[3] The average movement time t_{mov} is assumed to be 24 s which corresponds to driving 100 m (328 ft) with 15 kph (9.3 mph)

3.4.2.2. Process execution time

The individual process times t_{ex} are calculated using a specific flow rate r_{rate} for the exchanged amount of goods n_{good}, such as containers or potable water. Specific amounts to be exchanged for the inbound and outbound flight are determined for processes which distinguish between loading and unloading procedures.

$$t_{ex} = \frac{n_{good}}{r_{rate}} \tag{3.22}$$

Boarding and disembarking

The passenger boarding and disembarking process time depends on various factors, such as the number of passengers and doors used, as well as the seating layout and hand luggage distribution. To capture these effects holistically, the process time $t_{ex,pax,in}$ is determined using the agent-based simulation framework described in Section 3.2. For passenger egress time $t_{ex,pax,out}$ Equation 3.23 by Fuchte [12] is incorporated. The values for k_1 and k_2 are listed in Table 3.1.

$$t_{ex,pax,out} = k_1 \cdot n_{pax} + k_2 \tag{3.23}$$

Table 3.1.: Values for k_1 and k_2 using disembarking approach by Fuchte [12].

Configuration	Seat Abrest	Door	k_1	k_2
Single-aisle	6	L1	0.033	3.272
		L2	0.032	2.888
		L1 + L4	0.022	2.160
Twin-aisle	6	L1	0.023	1.316
		L2	0.019	1.455
		L1 + L4	0.015	0.868
	7	L1	0.024	1.265
		L2	0.020	1.394
		L1 + L4	0.016	0.835
	8	L1	0.024	1.162
		L2	0.021	1.283
		L1 + L4	0.016	0.767

Catering

During the catering operation, galley trolleys with food and beverages are switched between the aircraft and the catering vehicle. In general two types of galley trolleys are distinguished: half- and full-size trolleys. If galleys are placed at both ends of the aircraft, either two catering vehicles are required or a repositioning is necessary. The execution time is given by the trolley exchange rate r_{cat} and the number of full-sized trolleys n_{trol} to be unloaded and loaded. An average value of $r_{cat,med} = 1.2\frac{trolley}{min}$ is used for loading and unloading [114], since these tasks are often done simultaneously.

$$t_{ex,cat} = \frac{n_{trol}}{r_{cat}} \tag{3.24}$$

Cleaning

The cabin cleaning is tailored to airline specific requirements. Often only garbage is removed and the overall cabin condition is checked during a transit stop at a non-hub airport. At the home base, the seats and tray tables are cleaned as well as the carpet. Furthermore, the surfaces in galleys and lavatories are cleaned [112]. The required cleaning time $t_{ex,clean}$ depends on the aircraft size in terms of passenger seats n_{seat}, galley size as a measure of number of trolleys $n_{gal,trol}$ and number of lavatories n_{av}, and the number of employed cleaners n_{clean}. For each cleaning task, average durations are assumed.[4]

$$t_{ex,clean} = \frac{n_{seat} \cdot (t_{seat,sur} + t_{seat,vac}) + n_{gal,trol} \cdot t_{gal,trol} + n_{lav} \cdot t_{lav}}{n_{clean}} \tag{3.25}$$

Cargo

The cargo unloading and loading covers the handling of bulk cargo, which are individual passenger bags or other goods, and the exchange of ULD. ULD are standardized containers fitting into different aircraft fuselage geometries. Access to the cargo compartment is predominantly given by one door in front of and behind the wing box [54]. The handling of ULD is more automated resulting in higher flow rates. The average rate for bulk cargo is $r_{bulk} = 8\frac{kg}{s}$ and for ULD depending on their type, where for the common LD3 type ULDs the rate is $r_{uld} = 0.53\frac{ULD}{min}$ [112]. The cargo process time for unloading and loading accounts in each case for $t_{ex,cargo}$ where the longer process between bulk and ULD is decisive, since they can be performed concurrently. Below the differentiation between loading and unloading rates is omitted.

$$t_{ex,cargo} = max(t_{ex,cargo,bulk} = \frac{n_{bag} \cdot w_{bag}}{r_{bulk}}; t_{ex,cargo,uld} = \frac{n_{uld}}{r_{uld}}) \tag{3.26}$$

Refueling

The refueling time $t_{ex,fuel}$ is calculated with Equation 3.27, taking into account an exponential decrease in fuel flow due to an increasing static pressure in the tank as well as an increasing drag caused by the closing of valves connecting the installed tanks [119, 160].

[4] The individual task execution times account for: seat surface cleaning $t_{seat,sur} = 10s$, carpet vacuum $t_{seat,vac} = 8s$, galley cleaning per trolley $t_{gal,trol} = 16s$ and for each lavatory $t_{av} = 240s$.

$$t_{ex,fuel} = \frac{1}{\alpha} \cdot \ln\left(1 + \frac{V_{fuel} \cdot \alpha}{r_{fuel,0}}\right) \tag{3.27}$$

Where α denotes the alpha factor as a value for resistance of the fuel tank, V_{fuel} is the volume of fuel being replenished $[l]$ and $r_{fuel,0}$ is the fuel flow rate $[\frac{l}{min}]$ at $t = 0$. The alpha factor can be determined iteratively based on OEM data.

Ground power

After the engines and APU are turned off, additional power is required for lights and air-conditioning. The ground power supply is often integrated into the boarding bridge at a gate position. At remote positions, a ground power unit (GPU) with a diesel generator is used to provide the required power. Since the power supply is connected during the whole turnaround event, the $t_{ex,power}$ equals the turnaround time t_{ta}.

Potable water and waste water

The potable water service replenishes the tanks with fresh drinking water V_{water} with a preservation admixture. This procedure is performed after each long-haul flight and less often for regional and short-haul operations. The average pumping rate[5] amounts to $r_{water} = 65\frac{l}{min}$ [114, 119] and the potable water execution time $t_{ex,water}$ is given by:

$$t_{ex,water} = \frac{V_{water}}{r_{water}} \tag{3.28}$$

The waste water service includes the pump down of waste water V_{waste} and the supply of disinfectant flushing water situated in tanks in the aft fuselage. This procedure is performed after each long-haul flight and less often for regional and short-haul operations. The average pumping rate is $r_{waste} = 38\frac{l}{min}$ [114, 119] and the waste water execution time $t_{ex,waste}$ is given by:

$$t_{ex,waste} = \frac{V_{waste}}{r_{waste}} \tag{3.29}$$

Pushback

A pushback of nose-in parked aircraft is required at most airport parking positions. Therefore, a towing truck is connected to the nose landing gear and the aircraft is pushed backwards out of the parking position. The pushback process is not part of the turnaround, since it happens after the blocks are removed (off-block). The pushback time is assumed to be an average of $t_{ex,pb} = 120s$.

[5]Here the median of the rates r_{water} stated by Sanchez [119] $67\frac{l}{min}$ and Bevilacqua et al. [114] $63\frac{l}{min}$ is taken.

3.4.3. Identification of critical processes

The determination of the total turnaround time t_{ta} follows the CPM method. Based on the execution time of all involved activities and their dependencies, the critical activities along the longest path are determined. The critical path is the sequence of activities $t_{proc,crit}$ with the shortest time possible to complete the turnaround (see Equation 3.30). Any disruption of an activity on the critical path directly impacts the total turnaround time. A shortening of the critical path becomes feasible through increased parallelization or additional resources [99].

$$t_{ta} = \sum_{i=1}^{k} t_{proc,crit,i} \tag{3.30}$$

Figure 3.17 illustrates the critical paths which are likely to appear based on process restrictions. The operations start with the positioning of the power connector and end with its removal. The critical path often consists of the passenger and aircraft cabin activities, and in several circumstances the fueling operation may become the critical path. This results from requirements stated in EU-OPS 1.305 (FAR 121.570) [57, 70] where the aircraft is refueled after the last passenger has left the aircraft. Furthermore, processes inside the aircraft cabin, such as the exchange of trolleys and cleaning of cabin interior, are performed when passengers are not present. Other activities, such as unloading, loading and aircraft servicing, could be performed without influence from other processes (see Section 2.2.2).

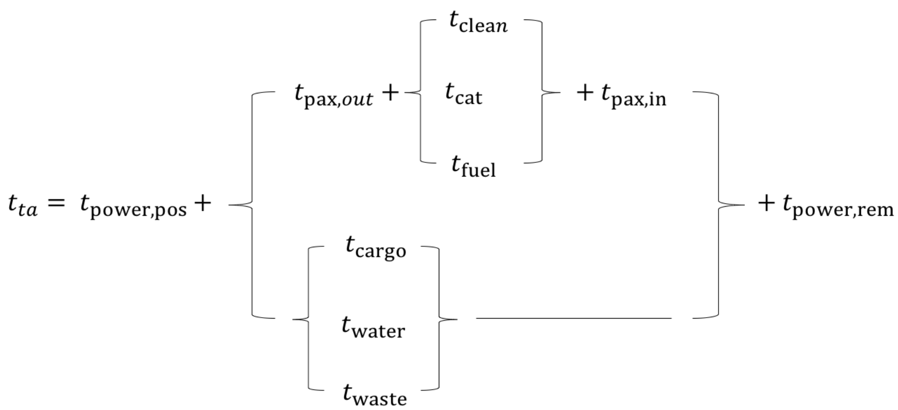

Figure 3.17.: Possible critical paths during turnaround operation.

3.5. Aircraft operating cost

The total operating cost (TOC) of an airline can be divided into DOC and indirect operating cost (IOC). The IOC are non-aircraft related costs which be subdivided into: burden costs and administration, estate and ground equipment, passenger and freight. The passenger cost category includes all cost elements associated with the transportation and handling of passengers, such as catering, baggage handling, ticketing, sales, marketing and distribution. Respectively, the freight category includes all expenditures concerning freight transportation. In addition, the cost for maintaining and depreciating estate and airline ground equipment are comprised in the IOC [161]. The DOC are aircraft related expenditures, therefore changes in the aircraft conceptual design will have a direct impact on their total value.

This section highlights the characteristics of the applied DOC estimation model. First, characteristics of the individual cost elements attached to cash operating cost (COC), COO and additional operation cost (AOC) are introduced, then the main focus is on the activity-based ground handling cost component. Concluding properties of life cycle cost estimations are explained.

3.5.1. Direct operating cost estimation

DOC are defined as expenditures allocated to specific items, and therefore, vary according to the type of aircraft used and the rate of utilization. They cover COC, COO and AOC. The DOC are in general expressed as cost per trip $[T]$, block hour $[BH]$ or seat kilometer/nautical mile $[\frac{SK}{SM}]$.

$$C_{DOC} = C_{COC} + C_{COO} + C_{AOC} \tag{3.31}$$

The cost estimation approach applied is mainly based on the model by Wesseler [162]. As depicted in Figure 3.18, the model processes the aircraft flight and ground operation performance to assess different configurations in a holistic way.

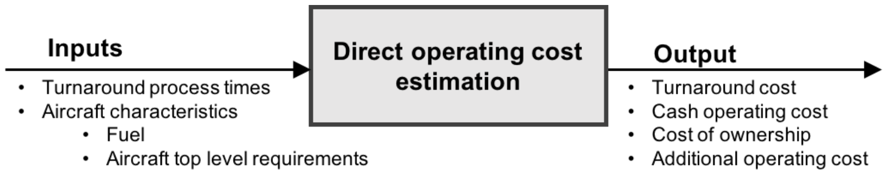

Figure 3.18.: In- and output for the direct operating cost estimation.

Cost of ownership

The COO covers depreciation, interest and hull insurance costs, which are mainly based on the aircraft market value and the annual aircraft utilization (see Equation 3.32). The aircraft market value is determined using parametric cost function based on Productivity Index for Commercial Aircraft (PIC). The PIC uses aircraft parameters known during the conceptual design including aircraft's range, speed, cabin volume, number of passengers and take-off field length (TOFL) [163, 164]. The depreciation cost C_{dep} is allocated to the initial cost of the investment over a period of time using a straight line method to a residual value. Interest costs C_{int} relate to the initial capital investment for the procurement of an aircraft. The insurance cost C_{ins} comprises aircraft hull insurance, war and political risk, deductible insurance and third party liability insurance [162].

$$C_{COO} = C_{dep} + C_{int} + C_{ins} \tag{3.32}$$

The aircraft utilization depends mainly on the operator's business model and the average flown stage length. Based on the data of Mirza [27] illustrated in Figure 3.19, a correlation between the turnaround time t_{ta} and flights per year n_{flight} is derived for three stage lengths. The values for k_1 and k_2 are listed in Table 3.2. This allows to account for the influence of improved turnaround operations on COO level.

$$n_{flight} = k_1 \cdot t_{ta} + k_2 \tag{3.33}$$

Table 3.2.: Aircraft utilization: values for k_1 and k_2.

Stage Length		k_1	k_2	R^2
500nm	926km	-18.270	3,099	0.994
1,500nm	2,778km	-4.958	1,374	0.952
2,827nm	5,236km	-1.050	788	0.998

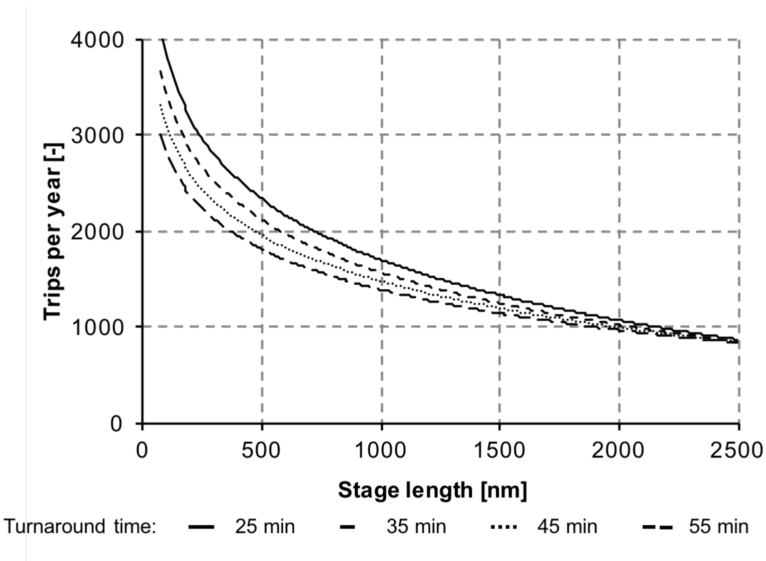

Figure 3.19.: Effects of turnaround time variations on aircraft utilization [27].

Cash operating cost

The COC sums up expenditures for fuel, crew, maintenance, airport and air service provider (ASP) charges. The fuel costs C_{fuel} are the product of mission fuel and fuel price. The principal crew cost model C_{crew} covers expenditures for flight and cabin crew.

It is based the Association of European Airlines (AEA) methodology where the crews hourly rate is a function of aircraft MTOW and number of passengers [165, 166]. The ASP charges C_{ASP} are levied for navigation services provided by every country being over-flown as a function of aircraft MTOW and distance flown [167].

$$C_{COC} = C_{fuel} + C_{crew} + C_{DMC} + C_{ap} + C_{ta} + C_{ASP} \tag{3.34}$$

The maintenance cost C_{DMC} cover expenditures for direct maintenance cost (DMC) which cover labor and material cost associated with airframe and engine. Indirect maintenance cost (IMC) for overhead, administration, tooling, testing equipment and quality control costs are not accounted for in the pursued approach. Operational dependencies, such as flight cycle and flight time are considered, as well as, aircraft aging effects and de-rating of the engines. The engine DMC are determined using parametric cost functions [168]. The airframe DMC covering airframe structure, systems and components, are calculated with an analogous costing method based on the Air Transport Association of America (ATA) chapter categorization [169]. In the context of cabin modifications, sensitivities of ATA chapter 25 - equipment/furnishing and 52 - doors are accounted for in DMC. Chapter 25 covers the flight and passenger compartment, galleys and lavatories, as well as emergency equipment and insulation. Passenger and cargo doors, emergency exits as well as service doors and hatches are summarized under ATA chapter 52 [170]. The typical DMC shares of these ATA chapters is summarized in Table 3.3.

Table 3.3.: DMC share of cost related to ATA 24 and 52 [162].

Aircraft Configuration	Cost Share [%]	
	ATA 25	ATA 52
Single-aisle	12.0	3.0
Twin-aisle	11.4	2.1

The airport charges C_{ap} cover expenditures for landing, passenger, terminal navaid, lighting, terminal user and service charges. These charges vary between airports, region and time, and should cover operating and maintenance costs, capital costs and the depreciation of airports [167]. The airport charges are determined using parametric cost functions based on MTOW and number of passenger [171]. A detailed activity-based ground handling charges model is highlighted in the following Section 3.5.2.

Additional operating cost

The AOC cover external noise, NO_x-emission charges and CO_2-emissions charges according to the European Emission Trading Scheme (ETS). The NO_x calculation is based on the pollutants of engine emissions defined by the ICAO engine data base [172]. The noise charge model uses aircraft specific standardized noise values for arrival and departure [173].

$$C_{AOC} = C_{noise} + C_{NO_x} + C_{CO_2} \tag{3.35}$$

Life cycle cost estimation

Operating expenses do not remain constant during the life cycle of an aircraft. During the first years, maintenance related costs are often minimal since warranty contracts cover most of the occurring incidents. Over a period of 12-15 years, aircraft aging and the detoriation of the engine performance can increase maintenance costs considerably. Considering the economic inflation over the aircraft life span allows for the determination of the associated DOC in each year [162].

3.5.2. Ground handling cost model

The ground handling charges cover expenditures for ramp activities such as push back, cargo handling, boarding bridge use and ground power supply. Plötner et al. [173] derived a parametric cost function for the ground handling cost based on the aircraft MTOW using the data of 425 different airports from the IATA Airport Charge Manual [167] (see Equation 3.36).

$$C_{ta} = 0.35 \cdot W_{MTOW} + 56 \tag{3.36}$$

Operational dependencies of the aircraft parking position and the influence of the turn-around time are not covered. Each airport may not cover all required processes to complete an aircraft turnaround and hence the data set might be incomplete. Furthermore, this generic approach does not account for changes in the aircraft dispatch operations, such as an increased assignment of resources or the abolishment of individual processes. Therefore, a sophisticated activity-based model based on Crönertz [112] is applied to determine the ground handling charges. The approach models cost related to a ground service provider based in Europe.

The ground handling cost C_{ta} are the sum of the individual cost for each activity. Here, processes covered are part of usual ground operation procedures and activities. Air conditioning and usage of air starters are neglected in the cost calculation as well as catering expenses, since the latter are airline-specific and belong to the IOC.

$$\begin{aligned} C_{ta} = \sum_{i=1}^{k} C_{act,i} = C_{pax} + C_{clean} + C_{cargo} + C_{fuel} + C_{power} + \\ C_{water} + C_{waste} + C_{pb} \end{aligned} \tag{3.37}$$

The individual process cost C_{act} for each activity are determined based on the used resources in terms of labor C_{labor}, equipment C_{equip} and supplies C_{sup}, and their specific cost unit rates c_{res}, number of used resources $n_{res,i}$ and operating times t_{act} (see Equation 3.39). The operating times are derived from the turnaround module described in Section 3.4. Setup times, other than the positioning and removal times, are neglected in the cost calculation, since they are highly dependent on the airport layout. The specific unit cost rates are based on the findings of Crönertz [112] (see Appendix B.1). In general, the type and size of equipment used is dependent on the aircraft type and transported goods.

$$C_{act} = C_{labor} + C_{equip} + C_{supplies} \tag{3.38}$$

$$C_{labor;equip} = \sum_{i=1}^{k} c_{res,i} \cdot n_{res,i} \cdot t_{act,i} \tag{3.39}$$

The labor working time can deviate from the activity duration t_{act}. During the potable and waste water service, a service truck and an employee are required for the whole process time. In contrast, the provision of passenger bridges and stairs, require a service employee only during the positioning and removal process.

Supplies cover a fixed cost for potable water, cleaning fluids and Diesel for the GPU. Furthermore, supplementary equipment and associated labor are accounted for as supply. In the case of operation on a remote aircraft position, necessary buses and their drivers fall under supplies. The same holds for additional tractors, drivers and dollies required for the cargo exchange. Based on the number of ULD and amount of bulk cargo, loading teams and loading equipment are composed. The cleaning expenditures are often fixed based on the number of passengers. An equation (3.40) for scheduled operations is derived based on the data from Crönertz [112][6].

$$C_{cleaning} = -0.0004 \cdot n_{pax}^2 + 0.5331 \cdot n_{pax} + 7.4735 \tag{3.40}$$

3.6. Framework application workflow

The framework presented here, it targets a holistic assessment of the aircraft operation during the conceptual design phase to address the challenges in current operation. It comprises: cabin design heuristics, passenger flow simulation, turnaround modeling and operational cost assessment. Mission performance analyses are integrated with trade factors produced with state-of-the-art aircraft design tools. Each module is based on existing approaches which are tailored to the specific requirements of this research. The developed framework addresses the Expected Contribution (EC) 1 of this thesis.

[6] Polynomial regression with $R^2 = 0.98978$.

As a central element connecting the passenger flow simulation and the turnaround module, a meta model following the EMOF [141] standard model-driven engineering provided by OMG is chosen. This addresses the EC 2. It contains the data structure, representation and allows to specify re-usable model elements. Thus, a model exchange with other frameworks following the EMOF specification is enabled.

Applying cabin design heuristics produce basic fuselage dimensions, such as the diameter and length, based on CTLR. They form the starting point for a detailed cabin layout generation to investigate the passenger processes. The passenger flow simulation module translates the cabin geometries into a grid-based representation where passenger can interact with the environment and one another. Applying distinct cost values to each node creates a pseudo three-dimensional cabin representation. The agent's behavioral repertoire comprises walking, waiting and passing as well as luggage stowing and dealing with row interferences. The passenger characteristics in terms of luggage, walking speed and collision strategy pattern allows for the representation of different traveler types. The focus is set on a detailed modeling of the HL storage process.

Changes of the fuselage dimensions and cabin interior, in terms of weight, are captured through fuel burn trade factors at the aircraft level. They are produced using the commercial conceptual aircraft design software APD by Pacelab [156] where the design process is based on handbook methods in an iterative process [151, 152, 157].

The turnaround simulation module processes the passenger process times and fuel burn factors together with data which is available during aircraft conceptual design to determine the turnaround times. For each turnaround activity the positioning, removal and execution time is estimated separately. Dependencies in terms of parallelization or consecutive execution are incorporated to identify the critical path covering all turnaround sub-processes.

Concluding with an operating cost assessment, the investigation of cabin configurations becomes feasible. The applied DOC module by Wesseler [162] covers COO, COC, AOC and take life cycle effects during the aircraft operating life span into account. Furthermore, the influence of improved ground operation and changing maintenance routines are captured. The focus is set on a detailed modeling of the ground handling cost to cover changes in the aircraft ground operation as introduced by Crönertz [112].

4. Framework benchmarking for contemporary single- and twin-aisle aircraft

The presented operational assessment framework consists of validated state-of-the-art modeling approaches for the aircraft design and operating cost estimation as well as newly developed approaches for the passenger flow simulation and turnaround process modeling. The data generated by these modules can influence the results of the subsequent modules. Thus, a benchmark of the entire framework is undertaken to ensure the validity of the generated results. Contemporary SA and TA aircraft are used as reference. In the following, the specific characteristics of the reference aircraft are highlighted and the results are compared to available data.

4.1. Single-aisle and twin-aisle reference cases

The choice of the reference aircraft as a benchmark was mainly driven by the availability of data and the targeted aircraft market. The framework is applied to determine the DOC of an Airbus A320neo for the SA segment and with an Airbus A330-300 reference for the TA category. Both configurations are low-wing aircraft with two wing-mounted engines. The A320neo is based on the A320 and entered service in 2016. Despite the maximum range of 3,500 nm (6,482 km), the predecessor A320 usually operates on short-to-medium haul routes where 49 % of the conducted flights were below 500 nm (926 km) in 2016 (see Figure 4.1) [9]. The average fuel consumption accounts for 0.0278 $\frac{kg}{PAXnm}$ taking a 1,000 nm (1,852 km) trip as datum. The cabin features 180 seats in a SA six-abreast layout [59]. The A330-300 targets the medium-to-long haul market, where the majority of flights are operated between 1,000 nm and 5,000 nm (1,852 km - 9,260 km) [9] with a fuel consumption of 0.0417 $\frac{kg}{PAXnm}$ on a 3,000 nm (5,556 km) trip. Airlines frequently select two-class cabin layouts with 36 business and 264 economy seats [174].

The required data was extracted from OEM publications, such as the Aircraft Characteristics for Airport Planning [59, 174] and from the CeRAS platform [175]. The aircraft top level requirements (ATLR) for the two reference cases is summarized in Table 4.1.

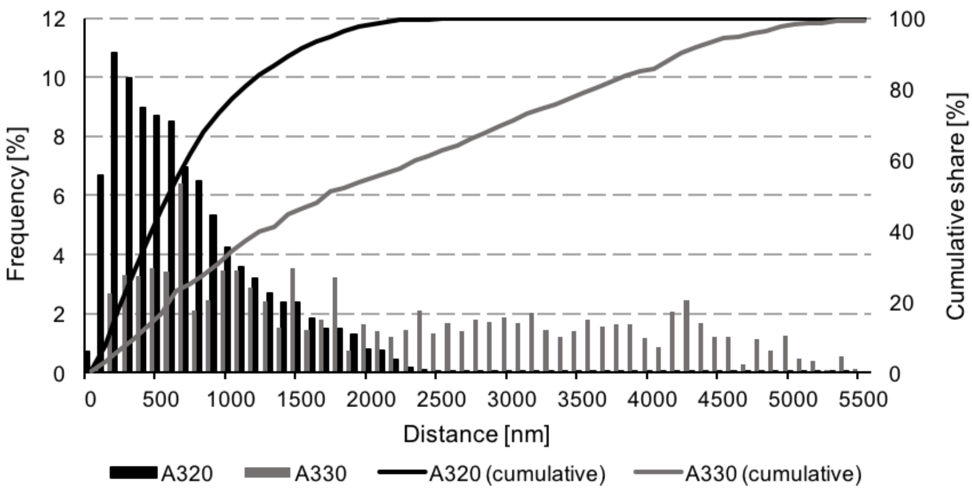

Figure 4.1.: Flown distances of the A320 family and A330 in 2016 based on OAG data [9].

Table 4.1.: Characteristics of the reference aircraft A320neo and A330-300 [59, 174, 175].

Parameter	A320neo	A330-300
Entry into service	2016	1994
Passengers	180	36/264
Design range	6,482 km (3,500 nm)	9,014 km (4,867 nm)
MTOW	85.3 t (188,054 lb)	217 t (478,403 lb)
Take-off field length	1,993 m (6,539 ft)	2,770 m (9,110 ft)
Wing span	35.80 m (117.45 ft)	58.00 m (190.29 ft)
Fuel burn - 1,000 nm	0.0298 kg/PAX/nm	0.0423 kg/PAX/nm
Fuselage width	3.95 m (13.0 ft)	5.64 m (18.5 ft)
Fuselage length	37.57 m (123.3 ft)	62.89 m (206.3 ft)
Cabin layout	single-class	two-class
Seat abreast	3-3	2-2-2/2-4-2
Seat pitch	0.76 m (30 in)	1.52 m/0.81 m (60 in/32 in)
Seat width	0.46 m (18 in)	0.53 m/0.46 m (21 in/18 in)
Aisle width	0.48 m (19 in)	0.53 m/0.48 m (21 in/19 in)

4.2. Cabin design heuristics

The overall dimensions and location of the cabin monuments are depicted in Figure 4.2. Applying the cabin design heuristics introduced in Section 3.1 generates basic fuselage dimensions without going into a detailed cabin design. Table 4.2 summarizes the results of the fuselage length and width calculations. The fuselage length is over-estimated with a deviation of 1.0 % in the case of the A320neo and 2.2 % for the A330-300 based on the available cabin data [59, 174]. The fuselage width shows a deviation of -2.7 % and -2.2 %.

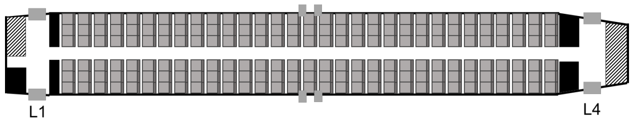

(a) A320neo

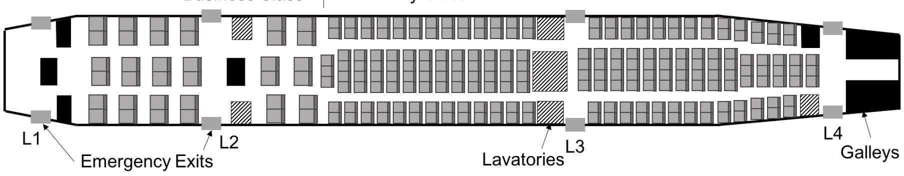

(b) A330

Figure 4.2.: Aircraft cabin layout configurations (based on [59, 174]).

Table 4.2.: Basic fuselage dimension applying cabin design heuristics.

Parameter	Aircraft	Dimension [m]		Deviation	
		OEM	Heuristic	[m]	[%]
Fuselage length	A320neo	37.57	37.98	-0.4	1.1
	A330-300	62.89	64.27	-1.4	2.1
Fuselage width	A320neo	3.95	3.85	0.1	-2.7
	A330-300	5.64	5.52	0.1	-2.2

4.3. Passenger egress and ingress simulation

The benchmarking of the developed passenger flow module is conducted using existing data from aircraft OEM, simulation results [12] and obtained empirical data for current aircraft [16, 132, 133]. The usage of empirical data is in general strongly dependent on the data quality in terms of type of tracked passenger characteristics, seasonal and region specific properties, airline business model, aircraft cabin layout as well as noteworthy boundary conditions.

A detailed model of the cabin layout is generated to analyze the passenger processes. The passengers have randomly assigned seats and do not follow any specific boarding scheme. They use the forward left door (L1), in case of the A320neo, and the left quarter door as a second door (L2), in case of the A330-300 to enter the cabin, mimicking the usage of a jet bridge. Passengers are assumed to be queuing up in front of the cabin door and then enter the cabin as soon as there is enough space. The passenger properties are randomly generated based on the distribution of physical characteristics to yield the boarding time in statistical sense. Figure 4.3 illustrates the distribution of the hip width, body depth and height, as well as walking speed. The share of female passengers accounts to 50 %. The input values are derived for European and US American passengers. The conducted studies assume a seat load factor (LF) of 100 % and a high HL degree. That means 20 %

of passengers have small luggage items, 30 % have a medium size laptop bag and 50 % have a trolley. The values for seat pitch, width and aisle width are based on contemporary cabin layouts [59, 139, 174] (see Table 4.1).

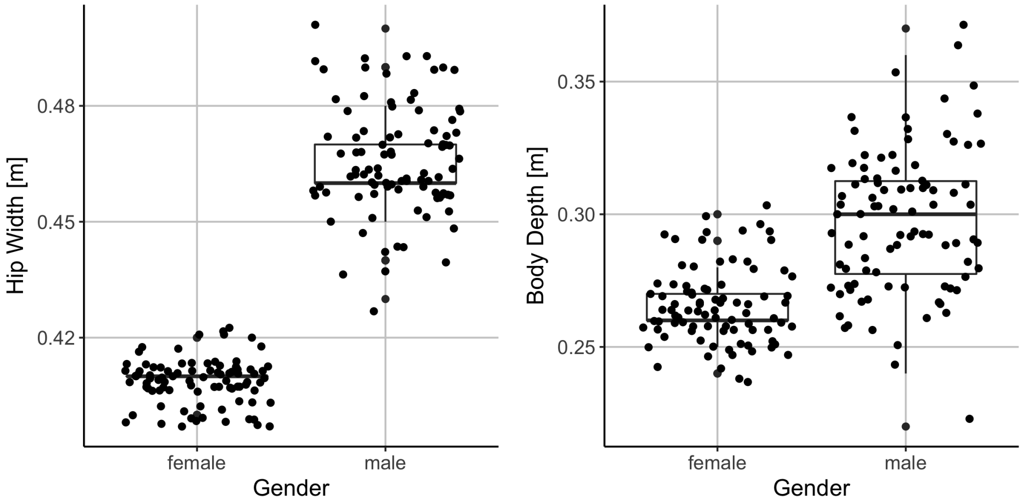

(a) Hip width (b) Body depth

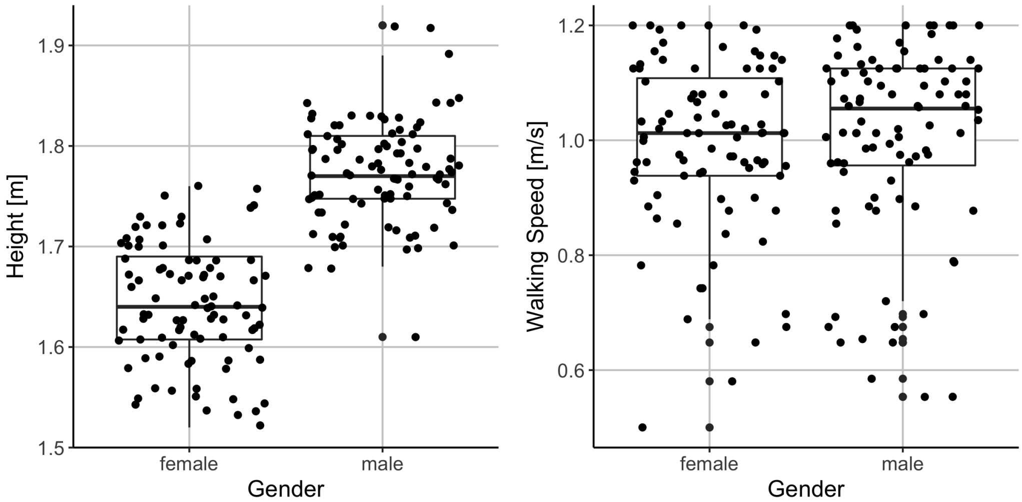

(c) Body height (d) Walking speed

Figure 4.3.: Distribution of passenger characteristics (box-plots show median, first and third quartiles, n=180).

The distribution of the passenger boarding times is illustrated in Figure 4.4a. The results show a mean boarding time of 16.08 minutes (σ = 0.96 minutes, CV^1 = 5.97 %) for the A320neo and 14.66 minutes (σ = 1.44 minutes, CV = 9.82 %) for the A330-300 (see Table 4.3). The increasing number of passengers, the TA configuration and the usage of two doors cause a higher variation of the results in the case of the A330-300. Figure 4.4b depicts the generated mean result compared to available passenger ingress data in dependency of the number of passengers. It becomes apparent that results produced by

[1] The CV is defined as the ratio of the standard deviation (σ) and the median (μ).

the passenger flow module lie in the same range as other available simulation frameworks, as well as OEM data. Evaluating the gathered data revealed that the simulations tend to underestimate boarding times compared to empirical data due to the exclusion of external factors, like no-show passengers. Further potential triggers for deviations with cited study results [12, 16, 132, 133] include different luggage distribution, passenger distribution and characteristics and different resolution of the gradient-based cabin model. The deviation amounts on average with available data to 11 % for the A320neo and 15 % for the A330-300.

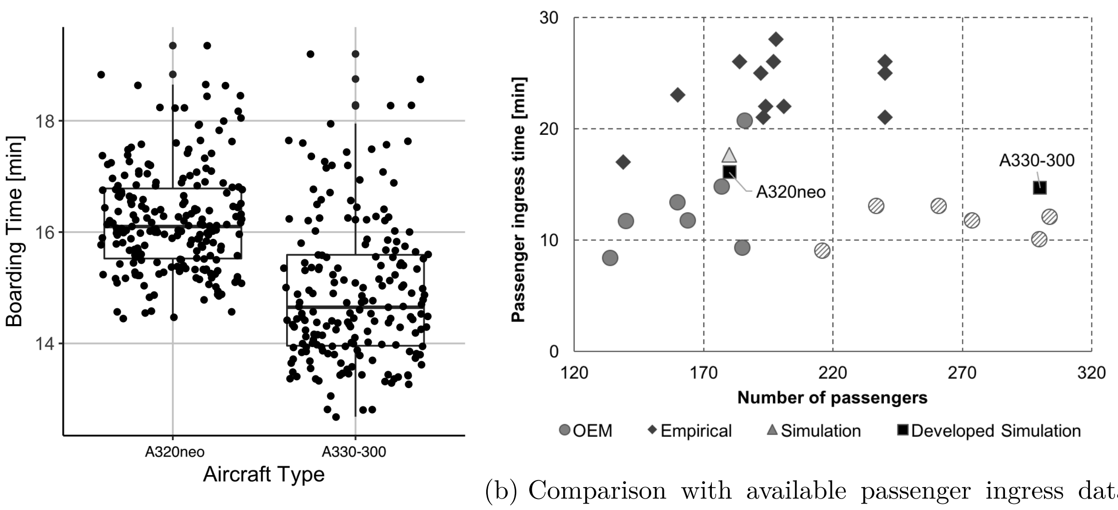

(a) Distribution of simulation module results (n=200).

(b) Comparison with available passenger ingress data from aircraft OEMs, simulations and empirical studies (TA configuration is hatched).

Figure 4.4.: Benchmarking of the simulation module results for A320neo and A330-300.

Table 4.3.: Summary of simulation statistics.

Aircraft	Boarding time [min]	SD [min]	CV [%]	Deviation [%]
A320neo	16.08	0.96	5.97	11
A330-300	14.66	1.44	9.82	15

4.4. Turnaround simulation

The turnaround module is based on existing empirical data and model approaches [43, 114, 119] to simulate the turnaround operation. In the following, a comparison of the developed model with data from OEM [59, 174] is conducted. Information about the general ground handling arrangement and exchanged goods are taken as a reference to mimic the OEM handling scenarios. Despite that, here the inbound and outbound flights are assumed to be equal in terms of the amount of passenger, cargo, catering, fuel and liquids to be exchanged. The passenger process times are taken from Table 4.3.

Conducting the turnaround at a gate position allows the jetbridge to dock on the left front door for the A320neo, allowing passenger egress and ingress. This enables electrical energy to supply through the jetbridge and for cleaning personnel use of the integrated stairs. The catering is performed using two trucks on the right forward and aft service door. Cargo containers are transported with dollies to the aircraft and are loaded with a container loader. The bulk cargo is separately stored using a bulk cargo loader. Potable water and waste water vehicles dock in the aft aircraft section and the fuel truck under the wing to perform their services. This arrangement is similar for the A330 except an additional jetbridge is docked on the left quarter door and cleaning personnel use extra airstairs docked at the left aft door to enter the cabin. In total, three catering trucks serve galleys due to higher demand of food and beverages on long-haul flights.

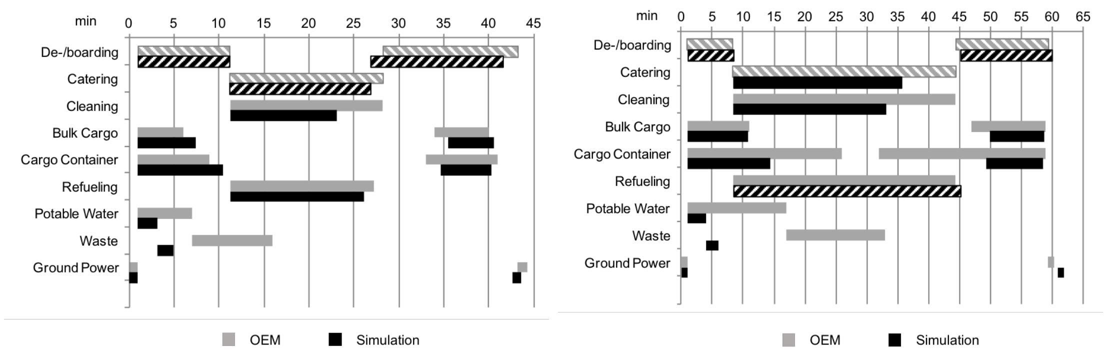

(a) A320neo design mission

(b) A330-300 on a 3,000 nm off-design

Figure 4.5.: Turnaround Gantt chart for the A320neo and A330-300. The critical path is hatched.

Figure 4.5 shows a comparison of the turnaround module results for the A320neo and A330-300 with the corresponding OEM data. For the A320neo the estimated turnaround accounts for 42.5 minutes which is about 4 % lower than the value stated by the OEM manual. The critical paths are constituted by passenger egress, catering and passenger ingress. Deviations exist in cargo operation times and the potable and waste water service due to different assumptions in the amount of exchanged goods. The OEM manual assumes a complete exchange of cargo, catering and liquids, while the turnaround module estimates the amounts for the current flight. The potable and waste water service shows large deviations, since these procedures are often not performed after each flight and therefore the transferred liquid volume is larger. The results are similar for the A330-300 with a deviation of 1 % of the total turnaround time of 60 minutes. However, the critical path switches from catering to refueling due to the lower assumed amount of exchanged galley trolleys by the turnaround module.

4.5. Direct operating cost

Since the DOC module is based on the validated approach by Wesseler [162], the focus is on the introduced changes from the turnaround cost module based on Crönertz [112]. The stated cost values are inflationary adjusted [176] to reflect 2016 levels in US-Dollars (USD) and given results in Euro are transferred into USD [177].

Table 4.4.: DOC estimation study settings.

Parameter	A320neo	A330-300
Block hours per year	5,398 BH	5,556 BH
Fuel price	USD 2.00	USD 2.00
Mission	3,000 nm (5,556 km)	3,000 nm (5,556 km)
Block hours per trip	7.26 BH	7.13 BH
Block fuel	15,622 kg (34,441 lb)	35,439 kg (78,130 lb)

Figure 4.6 depicts the absolute turnaround cost values for the A320neo and A330-300. The calculated costs using a simplified approach by Plötner et al. [173] apply a correlation with MTOW. They account for 1/4 of the cost estimated with the sophisticated activity-based approach by Crönertz [112]. The developed turnaround model incorporates simplifications in the determination of the required resources and disregards the preparation time for workers and GSE. Thus, a deviation of 24 % for the A320neo and 28 % for the A330-300 can be identified.

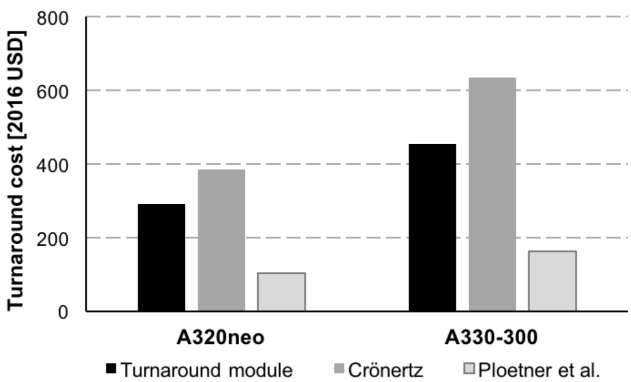

Figure 4.6.: Absolute turnaround cost comparison of the developed turnaround model, approach according to Crönertz [112] and Plötner et al. [173] (gate position).

Incorporating the turnaround cost results with the DOC assessment shows a cost share of less than 1 % for both aircraft, as illustrated in Figure 4.7. The absolute DOC per passenger nautical mile account for USD 0.0544 for the A320 and USD 0.0620 for the A330-300 on a 3,000 nm off-design mission. The share of each cost component strongly differs due to aircraft performance characteristics and their operation. If flight legs are consistent in the short-haul segment, the share of airport related charges raises due to the increased number of starts and landings, as apparent when comparing the A320neo and A330-300 DOC. The applied activity-based turnaround model increases the total DOC by 0.5 % in the stated scenarios. A summary of the cost values can be found in Appendix B.2.

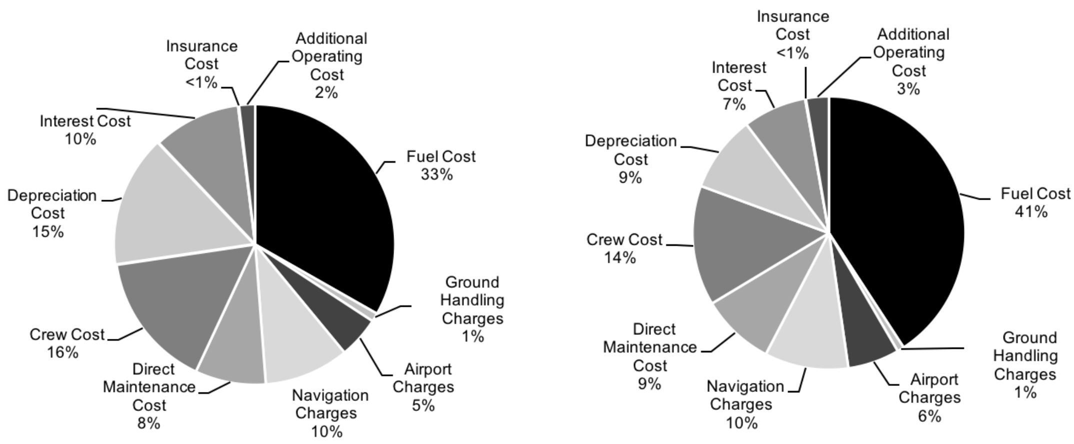

(a) A320neo (b) A330-300

Figure 4.7.: DOC pie charts for a 3,000 nm off-design mission. Cost shares are per passenger nautical-mile.

4.6. Summary

The conducted benchmark using a A320neo and A330-300 as reference demonstrated the applicability of the developed operational framework. Table 4.5 summarizes the results and the deviation to available data. The cabin design heuristic show minor deviations of 2 to 3 %. The results generated by the passenger flow simulation lie in the same range as available data where simulations have the tendency to underestimate the actual boarding time by 10-15 %. Processes on the critical path are represented with an appropriate accuracy to capture changes in the turnaround procedures. However, the turnaround module shows larger deviations for potable and waste water, cargo and catering processes due to variations in the estimated amount of exchanged goods compared to the OEM manuals. A model enhancement will be necessary, if these processes become the focus of concepts under investigation. The DOC are slightly higher due to the increased detail of

Table 4.5.: Summary of framework benchmark results.

Framework Module	Deviation [%]	
	A320neo	A330-300
Cabin design heuristic	3.0	2.0
Passenger flow simulation	11.0	15.0
Turnaround simulation	4.0	1.0
Direct operating cost	0.5	0.5

the turnaround cost estimations. Thus, the framework allows to capture the influence of improved turnaround operations on DOC.

5. Demonstration of ground operation assessment framework

In the following, the ground operational assessment framework is applied to several case studies. First, an overview of the investigated case studies is given. The second part of this chapter presents the results for the passenger flow simulation and subsequent insights from an aircraft level, turnaround, and cost perspective are given. Finally, a critical results recapitulation is conducted and recommendations for the design of future commercial transport aircraft are given.

5.1. Overview of case studies

The selection of case studies builds upon the findings of Section 2.3.2. They cover sensitivities of passenger characteristics, cabin layout modifications and two integrated studies. The focus is on the implementation of advanced concepts into each module of the assessment framework under predominant boundary conditions.

5.1.1. Passenger flow simulation

The focus is on passenger characteristics, such as the walking speed or the carried HL, and impact of changes to the cabin layout. The sensitivity analysis follows a one-factor-at-a-time (OFAT) approach. A reasonable number of studies and the identification of decisive parameters and their bandwidths are essential for the determination of an appropriate design space for novel concepts. This contributes to the EC 3 with the identification of concepts with enhanced performance through the application of the developed framework (see Section 1.2). Furthermore, several single concepts are combined into two case studies aiming to capture cascading effects. A summary of the investigated studies and sensitivities is given in Table 5.1 and highlighted in the following.

5.1.1.1. Monte Carlo simulation initialization

Monte Carlo simulations are conducted to gain insight to the performance of the cabin concepts investigated. The passenger anthropometrics and properties, such as walking speed or body dimensions, are distributed among the agents using probability functions before each simulation run. The number of required runs is estimated with the approach

Table 5.1.: Investigated studies and sensitivities.

Category	Parameter	Unit	Sensitivities		Integrated Studies	
			Min	Max	Study A	Study B
Passenger	Walking Speed	-	0.5	3.0	1.0	1.1
	Boarding Rate	PAX/min	5	40	30	30
	Load Factor	%	50	100	100	100
	Hand Luggage	-	none	very high	high	high
Cabin	Aisles	-	1	2	1	2
	Seat Abreast	-	6	8	6	7
	Doors	-	L1, L2, CD, CD-2 PAX, L1+L4, L2+L3		L2+L3	CD-2 PAX
	Hand Luggage Storage	%	100	120	110	120
	Seats	-	Default, LSP, SFS		LSP	SFS

by Byrne [178]. At least 30 simulation are run for each study to determine the coefficient of variation (CV) as a measure of variability. The CV is defined as the ratio of the standard deviation (σ) and the median (μ). The minimum number of model runs (n) to achieve the desired confidence interval width (w) of 0.05 is estimated with Equation 5.1, where $z_{\frac{\alpha}{2}}$ is the usual value of standard normal assuming a 95 % confidence level. The probabilistic results are the likelihood of each outcome.

$$n = (\frac{z_{\frac{\alpha}{2}}}{w} CV)^2 \tag{5.1}$$

5.1.1.2. Passenger characteristics and operational factors

Passengers are described by their body dimensions, walking speed and carried HL. The walking speed is a result of the passengers age, body shape, and body weight, as well as the amount of carried HL. A range between 0.5 and 3.0 times the nominal average walking speed was investigated to identify the impact of concepts allowing passengers to walk freely and thus faster.

The separation of passengers before entering the cabin, after the check-in, can be expressed with an average passenger boarding rate per door. The determination of the maximum performance of cabin layouts requires passengers to line up in front of the doors. A bandwidth from 5 to 40 passengers per minute (uniformly distributed) trying to enter the cabin was examined, which covers the range from 15-25 $\frac{PAX}{min}$ stated by OEM. The aircraft LF often deviates from the optimal degree of 100 % during daily operation. To account for these differences, the LF was varied between 50 % and 100 % to gain operationally valid results.

Passengers are allowed to bring HL and personal items into the cabin. The composition of the number and size of all items to be stowed inside the cabin varies for each flight.

Therefore, four scenarios were investigated ranging from no HL to a very high degree of HL which exceeds the available storage volume. Each scenario defines a percentage of passengers carrying no, small, medium and large HL items. Passengers carry a maximum amount of one bag and no additional time was accounted for, when they stow their bag under the seat. Table 5.2 summarizes the HL values.

Table 5.2.: Percentages of passengers carrying hand luggage items.

Hand Luggage Case	No HL [%]	Small Bag [%]	Medium Bag [%]	Large Bag [%]
No HL	100	0	0	0
Medium HL	10	50	30	10
High HL	0	20	30	50
Very High HL	0	10	25	65

5.1.1.3. Cabin layout modifications

The overall aircraft dimensions are driven by the payload integration. Here, single-class aircraft cabins with a high passenger seating density between 180 and 300 seats were investigated. As previously shown by the author [37], aircraft manufacturers have the choice between various configurations in terms of seat abreast, number of aisles as well as door positions within this passenger range. Taking the benchmarking cases A320neo and A330-300 (see Section 4.1) as boundaries, one SA configuration with a six-abreast and three TA layouts with a six-to-eight-abreast were examined, as illustrated in Figure 5.1.

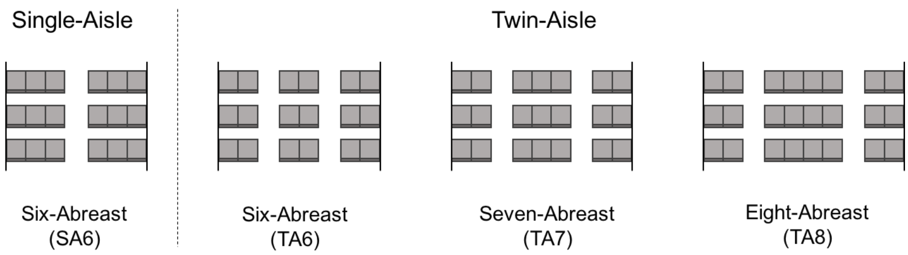

Figure 5.1.: Seat abreast variations.

Additionally to using only the forward left door to enter the cabin, six combinations of left-hand-side doors were analyzed, with a maximum of two doors utilized simultaneously during operation (see Figure 5.2). In this case, passenger use the closest door to their seat to enter the cabin.

As addressed in Section 2.2.3, an increased amount of HL results in a drop in boarding velocities. The effect of increased overhead bin storage volumes of 10 % and 20 %, specifically with space for large luggage items was investigated.

An ideal seating concepts aims to increase the moving space of passengers in the row and to enhance their access to the overhead bins [37, 38]. For the LSP, the aisle width re-

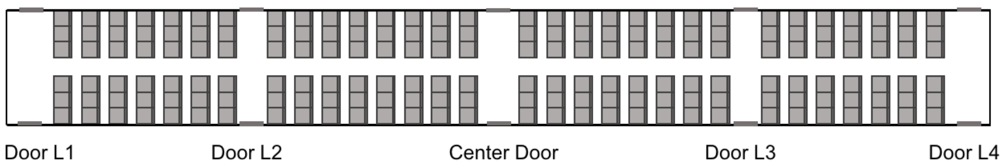

Figure 5.2.: Exemplary depiction of investigated door positions for a single-aisle six-abreast configuration (SA6).

mains unchanged during boarding. The SFS increases the aisle width threefold. However, passengers prefer to walk in the middle of the aisle, since overhead bins constrict the ease of walking on either side. The foldable seats allow passengers to step into the row, if the aisle seat is not yet occupied, and to stow their HL in the overhead bin without blocking the aisle. Passengers can stand up while remaining within the row, in the case of row interferences, when seated at the aisle. This reduces the duration of aisle interferences. When passengers seated at aisle seats have reached their row, they unfold the seat. This additional agent behavior updates the grid and blocks the associated vertices. The general configuration of the investigated folded and unfolded LSP and SFS is illustrated in Figure 5.3.

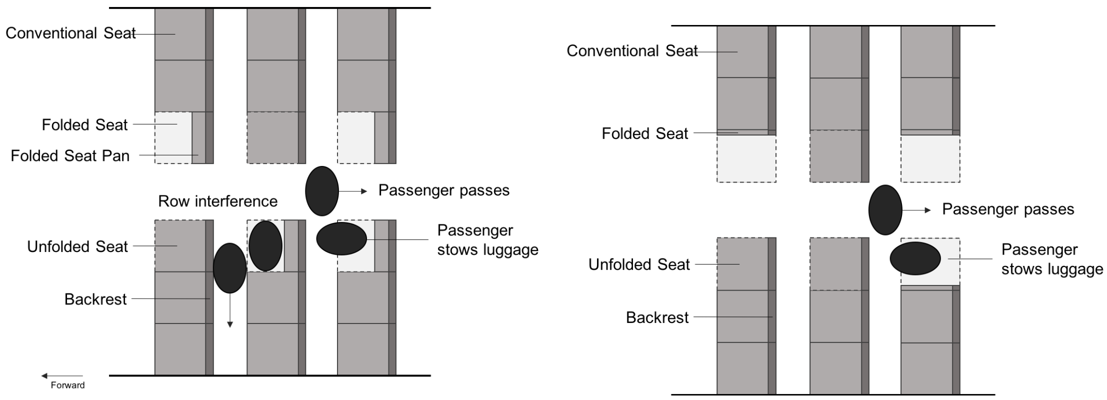

(a) Lifting seat pan (LSP). (b) Sideways foldable seat (SFS).

Figure 5.3.: Foldable seats in a six-abreast single-aisle (SA6) arrangement with folded and unfolded seats [38].

5.1.1.4. Integrated studies

A combination of the previously introduced concepts was targeted through the analysis of two integrated studies, Study A and Study B. Study A focuses on the SA segment and is based on the findings of Schmidt et al. [54], where Study B is a seven-abreast TA as seen in Isikveren et al. [93].

Figure 5.4 depicts the cabin layouts of the two studies. Study A, the six-abreast SA, features additional floor-level exits at quarter (L2) and three-quarter positions (L3) instead of at both ends of the fuselage where smaller emergency exits are integrated. The overhead bins are increased by 10 % through an optimized construction and the 180 passengers carry a high amount of HL. Furthermore, aisle seats are replaced with the LSP. Study B, the TA study, features a seven-abreast configuration for 240 passengers. In addition to the doors at both ends, a center door is integrated which allows two passengers to enter the door simultaneously. The aisle seats are replaced with the SFS allowing passengers to walk through aisles faster. The overhead bins are increased by 20 %. See Table 5.1 (p. 72) for a summary of the study settings.

(a) Study A: six-abreast single-aisle (SA6) with 180 passengers and LSP.

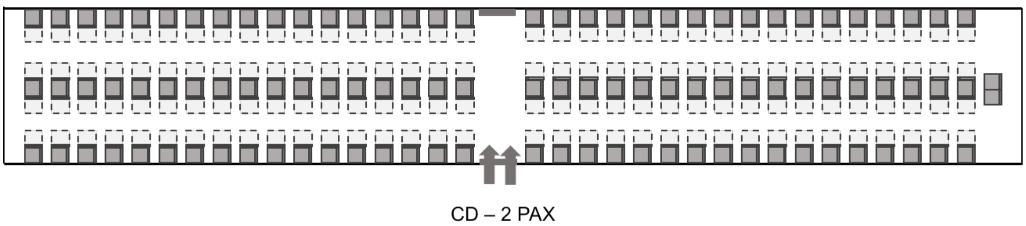

(b) Study B: seven-abreast twin-aisle (TA7) with 240 passengers and SFS.

Figure 5.4.: Cabin layouts of the integrated case studies.

5.1.2. Integration of cabin layouts into aircraft design environment

Applying the cabin design heuristics and designing a detailed cabin layout for the afore mentioned case studies allows the overall dimensions for the integration into the aircraft design environment to be determined. The design studies undertaken were derived from a state-of-the-art short-to-medium haul SA aircraft type [37]. Their aim was to produce trade factors to quantify trade-offs between the cabin layout configurations investigated and not to provide optimized design studies. For each evaluated design described by number of passengers and aisles, and seat-abreast, different aircraft were sized using fuselage diameter and lengths as input parameter. The investigated stage lengths covered a 500 nm, 1,500 nm as well as the design mission with 2,827 nm. The resulting designs complied with the following constraints [37]:

- Weight per passenger is 100 kg (220 lb)
- Tail clearance should remain constant, if feasible, but shall not fall below 10° to avoid tail strikes. This was accomplished via adjusted landing gear length.
- The design range was constant, targeting short-to-medium haul operations and consequently the MTOW adapted accordingly.

- Additional cabin weight was accounted as an OWE change.
- A clearance was required to prevent the engine nacelle from touching the ground in case of a nose landing gear collapse, as well as the wingtip from touching the ground in case of a main landing gear collapse.
- Wing spans should remain within ICAO Code C [179], if practical (depending on aspect ratio). The reference [175] aspect ratio of 9.25 was taken, if the resulting wing span was below 36 m (118 ft).
- Constant tail volume coefficients were assumed to implement the effects of changing fuselage length.
- Landing gear positions should result in the same ground stability of the aircraft.
- Wing loading was kept constant.
- Thrust to weight ratio was kept constant.

The latter two bullet points ensured that all configurations have similar field and cruise performance. Feasibility of the resulting configurations was cross-checked in terms of performance.

For each configuration the service level, in terms of galley and lavatory space per passenger, and the comfort described by the passenger density, remained constant. The additional weight of the LSP was assumed to be 2 kg (4.4 lb) and the SFS accounted for 3 kg (6.6 lb) per seat [94].

5.1.3. Turnaround modeling

The modeled turnaround process mimicked the aircraft dispatch at an airport gate position using jetways or stairs at a remote position for passenger processes. The inbound and outbound flight were assumed to be equal in terms of the amount of passenger, cargo, catering, fuel and liquids to be exchanged. The exchanged cargo covered only the baggage of the passengers, no additional cargo was accounted for. Three cases covering a 500 nm, 1500 nm as well as the design mission were analyzed in terms of replenished fuel. In this context, the focus was on exploration of processes on the critical path through the enhancement of the passenger egress and ingress.

The general ground handling arrangements are depicted in Figure 5.5a at a gate position and for the remote case in Figure 5.5b. Conducting the turnaround at a gate position allows to use the jetbridge for passenger egress and ingress. This enables the supply of electrical energy through the jetbridge. Catering is performed using two trucks on the right forward and aft service door. Cargo containers are transported with dollies to the aircraft and are loaded with a container loader. The bulk cargo is separately stored using a bulk cargo loader. Potable water and waste water vehicles dock in the aft aircraft section

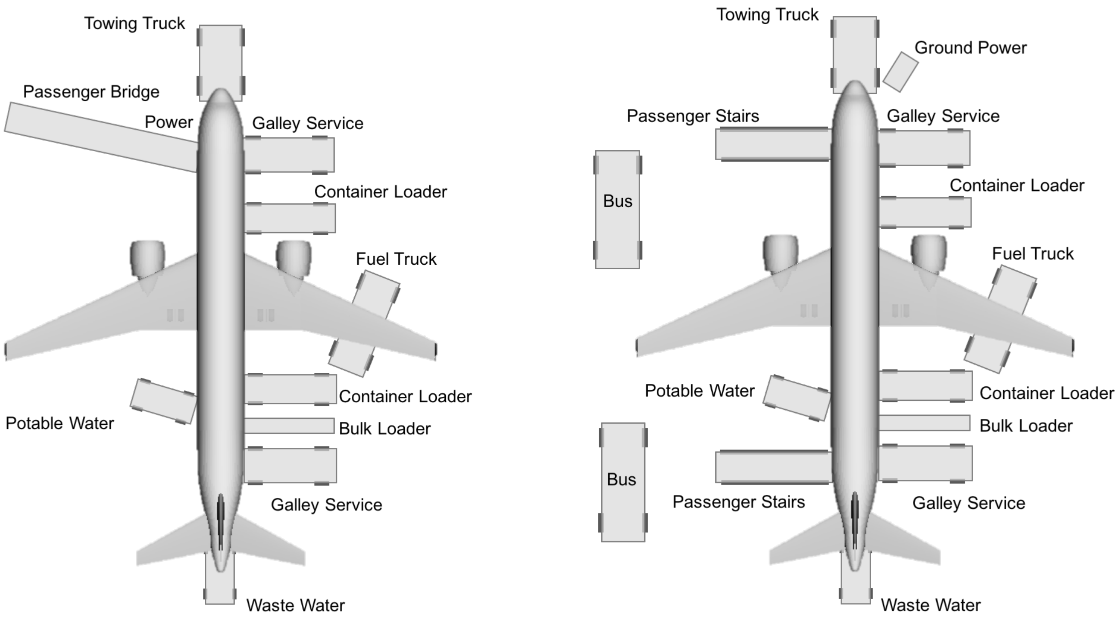

(a) Gate position (b) Remote position

Figure 5.5.: Arrangement of the GSE during the turnaround for the 180 passenger single-aisle configuration.

and the fuel truck docks under the wing to perform their services. For remote turnaround operations (see Figure 5.5b), buses transport the passengers to the aircraft and they board the aircraft through airstairs. Furthermore, electrical energy is supplied by a GPU.

5.1.4. Operating economics

All stated cost values were adjusted for inflation [176] to reflect 2016 levels in USD. Euros were transferred into USD using an average exchange rate of 1 Euro = 1.11 USD from 2016 [177] allowing a comparison of the generated results. Socio-economic factors, such as the average labor salary, the ASP unit rate or interest and insurance rates remained fixed during the investigated life-cycle. The economic aircraft life span was a fixed value of 25 years. The airport charges reflected a global average. A detailed list of the input values can be found in Appendix B.1.

Sensitivity studies covered variations of the aircraft OWE and turnaround cost. Furthermore, the baseline annual aircraft utilization was determined with approach by Mirza [27] highlighted in Section 3.5.1 and changes due to turnaround variations were captured accordingly. The fuel price was varied between 1 and 5 USD per gallon with a 2 $\frac{USD}{gal}$ datum for 2016 to account for uncertainty during the aircraft life-cycle. The impact of higher aircraft acquisition cost due to implemented new concepts were accounted with up to 5 % of the baseline aircraft value. Additional maintenance effort was captured for ATA chapter 25 - equipment and furnishing.

5.2. Results for passenger egress and ingress simulation

This section highlights the results of the investigated sensitivity studies considering the introduced passenger characteristics and cabin layout modifications. Figure 5.6 shows the distributions of the reference cases, which for each study have a high degree of HL and passengers use the forward left door (L1) to enter the cabin. The difference between SA and TA configurations amounted to 40 % in absolute boarding time. The six-abreast SA required 15.82 minutes ($CV = 5.01\%$) for 180 passengers to board where the lowest boarding time of 9.55 minutes ($CV = 5.68\%$) was achieved with a six-abreast TA configuration. The CV remained constant around 5-10 % throughout the studies.

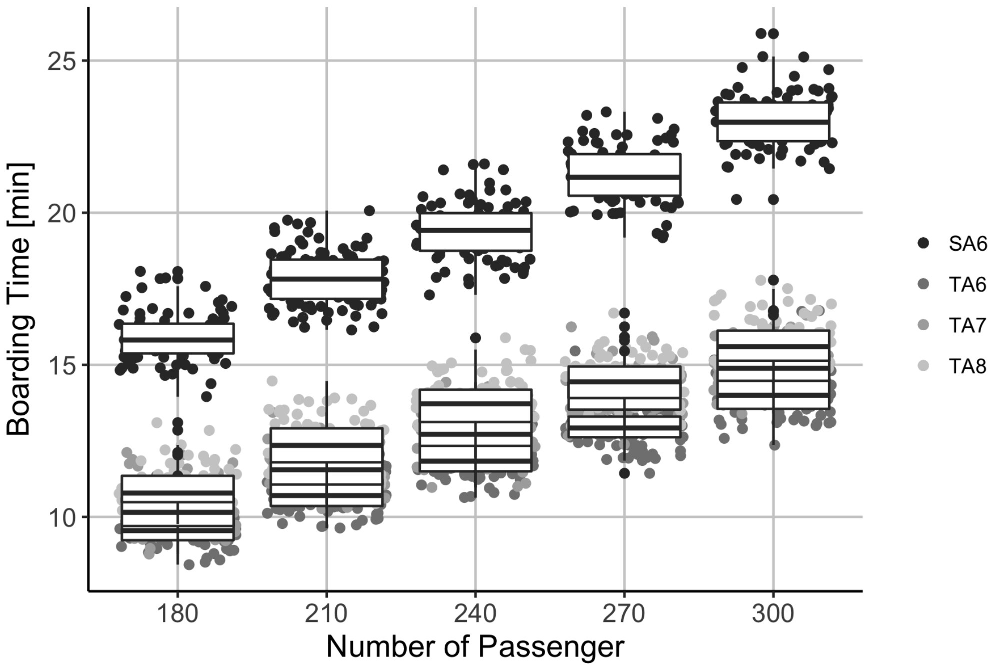

Figure 5.6.: Distribution of the passenger ingress time, high degree HL and door L1 (boxplots show median, first and third quartiles, n=100).

5.2.1. Passenger walking speed

The impact of deviations from the nominal average passenger walking speed on the boarding time is illustrated in Figure 5.7. Here, the results are plotted for the SA six-abreast configuration using the most forward door (L1). An increase of the average walking speed resulted in lower boarding times of up to 15 %. A saturation was identified between an increase of 1.5-2.0 of the nominal speed, which is equivalent to jogging. Thus, higher walking speeds did not have a significant impact on the boarding times. This was valid for all investigated cabin sizes ranging from 180 to 300 seats. A bisection of the nominal walking speed had significant impact on the ingress times with an increase of up to 20 %. These trends were also identified for the TA configurations.

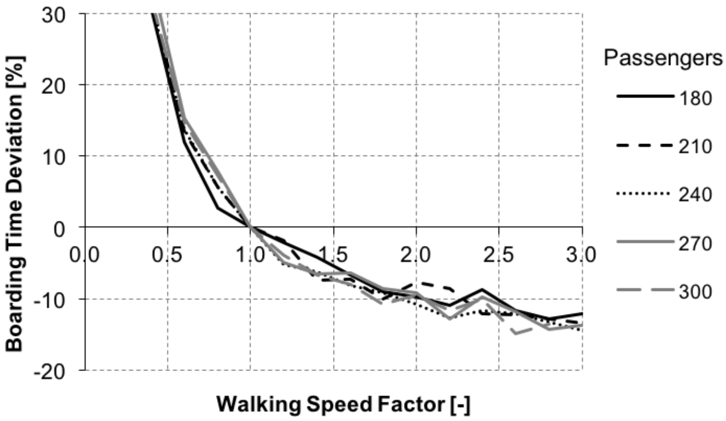

Figure 5.7.: Influence of the passenger walking speed on the overall boarding time. Single-aisle six-abreast configuration (SA6) using the most forward door (L1) (n=50).

5.2.2. Passenger boarding rate

Figure 5.8 depicts the influence of the passenger boarding rate per door on the overall boarding time. The six-abreast SA showed a saturation between 15-20 $\frac{PAX}{min}$ (Figure 5.8a) where the saturation was shifted to a passenger boarding rate of 25-32 $\frac{PAX}{min}$ for the seven-abreast TA (see Figure 5.8b). Thus higher passenger boarding rates did not reduce the passenger ingress time. The overall relative benefit was higher for larger cabins compared to fewer passengers. The same trends was observed, if two doors were used simultaneously for passenger ingress.

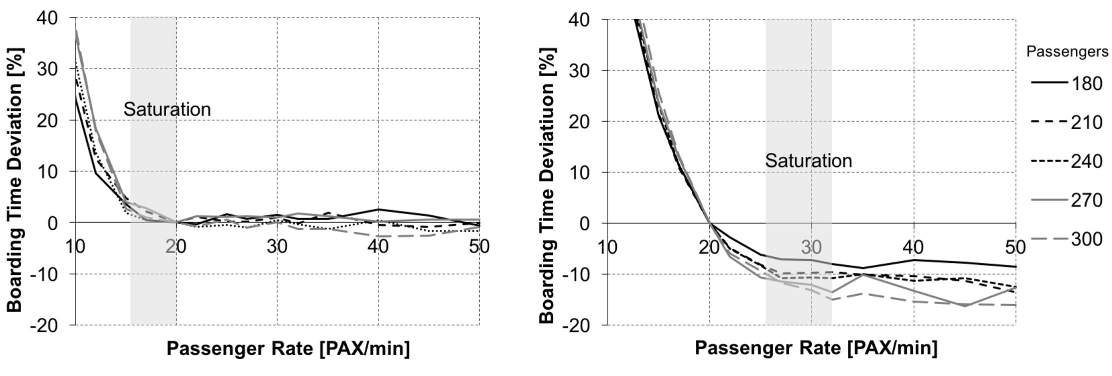

(a) Single-aisle six-abreast configuration (SA6).

(b) Twin-aisle seven-abreast configuration (TA7).

Figure 5.8.: Absolute boarding times for variations in the passenger boarding rate using the most forward door (L1) (n=50, legend is valid for both plots).

5.2.3. Aircraft load factor

The impact of a reduced aircraft LF is illustrated in Figure 5.9. A reduction of the LF resulted in a reduced boarding time throughout the investigated passenger range, where the benefits show a linear behavior. For the six-abreast SA, the boarding time was lowered by 43-46 % for a LF of 50 % and 12-15 % for a common operational LF of 85 %. The same behavior was observed for TA configurations.

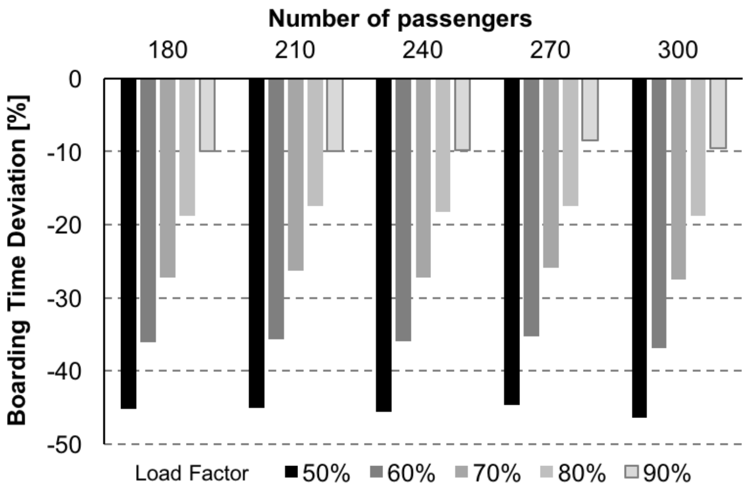

Figure 5.9.: Deviation in the boarding time when the aircraft load factor is smaller than 100 %. Single-aisle six-abreast configuration (SA6) using the most forward door (L1).

5.2.4. Hand luggage type and amount

The impact of carrying and stowing HL was substantial for all investigated cases. Figure 5.10a depicts the deviation between no HL present and the three HL distributions with a medium, high and very high degree. Focusing on the SA configuration, the deviation accounted for 54 % in case of medium HL with 180 passengers and up to 67 % in the case of a very high degree. A shrinking of the deviation was identified for a larger number of passengers. For 300 passengers, the gap amounted to 47 % for medium HL and 61 % for a very high degree. The seven-abreast TA followed the same trend, where the absolute deviations were 25 % for a medium HL degree and 40 % for a very high amount with 180 passengers.

The TA configuration provides 12 % more personal stowing space per passenger and 31 % more large luggage items storage space compared to the SA. The filling degree of the overhead bins, as shown in Figure 5.10b, amounts to around 40 % in case of medium HL and rose with an increasing amount of HL. When the space above a passenger's seat is already full, they must look for another spot inside the cabin. In the high HL case, ten passengers had to look for a spot in the TA and 40 passengers in the SA. These number rose to 28 and 75 for the very high HL degree. All HL fit into the overhead bins for the SA, however with a minimal amount of excess space. If all bins were full or did not provided enough space for large HL items, the number of unstowed items rose. For a very high level of HL in a SA configuration, an average of 31 bags could not be stowed in the overhead

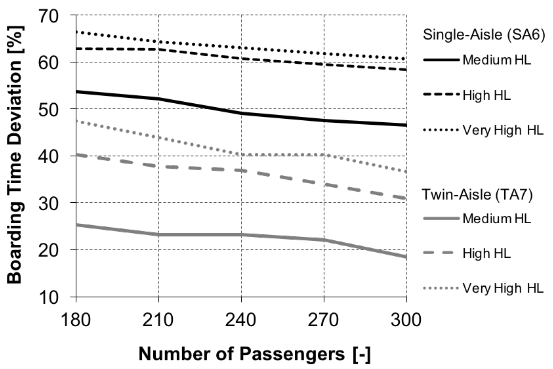

(a) Deviation between no HL present and the three HL distributions with a medium, high and very high degree.

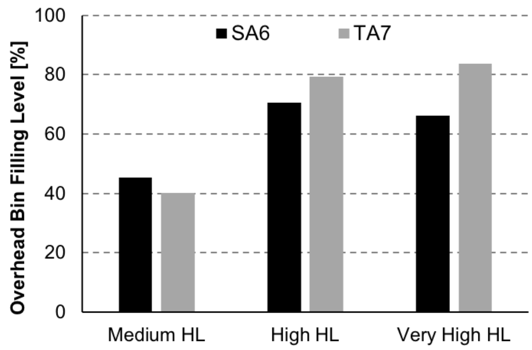

(b) Filling degree of the overhead bins.

Figure 5.10.: Impact of the HL on the boarding times (n=50, door L1).

bins. These unstowed items were not accounted for in Figure 5.10b, since they would be loaded into the bulk luggage compartment. The remaining overhead bin space describes the sum over all installed bins, which is not necessary usable for additional items as it is distributed within the cabin.

5.2.5. Seat abreast

Three different seat abreast variations between six and eight were examined for TA cabins (see Figure 5.1). Figure 5.11 depicts the boarding time deviation with the TA six-abreast case as datum. A larger seat abreast resulted in higher boarding times and no distinct dependency on the cabin size was identified. The seven-abreast configuration showed 4-7 % longer ingress times and the eight-abreast 9-17 %.

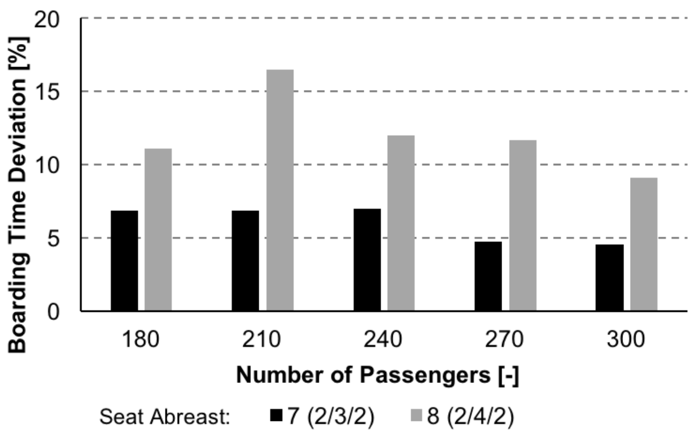

Figure 5.11.: Impact of the seat abreast for twin-aisle configurations (baseline: six-abreast twin-aisle (TA6), door L1, n=50).

5.2.6. Doors

In the following, different door positions and number of simultaneously used doors for passenger ingress were reviewed. The SA and TA studies using door L1 with HL served as datum for the results depicted in Figure 5.12. Using door L2, also called the quarter door, instead of L1 showed lowered boarding times of around 10 % for 180 passengers in SA and TA configuration. The benefits increased with higher passenger numbers and favors the SA with a maximum gain of 17 %. The center door (CD) performed slightly better than the quarter door (L2) for both cases.

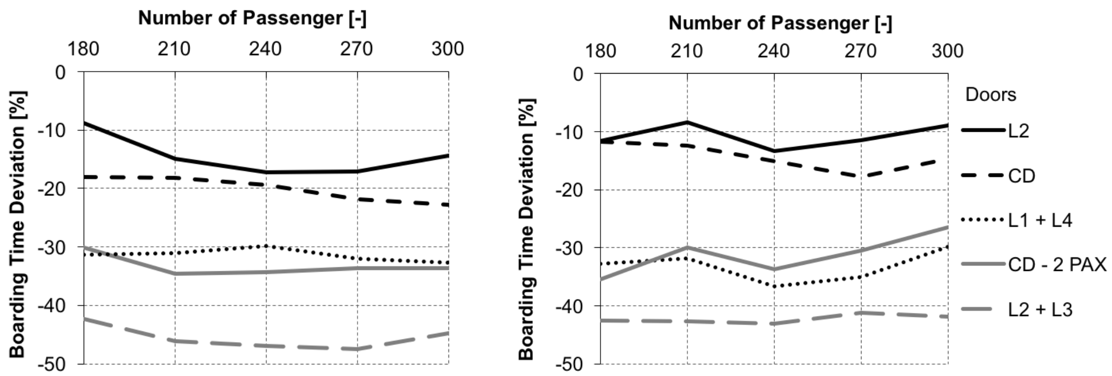

(a) Six-abreast single-aisle (SA6). (b) Seven-abreast twin-aisle (TA7).

Figure 5.12.: Influence of the position and number of doors used for passenger ingress (legend is valid for both plots, n=50).

The dual door boarding procedures with the most forward and aft cabin doors (L1 and L4) showed significant advantages compared to the single door (L1) configuration. For both configurations, an efficiency gain in the boarding procedure of 30-37 % was observed. A similar performance can be achieved with a center door allowing two passengers to enter the cabin simultaneously (CD - 2 PAX). The shortest passenger boarding was enabled through the combination of a quarter and three-quarter door (L2 and L3). This concept showed reduced ingress times for the SA of 42-48 % and 41-43 % for the TA.

5.2.7. Foldable seats

Figure 5.13a illustrates the sensitivities when the aisle seats are replaced with foldable seats. The plot compares the LSP and the SFS concepts with a reference case featuring a conventional seating layout. The SFS showed a slightly increased performance for the SA configuration compared to the LSP with a deviation of 1-5 % and an overall benefit of 28-31 %. Similar trends were observed for the TA configuration. However, the absolute deviation between a cabin equipped with conventional seating was in the range of 17-29 %. A shrinking of the benefit for higher numbers of passengers could be identified for both configurations.

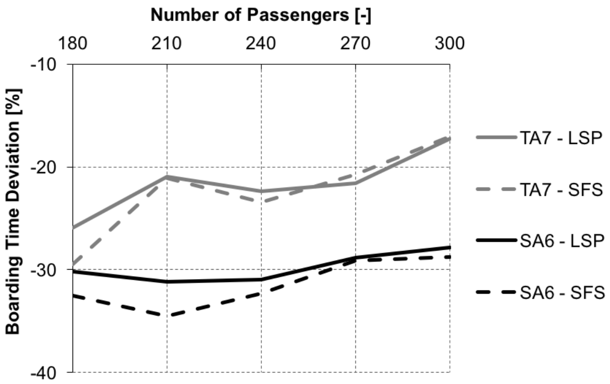

(a) Boarding performance for single- and twin-aisle configurations with LSP and SFS compared to conventional seating.

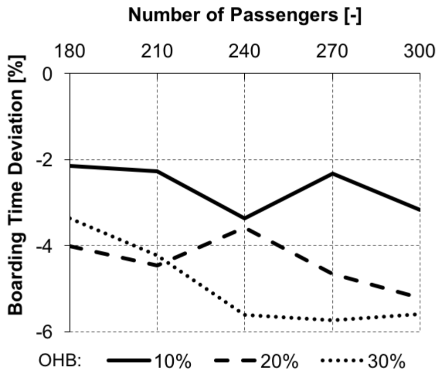

(b) Impact of increased overhead bin storage volume (six-abreast single-aisle (SA6), very high HL case).

Figure 5.13.: Results for foldable seats and increased overhead bin storage space (n=50, door L1).

5.2.8. Luggage storage concepts

The stepwise increase of the overall cabin overhead bin storage volume is depicted in Figure 5.13b for the very high HL case. The highest benefit with 6 % was identified for 270 passengers and a 30 % overhead bin volume increase. The benefit shows almost a linear behavior for each stepwise increase throughout the passenger range. The deviation for a 10 % volume increase accounted for an average of 2 % throughout the investigated passenger range.

5.3. Aircraft level assessment

The investigated aircraft configurations ranged from 180 to 300, being equivalent in fuselage length (l_{fuse}), with four different fuselage diameters (w_{fuse}). The MTOW per passenger is plotted in 5.14a. The specific MTOW decreased with an increasing number of passengers. The SA configuration had a 10 % lower specific MTOW for 180 passengers compared to the six-abreast TA being the TA with the lowest specific MTOW. The deviation amounted to 7 % for 300 passengers where the SA configuration showed a slight increase of the specific MTOW.

The variation of the fuselage weight per passenger is depicted in Figure 5.14b. The weight increased with an increasing number of passengers where the difference between 180 and 300 passengers amounted to 1-14 %. A fuselage weight shift was noticeable for a diameter of 4.8 m (TA6) where for larger diameters a flattening of the weight increase was identified. The difference between a diameter of 4.0 m and 5.6 m accounts for 18-32 %. The furnishing mass per passenger remained with 25 $\frac{kg}{PAX}$ constant for all configurations.

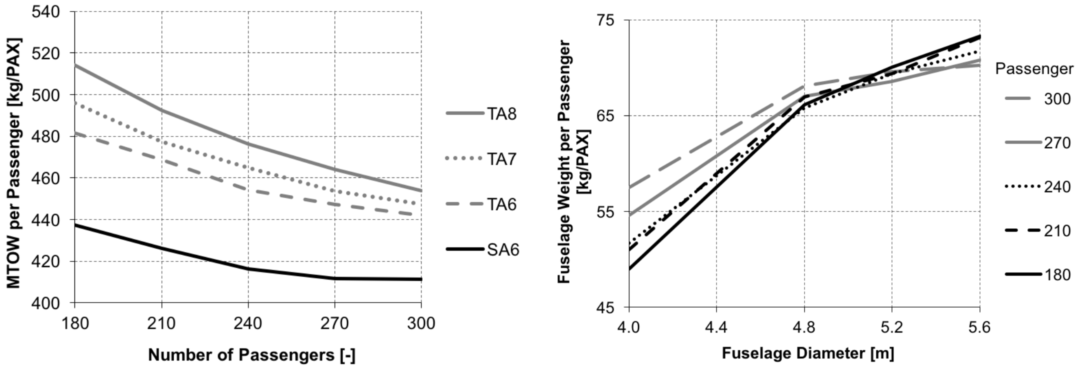

(a) MTOW per passenger. (b) Fuselage weight per passenger.

Figure 5.14.: Fuselage weight and MTOW.

Figure 5.15a illustrates the dependency of the number of passengers on the specific fuel burn per passenger and nautical mile exemplary for a stage length of 500 nm. The same trend was observed throughout the investigated missions. The specific fuel burn dropped with an increasing passenger number for all investigated configurations by 11-18 % comparing layouts with 180 and 300 passengers. The gap between SA and TA amounted to 10-17 % for 180 passengers and 8-12 % for 300 passengers depending on the seat-abreast, which is equivalent to the sensitivity of the fuselage diameter. The impact of an OWE change (ΔW_{OWE}) is shown in Figure 5.15b. An additional weight of 500 kg (1,102 lb) was translated into a 0.7 - 1.2 % increased fuel burn, where smaller relative fuel burn deviations was observed for higher passenger numbers.

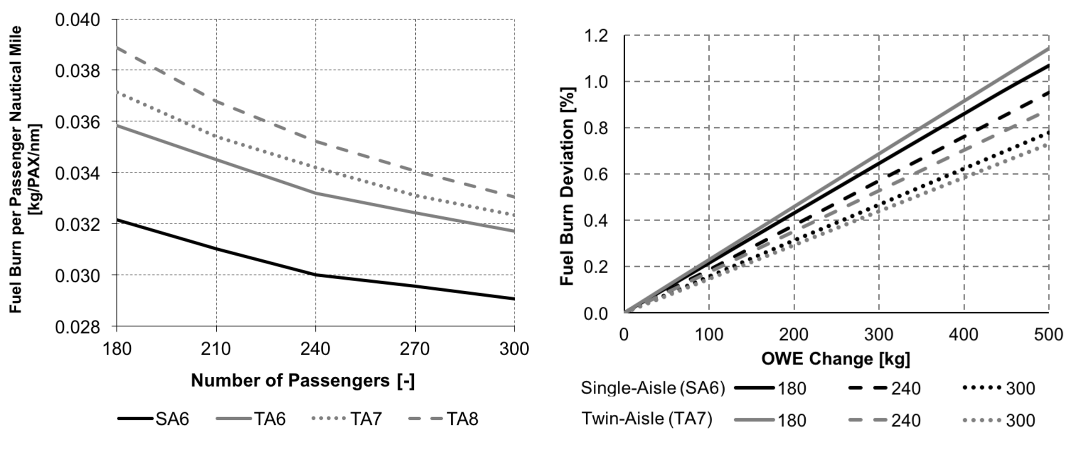

(a) Specific fuel burn per passenger nautical mile. (b) Impact of an OWE change on the fuel burn.

Figure 5.15.: Impact of the investigated aircraft configurations and OWE changes on the specific fuel burn (500 nm off-design mission).

5.4. Turnaround simulation results

Feeding the results of the passenger process investigations and the fuel burn assessment into the turnaround module allowed for a critical path analysis. Figure 5.16a illustrates the absolute turnaround times at a gate position for the passenger range and configurations under investigation. Here, the replenished fuel accounted for a 1,500 nm (2,778 km) off-design mission. The critical path was constituted by the GPU connection and removal, passenger egress, catering and passenger ingress using door L1. The GPU connection and removal times were fixed values for all cases and the catering time remains constant for an equal number of passengers. An advantage of around 21 % faster turnaround time was calculated for the TA configurations resulting from the shorter passenger processes and remained constant for the entire passenger range. The differences between the three TA configurations were less than 0.5 %.

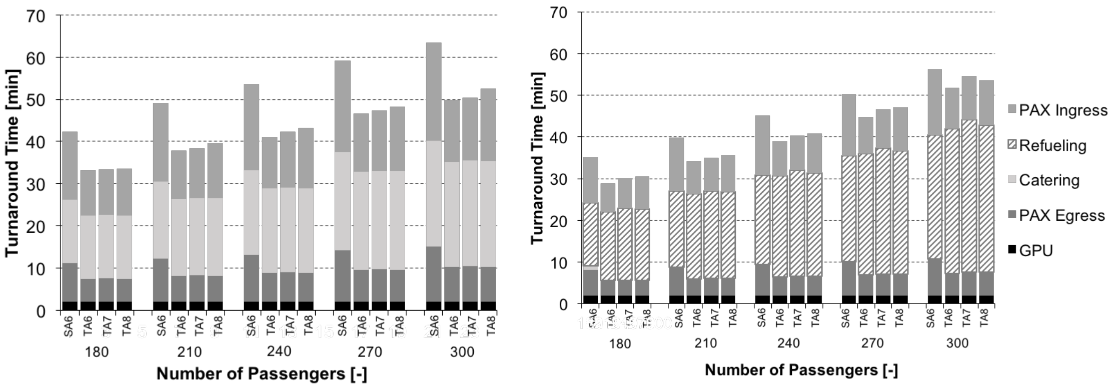

(a) Gate position, 1,500 nm off-design mission using one door (L1).

(b) Remote position, design mission of 2,827 nm using forward (L1) and aft door (L4).

Figure 5.16.: Absolute turnaround times for the passenger range and configurations under investigation.

Figure 5.16b depicts the absolute turnaround times for operation at a remote location using two stairs located at L1 and L4. The replenished fuel accounted for the design mission of 2,827 nm (5,236 km). Here, the critical path changed from catering to refueling, GPU connection and removal, passenger egress, and passenger ingress. The advantage of the TA was reduced to 15-10 % for configurations with 180-240 seats and for higher seat numbers the deviation accounted for around 5 %.

The impact of a boarding time reduction on the overall turnaround time is plotted in Figure 5.17a. Here, a range from 0 to -50 % reduced boarding times was investigated for operations at a gate position considering a 1,500 nm off-design mission using one door (L1). A 30 % boarding time reduction results in a 9 % shorter turnaround for the TA and 12 % for the SA.

Figure 5.17b maps the impact of a boarding time reduction due to the afore investigated studies for SA configurations on the turnaround time. The usage of a quarter door (L2)

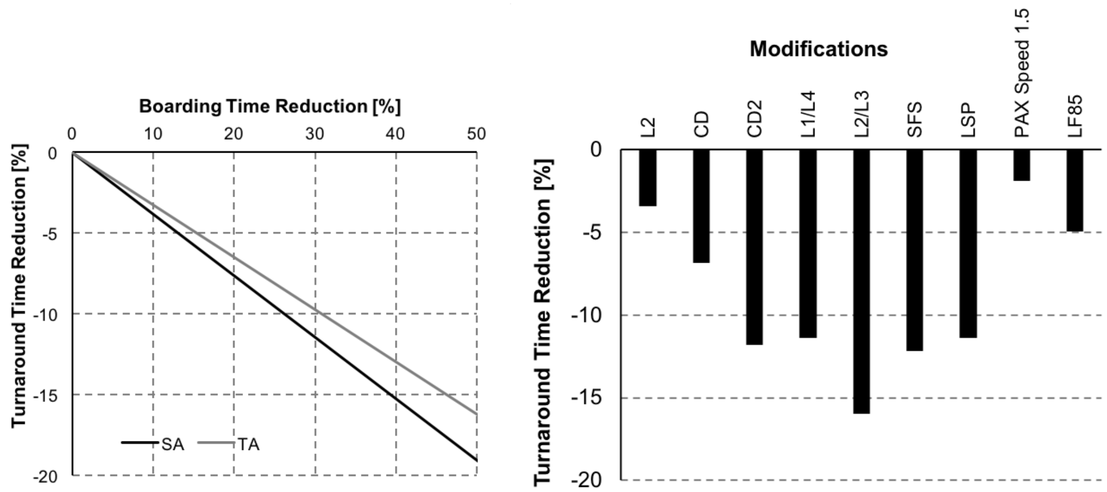

(a) Sensitivity of boarding time variation on the overall turnaround time.

(b) Summary of cabin modifications and their impact on the turnaround time (Single-aisle six-abreast configuration (SA6)).

Figure 5.17.: Sensitivity of boarding time variations (180 passengers, gate position, 1,500 nm off-design mission using one door (L1).

yielded 4 % lower turnaround times. Other door combinations, such as the quarter and three-quarter door, showed up to 16 % savings. The LSP and SFS achieved 12 % shorter turnaround times. A reduction of the LF to 85% resulted in a 5% reduction and an increase of the average walking speed of 50% translated to 2%. The relative reductions were smaller for the TA due to the shorter absolute turnaround times.

5.5. Aircraft operating cost

A DOC analysis became feasible with the previous presented results. In the following, the cost values are expressed as cost per passenger nautical mile to form a comparable metric. A comparison of the four investigated cabin configurations without any cabin

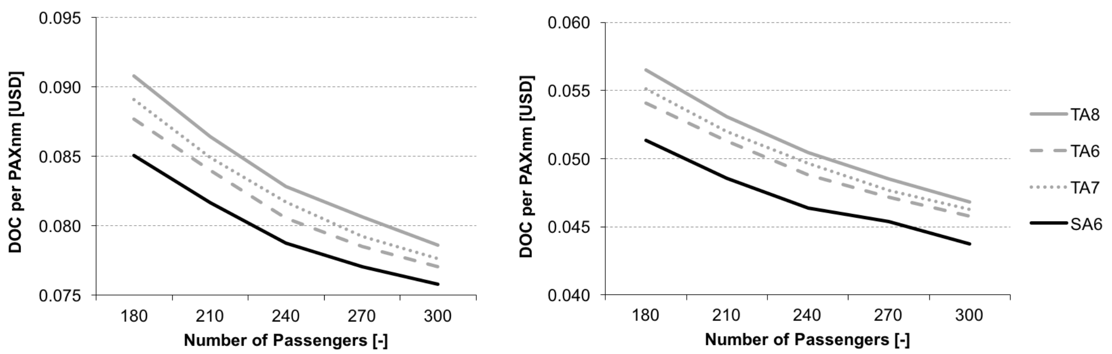

(a) 500 nm off-design mission.

(b) Design mission (2,827 nm).

Figure 5.18.: Absolute DOC per passenger nautical mile (legend is valid for both plots).

modifications on DOC level is depicted in Figure 5.18 for a 500 nm off-design mission and the design mission. The lowest operating cost were achieved by the six-abreast SA configuration, however the margin against the TA configurations was reduced with an increasing number of passenger. The deviation between 180 and 300 passengers accounted for 12-15 %.

Figure 5.19 depicts the absolute DOC for the six-abreast SA and the seven-abreast TA with passenger numbers ranging from 180 to 300. The share of each cost elements varied depending on the mission length. Airport charges, fuel cost and cost of ownership were predominant on the 500 nm off-design mission, where a shift towards navigation, crew and an even higher share for fuel cost could be identified on the design range.

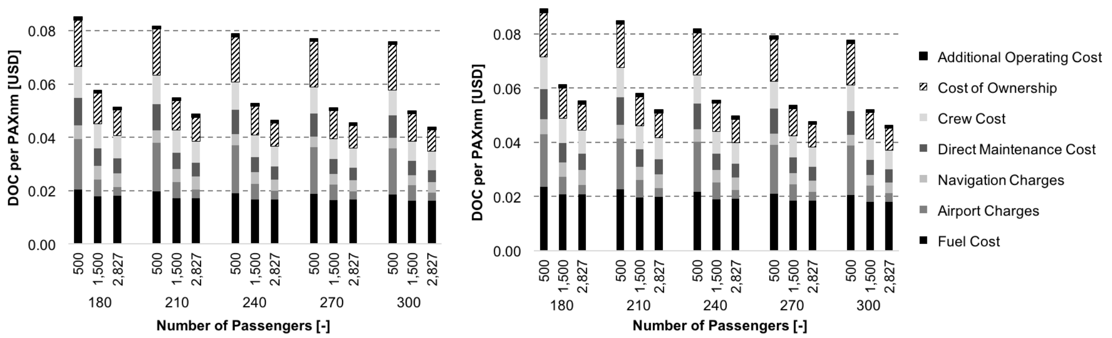

(a) Single-aisle six-abreast (SA6).

(b) Twin-aisle seven-abreast (TA7).

Figure 5.19.: Absolute DOC per passenger nautical mile (legend is valid for both plots).

The DOC amounted to 0.0851 $\frac{USD}{PAXnm}$ on a 500 nm mission and to 0.0513 $\frac{USD}{PAXnm}$ on the design range considering 180 passengers in a six-abreast SA configuration (see Figure 5.19a). The absolute cost decreased with an increasing number of passengers and the change amounted to 15 % when comparing the 180 and 300 passenger configurations on the design range. The trend was similar for the TA with higher absolute values (see Figure 5.19b). The deviation between SA6 and TA7 configuration accounted to 2.4 % considering 300 passengers on the design range and to 5.7 % on a 500 nm mission.

5.5.1. Cost of ownership sensitivities

The sensitivities of higher aircraft investment cost due to integrated novel concepts on COO basis are illustrated in Figure 5.20. Higher acquisition costs increase the COO, which cover depreciation, insurance, interest and correlate with the PIC (see Section 3.5.1). Additional cost of USD 1 million increased the DOC by 0.38 % for the SA on a 500 nm mission and by 0.33 % on the design mission. The impact for the seven-abreast TA accounted for 0.34 % and 0.31 % respectively.

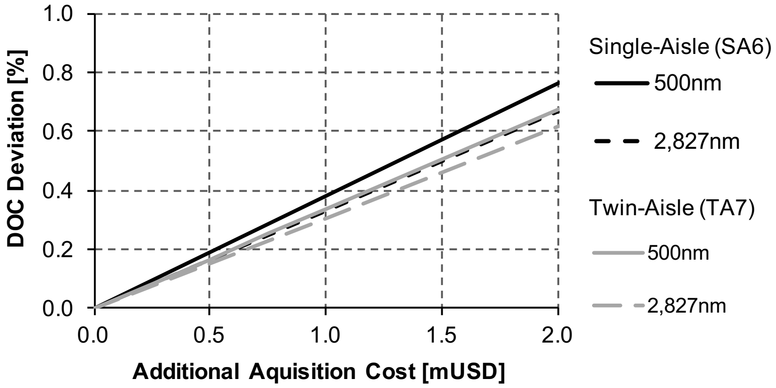

Figure 5.20.: Impact of higher acquisition cost on the DOC (240 passenger configuration).

5.5.2. Airframe maintenance cost sensitivities

The impact of increased maintenance effort due to novel cabin concepts and systems was investigated for parts categorized under ATA 25 - furnishing and equipment. An increase of maintenance costs associated with ATA 25 showed a linear behavior, as depicted in Figure 5.21a, where 10 % higher cost resulted in 1.5-1.6 % higher DMC. On DOC level the influence ranges from 0.10-0.12 %.

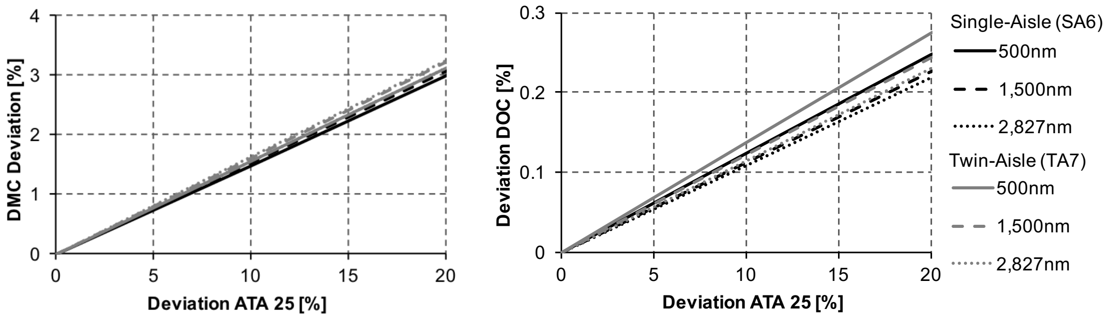

(a) DMC level (b) DOC level

Figure 5.21.: Influence of increased maintenance expenditures concerning aircraft parts categorized under ATA 25 - furnishing and equipment (240 passenger configuration, legend is valid for both plots).

5.5.3. Ground handling cost sensitivities

The absolute ground handling cost for operations at gate positions are illustrated in Figure 5.22a for the investigated aircraft and passenger range. The handling cost increased with an increasing number of passengers due to longer refueling, cleaning and passenger process times. They averaged around USD 300 for 180 passengers and increased by 30 % for 300 passengers. The difference between SA and TA configurations accounted for 4 %. During remote operations, two stairs were commonly used requiring additional buses to transport the passengers resulting in higher cost for passenger GSE. Here, the difference between

SA and TA configurations accounted for 14 % with an absolute cost of USD 300 for TA with 180 passengers.

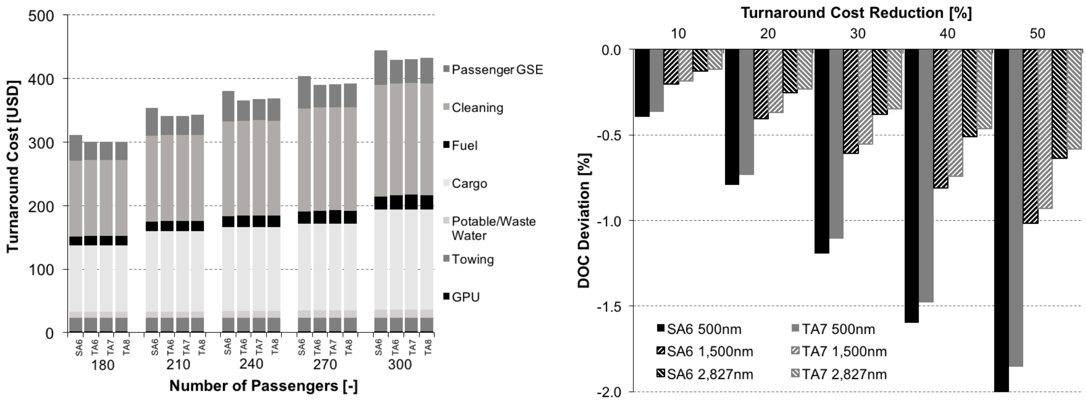

(a) Gate position using one door (L1), 1,500nm mission.
(b) Turnaround cost sensitivity on DOC level.

Figure 5.22.: Absolute ground handling cost values and cost sensitivity on DOC level.

The impact of potential cost reduction of ground handling operations on a DOC level are depicted in Figure 5.22b. The largest influence was identified for short-haul missions of 500 nm, where a cost reduction of 50 % yielded around 2 % lower DOC for the six-abreast SA and seven-abreast TA. For the design mission, the advantage accounted for around 0.6 %.

5.5.4. Aircraft utilization

The impact of a varying aircraft utilization is captured by the COO, since they cover depreciation, interest and insurance costs. Figure 5.23a shows the sensitivity of potential turnaround time reductions, which leads to higher aircraft utilization according to Mirza [27] (see Section 3.5.1), on a COO level. A turnaround time reduction of 40 % yielded the

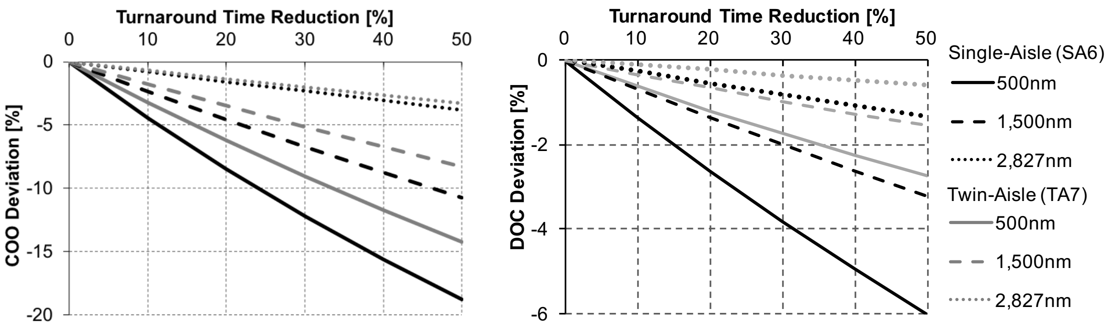

(a) Impact on COO.
(b) Impact on DOC.

Figure 5.23.: Influence of reduced turnaround times on COO and DOC (240 passenger configuration, legend is valid for both plots).

largest impact on the 500 nm mission with 16 % lower COO for the SA and 12 % for the TA. For the design mission this translates to a reduction of around 2 %. On DOC level, this was translated to 4.9 % reduced cost for the SA and 2.2 % for the TA.

5.5.5. Fuel price sensitivities

The fuel price for Jet-A1 is of volatile nature, hence a sensitivity analysis of the fuel price was undertaken to show a potential impact of cabin concepts increasing the OWE and to allow for conclusions in future scenarios. Figure 5.24a depicts the cost shares of each DOC element for fuel prices between 1 and 5 $\frac{USD}{gal}$, where 2 $\frac{USD}{gal}$ is the nominal value. A fuel price bisection increased the cost shares of all remaining operating expenses and this was especially the case on the 500 nm mission. Hence, cost savings in these categories due to novel concepts would have a larger impact on the absolute DOC. An increase of the fuel price had the opposite effect, where in the case of a Jet-A1 price of 5 $\frac{USD}{gal}$, the fuel cost share was dominant with 45-60 %.

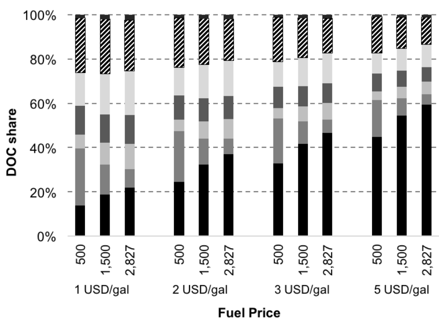

(a) Cost shares

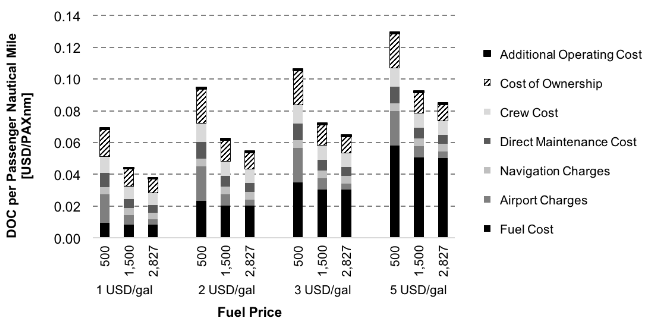

(b) Absolute operating expenses

Figure 5.24.: Fuel price sensitivity for the six-abreast single-aisle (SA6) with 240 passengers (legend valid for both plots).

The absolute cost values were strongly driven by a fuel price variation as illustrated in Figure 5.24b. The absolute fuel cost correlated directly with the fuel price. The DOC were reduced by 27 % for a nominal kerosene price of 1 $\frac{USD}{gal}$ and they showed an increase of 37 % for 5 $\frac{USD}{gal}$ considering a 500 nm mission.

5.6. Results for integrated studies

The integration of several concepts was targeted through the analysis of two integrated studies. In the following, the results for the agent-based passenger flow simulation, aircraft level assessment, turnaround modeling and operational cost assessment are presented for a six-abreast SA with 180 passengers (Study A) and the seven-abreast TA with 240 passengers (Study B), as highlighted in Section 5.1.1.4. The reference cases feature no layout or process modifications as summarized in Table 5.3.

Table 5.3.: Reference cases and investigated integrated studies

		Reference Case		Integrated Studies	
Category	Parameter	A	B	Study A	Study B
Passenger	Number of Passengers	180	240	180	240
	Walking Speed	1	1	1	1.1
	Boarding Rate	30	30	30	30
	Load Factor	100	100	100	100
	Hand Luggage	high	high	high	high
Cabin	Aisles	1	2	1	2
	Seat Abreast	6	7	6	7
	Doors	L1/L2+L3	L1/CD-2 PAX	L2+L3	CD-2 PAX
	Hand Luggage Storage	100	100	110	120
	Seats	Default	Default	LSP	SFS
Aircraft	Delta OWE	0	0	+360kg	+720kg
	Delta Fuselage Length	0	0	+1m	+1m
Cost	Delta Maintenance	0	0	+10% ATA 25	+10% ATA 25
	Delta Acquisition	0	0	+1m USD	+2m USD

Figure 5.25a shows the distribution of the absolute boarding time for both studies. Study A showed an average boarding time of 6.65 minutes (CV = 11.15 %) and Study B yielded 6.31 minutes (CV = 8.50 %). A comparison with the baseline without any modifications resulted in an improvement of 66 % for Study A and 58 % for Study B. Taking the same door configuration as the reference provided a 26 % reduction for Study A using doors at quarter (L2) and three-quarter positions (L3) and a 31 % reduction for Study B using a center door allowing two passengers to enter simultaneously (see Figure 5.25b).

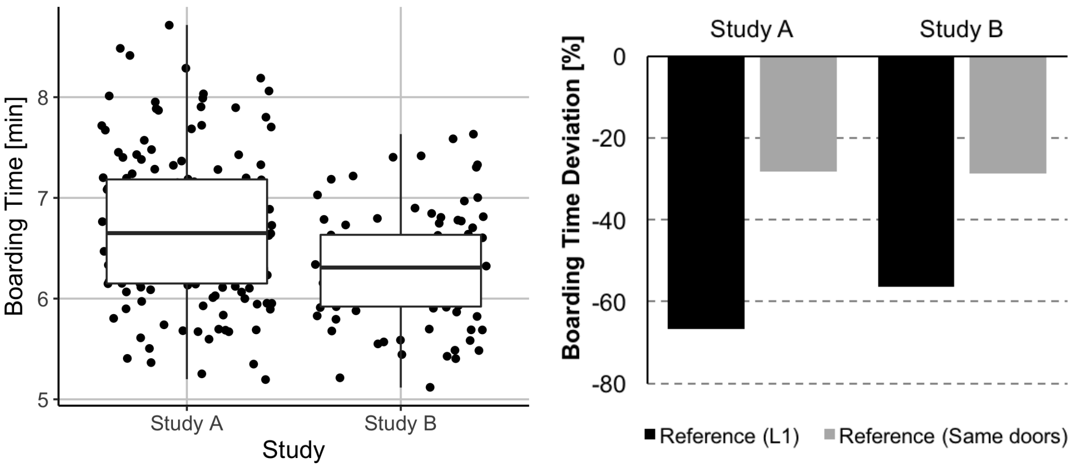

(a) Distribution of passenger boarding times (n=100).

(b) Comparison with reference results.

Figure 5.25.: Results of the integrated studies for the passenger flow simulation.

The integrated assessment on aircraft level accounted for the additional seat weight of the LSP and SFS as well as the longer fuselage due to an increased number of installed exits (see Table 5.3). Figure 5.26a shows, for Study A, a 1.4 % increased fuel burn on a 500 nm off-design mission and 1.3 % on the design mission and for Study B, 2.1 % and 2.0 % respectively.

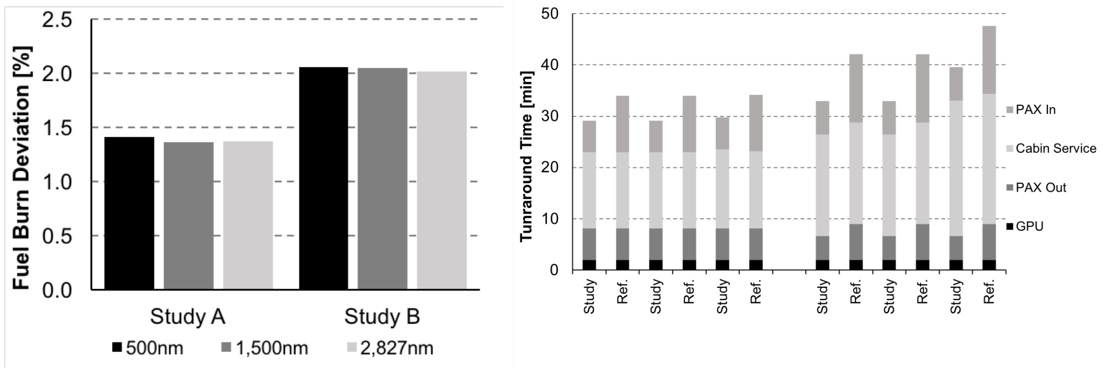

(a) Aircraft level assessment of increased OWE and fuselage length.

(b) Turnaround time comparison with reference cases.

Figure 5.26.: Aircraft level assessment and turnaround simulation results.

Figure 5.26b depicts the absolute turnaround times of both studies compared to the reference case. Here, the critical path was constituted by GPU connection and removal, passenger egress, cleaning and passenger ingress. In the case of the design mission, the critical path changed to refueling instead of cleaning. Study A resulted in an improvement of 14.6 % for the off-design missions compared to the reference and for Study B, the deviation accounts to 22.2 %.

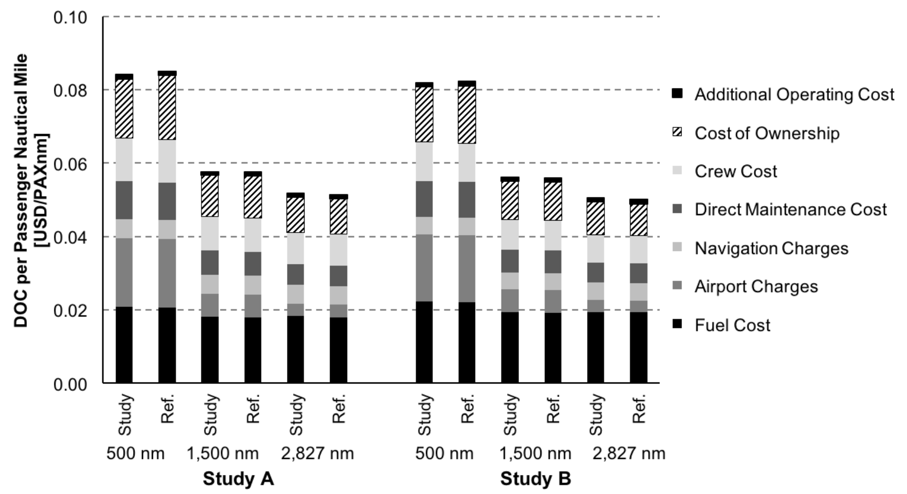

Figure 5.27.: Absolute DOC per passenger nautical mile.

The results on a DOC basis are depicted in Figure 5.27. The absolute DOC per passenger nautical mile accounted for 0.0842 $\frac{USD}{PAXnm}$ for Study A on a 500 nm mission and 0.0517 $\frac{USD}{PAXnm}$ for the design mission. Study B yielded similar values of 0.0820 $\frac{USD}{PAXnm}$ and 0.0505 $\frac{USD}{PAXnm}$.

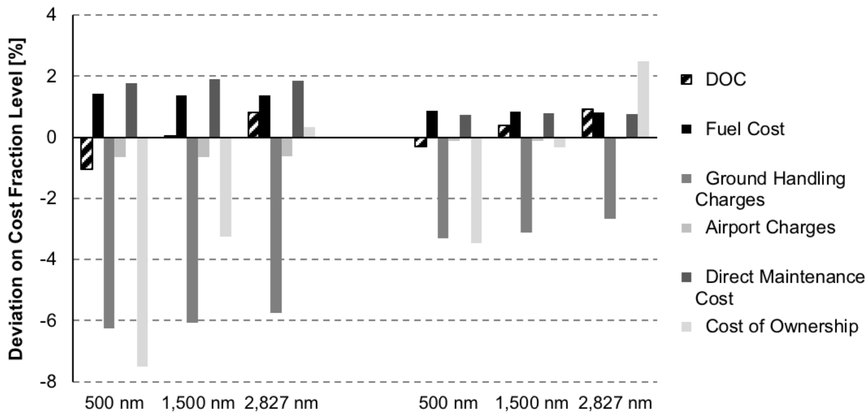

Figure 5.28.: Relative change of DOC cost components in comparison with reference case.

A comparison with the reference case showed a DOC reduction of 1.1 % for Study A on a 500 nm mission and a cost neutral outcome on a 1,500 nm mission, as illustrated in Figure 5.27. For the design range, an increase of 0.8 % was determined. Significant contributions to a cost reduction are made by lower ground handling costs (5.7-6.3 %) and COO (0-7.5 %), however their cost share accounted for only 3.7 % and 19.1 % on a 500 nm mission and was further reduced towards the design range. These savings could not offset the increased fuel (1.4 %) and maintenance costs (1.8 %) which represented a share of 29-37 %. The results for Study B showed a cost neutral outcome for the 500 nm and 0.9 % higher DOC for the design range. Here, the fuel costs were increased by 0.9 % and the maintenance costs by 0.8 %. The savings on ground handling costs accounted for 2.7-3.3 % but the COO were only reduced by 3.5 % on the 500 nm mission.

The absolute deviations of each cost share on DOC level is depicted in Figure 5.29. The share of higher fuel cost and maintenance expenses accounted for 0.5-0.6 % for Study A and 0.4 % for Study B. However, the cost reduction based on lower COO was reduced with an increasing stage length from -1.4 % to 0 % for Study A. In case of Study B, the COO were 0.5 % higher compared to the reference for the design mission. This resulted in higher DOC compared to the reference with an increasing stage length.

5.7. Result recapitulation

The studies undertaken aimed to identify promising candidate solutions in terms of their performance and allowed for the assessment of cascade effects with two integrated case studies. This contributes to the Expected Contribution 3, which targets a coherent down-selection through the application of the developed framework. Furthermore, the obtained

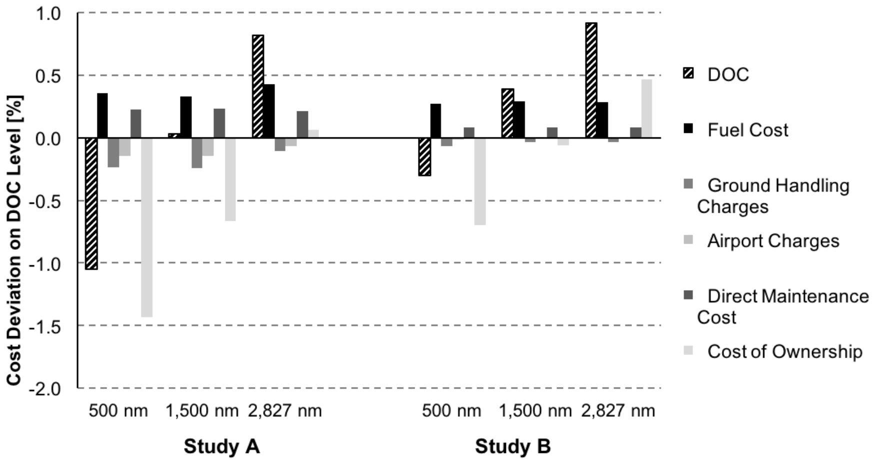

Figure 5.29.: Change on DOC level in comparison with reference case.

insights of the concept evaluation enable the identification of design criteria for the next generation of commercial passenger aircraft (Expected Contribution 4, see Section 1.2). In the following, the results are analyzed and the integration within current operations is highlighted.

5.7.1. Sensitivities

Passenger characteristics and operational factors

The passenger characteristics cannot be directly influenced by the cabin layout but can facilitate seamless passenger movements. The impact of the passenger walking speed of up to +5 % on the boarding time was notable considering a reasonable increase of +25 % of the nominal walking speed (see Figure 5.7, p. 79). The cabin should be designed to accommodate for an increase of the average walking speed through wider aisles and non-destructed ceilings. Carried HL additionally reduces the average walking speed.

The passenger boarding rate is mainly influenced by the passenger throughput of the check-in counters, which is of a stochastic nature [69]. Here, a uniform arrival distribution was assumed. As shown in Figure 5.8, a rate of 15-20 $\frac{PAX}{min}$ for SA and 25-32 $\frac{PAX}{min}$ for TA per door has to be guaranteed to max out the performance of the cabin. If more than one door is used for passenger processes, the rates must be multiples of these values. From a passenger perspective, this results in queuing up in the jetway or on the stairs reducing the experienced level of comfort. A passenger boarding rate in the saturation bandwith is appropriate to max out the cabin performance.

Airlines aim to sell every seat on a flight to reach a high seat LF. Recent trends showed a continuously increasing passenger LF of up to 84 % in 2015 [17], as stated in Section 1.1. On average, this resulted in reduced passenger ingress times of 12-15 % (see Figure 5.9,

p. 80) due to the lower passenger density, shortening queue lengths and increasing movement space for passengers. However, airlines and airports must account for a maximum LF during their infrastructure design and schedule generation to avoid delays where an increase of the LF reduces the operational buffer times.

The amount of HL taken on an aircraft is considerably high since passengers try to avoid extra fees for check-in luggage and shorten their door-to-door travel time by eliminating the extra waiting time at the baggage carrousel. However, the stowing and retrieving of those items increased the average boarding time substantially, especially if the cabin configuration features only one aisle (see Figure 5.10a, p. 81). The increase of the number and size of carried items had a negative impact on the boarding time in the three investigated HL scenarios. Going from a high to a very high degree of HL did not result in huge deviations in the simulations. A time penalty was accounted for the time passengers need to look for a suitable luggage storage space, however if the overhead bins reached their capacity, the process time of bringing the excessive amount of HL out of the cabin was not modeled. In reality, those items have to be stowed in the bulk cargo compartment after the overhead bins reach their capacity which could lead to a delayed boarding process.

In general, the TA provides more luggage storage space due to two additional overhead bins on the cabin centerline. In the HL scenarios considered here, an advantage was identified if the space for large items, such as trolleys, could be increased. Furthermore, an even distribution of the large bags along the cabin is favored, since it provides enough space for each passenger to stow their items close to their seat, thereby reducing the search for a suitable spot in the overhead bins. This could be achieved, if passengers are sorted according to the boarding scheme of Milne and Kelly [83] (see Section 2.3.2). From an airline perspective, a trade-off must be made between the ancillary revenues of check-in baggage and operational costs due to longer ground times or delays.

Cabin layout modifications

The results of the baseline studies, illustrated in Figure 5.6 (p. 78), determined an advantage of 40 % of the TA over the SA for the investigated passenger range. TA configurations allowed for the passenger flow to split into two separate streams after the door, which distributes the passenger more evenly throughout the cabin and shortens the queue lengths. The seat abreast was the decisive parameter within the TA configurations. A six-abreast layout enables a direct aisle access for four out of six seats in one row (see Figure 5.1, p. 73) reducing the row interferences substantially. In the case of an eight-abreast, only half of the passengers have a direct access to the aisle. Thus the passenger density in the aisle and ingress times increased for a larger seat-abreast, as depicted in Figure 5.11 (p. 81). The decision of the best seat abreast for a distinct number of passengers is driven by the fuselage slenderness ratio, which is the fuselage length divided by the diameter [12].

The investigation of different door positions and number of doors was already part of the studies by Fuchte [12]. His results covered an implementation of a quarter door (L2), as well as a scenario with two doors at both cabins ends (L1 and L4). The results presented in Figure 5.12 (p. 82) confirm the previously identified trends showing advantages for a quarter door in a SA configuration compared to a TA. The repositioning of the quarter door near the center of the fuselage (CD) was analyzed and showed efficiency gains of up to 22 %. However, the access of the center door (CD) is challenging due to their position over the wing and only few airports feature a jetbride which is capable to perform passenger processes at this position. Using two doors simultaneously resulted in an efficiency gain of around 30 %.

The queuing up of passengers up to the door due to aisle interferences in the first rows has a negative effect especially for the TA, since both aisles are blocked in this situation. Using a quarter door for boarding is commonly applied in daily operation especially for larger SA and TA aircraft. A dual boarding scenario using L1 and L4 is seen by LCC at remote parking positions. The scenario with the largest performance gain of 42-48 % used the doors L2 and L3. However, the access of the three-quarter door (L3) is challenging due to the close position behind the wing root [37].

The implementation of foldable seats provides a backwards compatible solution to increase the boarding efficiency between 28 % and 35 % for SA and between 17 % and 30 % for the TA (see Figure 5.13a, p. 83). However, the operational applicability of the concepts relies on the certification and passenger acceptance in terms of manageability, integration of inflight amenities and seating comfort. The folding mechanism introduces more complexity, which leads to higher maintenance efforts (ATA 25). Here, it was assumed that a passenger, who unfolded a seat, was not blocking the aisle. The benefits will be radically reduced if this could not be guaranteed during operation. A removal of the metal strap prohibiting HL to move around the cabin affects the stowage of luggage under the seat, which is a major drawback with current high amounts of hand luggage [37, 38]. Furthermore, the seat belt requires a redesign to prevent getting blocked. The concepts are still under development and are partly certified, however they are currently not integrated in commercially used aircraft [90, 92].

As highlighted earlier, the amount of HL had a large impact on the boarding process efficiency. It is common for storage space to be limited, which requires passengers to search for adequate space. An increase of the available storage could reduce those scenarios and the number of items to be stored in the bulk cargo compartment. However, the maximum boarding time reduction was identified to be 4 % considering 30 % more overhead bin space (see Figure 5.13b, p. 83). A more efficient design of the overhead bins increases the number of trolleys to be stored, as shown by Airbus [95] and Boeing [180]. An increase of the total storage volume would require a further reduction of passenger's space or a widening of the fuselage, especially for SA configurations. An easier access of the storage compartments and the prevention of aisle blocking would contribute to a further reduction of the passenger process times instead of increasing the storage space.

Aircraft level assessment

The aircraft configurations were designed with the same baseline layout in terms of doors as well as galley and lavatory space. The SA showed the best performance in terms of fuel burn per passenger nautical mile for the passenger range investigated (see Figure 5.15a, p. 84), where an increasing fuselage diameter is favorable for an increased number of passengers. A fuselage weight shift was noticeable for a diameter of 4.8 m (TA6) where for larger diameters a flattening of the weight increase was identified. Fuchte [12] showed that between 300 and 340 seats a shift exists, where the fuselage mass per passenger is up to 8 % lower for TA compared to SA configurations. The impact of additional OWE due to the folding seats resulted in 1-2 % higher fuel burn, if the weight per seat is 3 kg (6.6 lb).

Turnaround simulations

The turnaround results reflect current airport operations, where the critical path is constituted by cabin processes including passenger egress and ingress, catering or cleaning (see Figure 5.16, p. 85). Here, the catering process is longer than cabin cleaning. These process times are highly dependent on the aircraft operator business model. LCC try to reduce catering and cleaning to a minimum, which further reduces the time dedicated to this processes and hence the total turnaround time. An increased number of cleaners could be employed for the TA configurations to shorten the cleaning time, due to the increased cabin space. Avoiding the usage of doors next to galleys for passenger processes could allow for parallelization of catering and passenger processes. This scenario is possible with the use of a quarter door (L2) or quarter and three-quarter door (L2 and L3).

Recalling the average flight distance of current short-to-medium haul aircraft illustrated in Figure 1.1 (p. 1), only 3 % of the flights in 2014 were 2,000 nm and longer. Hence, the case where the refueling process becomes critical rarely occurred for the investigated range of missions.

The applied passenger simulation module focuses on the detailed analysis of the boarding process and uses statistical equations to determine disembarking times. Hence, deviations to current passenger egress behavior were not accounted for. Since the cabin is deboarded starting with the passengers close to the door until the furthest passengers have left, a marginal impact of the investigated concepts is assumed.

Aircraft operating cost

The analysis of the results on DOC level showed a strong dependency on the average flight mission. The sum of airport charges and COO accounted for 43 % on a 500 nm off-design mission, where their share was reduced to 25 % on the design mission comparing the cost shares for the 240-passenger six-abreast SA on different flight missions (see Figure 5.19a, p. 87). Hence, the impact of ground handling cost reductions or increased utilization was larger on short-haul missions. The disadvantage of a higher OWE had a reduced impact on these missions due to the smaller share of fuel cost.

Higher investment cost of the aircraft due to the integration of novel concepts increases the depreciation, interest and insurance cost of the aircraft. However, the impact on DOC level of an additional USD 1 million was marginal with around 0.3 % (see Figure 5.20, p. 88). The level of increased maintenance effort, in terms of cabin and furnishing expenses (ATA 25), due to missing operational robustness, resulted in 0.1 % higher DOC assuming 10 % higher expenses (see Figure 5.21, p. 88). The discomfort passengers face when a seat is not working as expected or the lost revenue of the airline if individual seats have to blocked during a flight was not accounted for. A malfunction of a foldable seat could also impede a smooth boarding procedure and lead to ground delays in a tight flight schedule.

The ground handling costs scale with the aircraft size and required equipment. Their share accounted for below 5 % of the DOC in all studies. Usually, airlines have SLA with the ground handling providers, which include a specific list of tasks for a fixed price. Here, the direct operating expenses for the executed handling tasks was accounted for. The larger impact of cost reductions can be accomplished on short-haul routes since the number of turnaround events is higher. LCC have proven that the usage of smaller regional airports with lower cost levels, together with a reduced level of service could yield remarkable cost savings [46, 48, 49].

Shorter passenger processes reduce the overall turnaround time, which increases the daily aircraft utilization. As illustrated in Figure 5.23 (p. 89), the largest impact was identified for short-haul operations, where a 40 % turnaround time reduction, as targeted by international regulators [7, 8], yielded up to 5 % reduced DOC. Consequently, airlines have to adapt their flight and maintenance planning to benefit from those time savings. However, often FSC offer various connecting flights to their customers requiring longer ground times. Furthermore, these enormous time savings would have a major impact on all involved stakeholders, such as airports and handling agents. A constraint might be the minimum connecting time (MCT) at airports, which is the required time for passengers and baggage to transfer between two flights. MCT varies between airports and depends on the distances between terminals and gates. An even further reduction of the turnaround might also affect brake-cooling times and cockpit procedures. From a passenger perspective, the booking behavior could be impacted in favor of shorter door-to-door travel times [54].

The German research project ALOHA (Aircraft Design for Low Cost Ground Handling) [71], which investigated new aircraft configurations and GSE to show reduction potential for DOC and ground handling process times, identified up to 4 % higher DOC. This was caused by the additional weight of the proposed high-wing configuration. Here, similar trends with an increasing weight could be identified, however the advantages through optimized passenger procedures could outweigh the weight disadvantage on short-haul routes.

Concepts, such as the foldable seats, which reduce process times, also introduce additional weight. The conducted fuel price sensitivity study shows that the absolute cost of COO, DMC and airport charges remained constant but the share of fuel expenses varies (see Figure 5.24, p. 90). Hence, the level for cost reductions favors lower fuel prices, meaning a weight neutral concept is required to gain cost savings.

5.7.2. Integrated studies

The results of the integrated studies showed that the huge passenger process time savings of 66 % for Study A and 58 % for Study B came with a penalty in terms of higher fuel burn and maintenance cost, which partially outweighed the savings on the DOC level (see Figure 5.29, p. 94). Additional exits along the fuselage were required to comply with current regulations (see Section 2.2.4) and thus increase the fuselage length, if the configuration under investigation did not innately implemented them. Furthermore, the foldable seats added additional weight to the cabin. The parallelization of passenger processes and catering through the repositioning of the doors did not have an impact on the overall turnaround time, since the critical path was constituted by the cleaning process.

Overall, Study A yielded a 1.1 % improvement on the 500 nm distance as the affected cost share is bigger than at design range. For Study B, only a cost neutral outcome was identified (see Figure 5.30). While the savings on the short-haul mission would not justify the investment of an OEM in a new aircraft design program, the gained efficiency improvements could contribute to the next generation of aircraft.

Further concept improvements are required in terms of weight and maintenance to reach a neutral outcome compared to the baseline aircraft. Figure 5.30 shows the results for a scenario with an equal fuselage length as the reference (A.1 and B.1). A weight neutral seat design and an equal fuselage length was analyzed in A.2 and B.2 (see Table 5.4). A scenario with similar fuselage dimensions yielded additional 0.3 % cost savings for Study A.1 and 0.4 % for Study B.1, where similar fuselage dimensions and a weight neutral seat design showed reduced DOC of 1.7 % for Study A.2 and 0.7 % for Study B.2. Hence, a weight neutral design could increase the savings on DOC level by around 1 %. However, an increased fuel price could easily outweigh these advantages even on short-haul missions.

Table 5.4.: Overview of further studies (x - modification present and o - not present).

Study	Additional OWE	Additional Fuselage Length
A/B	x	x
A.1/B.1	x	o
A.2/B.2	o	o

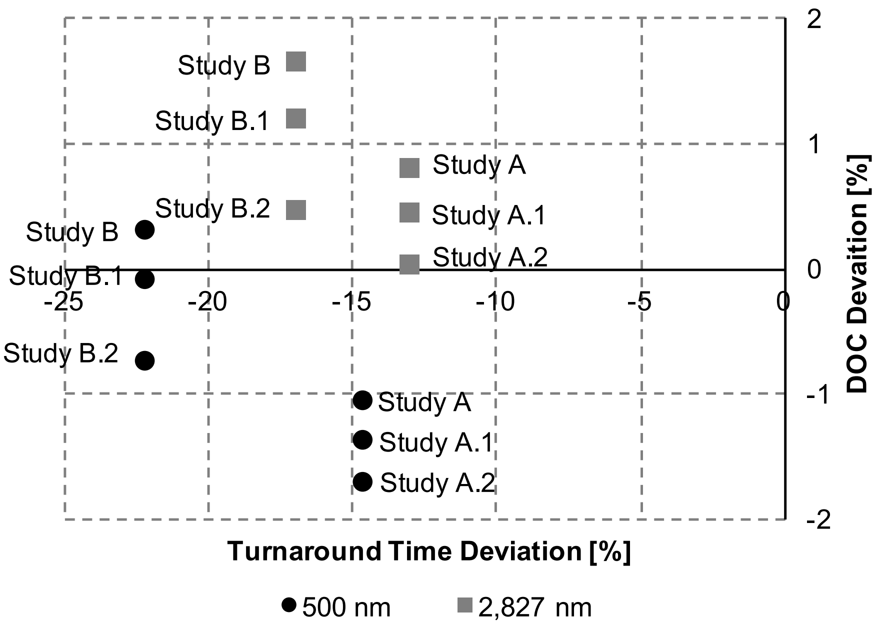

Figure 5.30.: Impact of weight reduction scenarios for investigated case studies.

A further seat weight reduction with the complex folding mechanism is disputable, since current economy aircraft seats are already pushing the weight limits between 5 and 10 kg (11 - 22 lb) per seat using advanced materials and construction techniques [181]. Aircraft seats face challenging certification constraints which limit the design of lighter seats [56, 57]. A shift towards a larger number of passengers is favored for the door layouts, since Study A with 180 passengers required two additional exits compared to the reference.

5.7.3. Recommendations for future aircraft design programs

During the early stages of new aircraft design program, the overall goal of novel cabin concepts is to allow for a seamless passenger egress and ingress through the avoidance of queues caused by aisle and row interferences. This can be achieved through concepts which allow for an adaption of the cabin according to specific requirements of each operational phase, such as seamless luggage stowing and retrieving realized foldable seats. Furthermore, moving the aircraft doors towards the center of the fuselage allows for the passenger flow to split and thus reduces the passenger process times.

The transfer of the passenger process time savings to reduced operating expenses comes often with penalties in terms of additional weight or changed ground handling procedures and equipment. A weight neutral design should always be targeted, since these drawbacks often outweigh the operational benefits. Specific aircraft programs for shorter design missions could maximize the advantages, if a sufficient demand exists on the market.

6. Conclusion and outlook

It is imperative that advancements in all aspects of current aircraft operations are developed based on the forecasted traffic growth rates. The focus here is on the turnaround as the connecting element between airport and aircraft. This special role of the turnaround results in various influences, such as airport capacity constraints, aircraft type diversity, prolonged passenger egress and ingress times, schedule disruptions, as well as airline cost reduction pressure.

A review of current operations and research showed that only a few concepts for novel ground operational and passenger processes have been thoroughly analyzed, even if they could offer large efficiency gains compared to current procedures. Since current models and frameworks are by the majority, not accessible and neither extendable, the development of a holistic assessment framework for advanced ground operational concepts is elaborated.

The framework presented comprises: cabin design heuristics, agent-based passenger flow simulation, turnaround modeling and operational cost assessment, as targeted in the Expected Contribution 1. Mission performance analyses are integrated with trade factors produced with state-of-the-art aircraft design tools. Each module is based on existing approaches which are tailored to the specific requirements of this research. The core of this research is dedicated to the development of the agent-based passenger flow simulation which has been made available for the community[1]. It incorporates a central meta model contributing to Expected Contribution 2. A benchmark with available data of current SA and TA aircraft validated the results. The underestimation of several turnaround processes did not have an impact on the overall turnaround time, as they were not part of the critical path.

The conducted studies covered SA and TA configurations with passenger numbers ranging from 180 to 300. The analyzed sensitivities comprised passenger characteristics, such as the walking speed or the carried HL, and impact of changes to the cabin layout. Furthermore, several single concepts were combined into two case studies aiming to capture cascading effects. This contributed to the Expected Contribution 3 through the identification of promising solutions.

An integrated study based on a six-abreast SA with 180 passengers and LSP showed significant passenger process time savings of 66 %. However, those savings come with

[1] The source code of the agent-based passenger flow simulation "PAXelerate" and any accompanying materials can be obtained from http://www.paxelerate.com [1].

penalties in terms of higher fuel burn and maintenance cost, which almost outweigh the savings on DOC level. A 1.1 % DOC improvement could be accomplished on an off-design mission of 500 nm (926 km). A 58 % shorter boarding time was determined for a second integrated study with 240 passengers in a seven-abreast TA configuration and SFS. A cost neutral outcome was identified on a short haul mission.

The findings of the integrated studies demand for further concept improvements in terms of weight, maintenance effort and their integration into current aircraft configurations. Considering a seamless passenger egress and ingress during the early stages of new aircraft design program should be one design criteria for the next generation of commercial passenger aircraft (Expected Contribution 4).

6.1. Critical assessment of methodology

The developed assessment framework consisted of state-of-the-art modeling approaches for the aircraft design and operating cost estimation as well as newly developed approaches for the passenger flow simulation and turnaround process modeling. The combination of divers software platforms required the specification of in- and output files which can be processes by all framework modules. During the implementation of the passenger flow and turnaround simulation module, the emphasis was on the usage of a coherent meta-model language according to the OMG [141]. However, any change of the program application programming interface (API) requires a continuous coordination of the affected interfaces.

The developed passenger flow simulation module is based on a microscopic approach applying agent-based modeling techniques as it is widely-used to model human behavior (see Section 2.4.2). Despite the detailed representation of the boarding procedure, statistical correlations are applied to estimate process times of the disembarkment. In general, the focus are the key behavior pattern to assess the selected concepts. Therefore, special processes covering passengers with restricted mobility, bulky luggage items, such as instruments, or the late arrival of passengers are disregarded. Furthermore, the walking speed does adapt to the current situation, in terms of agent density or acceleration and deceleration. Agents walk towards their seat and a directional change due to the search for luggage space or using the wrong entrance door is not covered. The input for the passenger characteristics and their distribution as well as the composition of the boarding passengers is based on available literature, which is often not comprehensive enough requiring data interpolation or assumptions.

The turnaround module is based on empirical equations and input distributions to estimate the connection, removal and process times. The quality of the estimations results from the used data. A differentiation of diverse airline service levels in terms of catering or cleaning was not implemented. Furthermore, simplifications in the determination of required resources are incorporated and the preparation time of workers and GSE is disregarded.

The commercial aircraft design software Pacelab APD [156] is commonly used with the aviation industry during the conceptual aircraft design phase. Building on handbook methods and empirical data, this tool investigated the crucial sensitivities of fuselage dimensions and OWE variations on the fuel burn. The foundation of the implemented methods is partially outdated and covers conventional aircraft configurations. Adaptions would be required to analyze advanced configurations.

The DOC approach from Wesseler [162] captures the cost shares for COC, COO and AOC. The ground handling cost estimation could not reflect sensitivities on a process and resource basis and so the methods by Crönertz [112] were adapted and integrated. The unit cost rates for labor and equipment are based on European cost levels and reflect the cost structure of an exemplary ground handling service provider. The model require region specific data for a world-wide application. The same accounts for the air traffic management (ATM) expenses which are based on the Eurocontrol charges.

6.2. Perspectives for future work

Based on the highlighted aspects of the critical assessment of methodology, framework enhancements are discussed in the following. Furthermore, a reasonable increase of the case study design space is explored.

Methods

A coherent meta-model representation was targeted during the implementation of the passenger flow and turnaround simulation. The interfacing with the Common Parametric Aircraft Configuration Scheme (CPACS)[2] data format [182] would enable a direct integration into preliminary aircraft design tools fostering a MDO process based on airport operational constraints. An interfacing with OpenCDT[3] as framework for conceptual aircraft design would allow for a seamless integration.

The passenger flow simulation module should be extended to simulate disembarking procedures as well. The social behavior of passenger traveling in groups of two or more should be accounted for. This becomes important for the assessment of boarding strategies. Using optimization algorithms would allow for the search of the most suited passenger entrance sequence for each concept under investigation. The performance of the A* pathfinding algorithm could be improved using a polygonal cabin representation allowing the passengers to move in straight lines instead of following a grid [183]. A further step would include the application of heuristic search algorithms which use heuristic knowledge in the form

[2]CPACS is available under Apache License 2.0 at http://www.cpacs.de

[3]The source code of OpenCDT and any accompanying materials are available under the terms of the Eclipse Public License (EPL) v1.0 at https://github.com/BauhausLuftfahrt/OpenCDT

of approximations of the goal distances to focus the search and solve search problems faster than uninformed search algorithms [150]. Furthermore, region and aviation specific passenger as well as process data gained through polls and experiments could improve the soundness of the produced results of the passenger flow and turnaround simulations.

Application

The conducted case studies covered a broad scope of sensitivities of SA and TA configurations. In the future, an even wider range of single- and multi-class cabin layouts in regional [184] and long-haul markets should be investigated. This includes the analysis of multi-deck designs with stairs or elevators and layout configurations. Since currently the stowing and retrieving of personal items has a significant impact on the boarding process, novel HL storage solutions should be analyzed. Beyond tube-and-wing aircraft configurations, also non circular cross-sections and BWB configurations could be targeted.

Currently, the view is fixed on a single turnaround event at the airport and interdependencies between stakeholders are neglected. Therefore, a scaling towards a total airport view including multiple stands, airlines and fleets is desirable. This enables the determination of the airport capacity in terms of gate utilization based on flight schedules. Building upon the identified aircraft ground performance and operating economics, an evaluation of the operational integration into current operations and airline fleets should be aspired. Furthermore, a profit-based evaluation from an airline-perspective could allow for a demand driven analysis on fleet-level.

References

[1] M. Schmidt. PAXelerate Release 1.0, Github Repository. 2017.

[2] Airbus. Global Market Forecast - Growing Horizons 2016-2035. Technical report, 2017. URL `http://www.airbus.com/company/market/forecast/`.

[3] Boeing. Current Market Outlook 2017-2036. Technical report, 2017.

[4] Advisory Council for Aeronautical Research in Europe (ACARE). European Aeronautics: A Vision for 2020. Technical Report January, 2001.

[5] Air Transport Action Group (ATAG). The Global Flightplan. In *Proceedings of the 19th Conference of the Parties (COP19) to the United Nations Framework Convention on Climate Change, updated with the results of the 38th ICAO Assembly*, number November, 2013.

[6] NASA. Advanced Air Vehicle Program, 2016. URL `http://www.aeronautics.nasa.gov/programs-aavp.htm`.

[7] Advisory Council for Aviation Research and Innovation in Europe (ACARE). Strategic Research & Innovation Agenda (SRIA) - Volume 1. Technical report, Brussels, 2012.

[8] Advisory Council for Aviation Research and Innovation in Europe (ACARE). Strategic Research & Innovation Agenda (SRIA) - Volume 2. Technical report, Brussels, 2012.

[9] OAG (Official Airline Guide). Scheduled Flight Database, 2016.

[10] H. Fricke and M. Schultz. Improving Aircraft Turn Around Reliability. In *Third International Conference on Research in Air Transportation*, pages 335–343, 2008. ISBN 9780615207209.

[11] N. J. Ashford, H. M. Stanton, C. A. Moore, P. Coutu, and J. R. Beasley. *Airport Operations*. McGraw-Hill, 3rd edition, 2013. ISBN 978-0-07-177585-4.

[12] J. C. Fuchte. *Enhancement of Aircraft Cabin Design Guidelines with Special Consideration of Aircraft Turnaround and Short Range Operations*. Dissertation, Technische Universität Hamburg-Harburg, 2014.

[13] Airbus. Airbus offers added seating capacity for the A320 Family while retaining modern comfort standards, 2014. URL `https://goo.gl/L2Rb1j`.

[14] Boeing. Boeing Launches 737 MAX 200 with Ryanair, 2014. URL `http://boeing.mediaroom.com/2014-09-08-Boeing-Launches-737-MAX-200-with-Ryanair`.

[15] M. Schmidt, K. O. Plötner, C. Pornet, A. T. Isikveren, and M. Hornung. Contributions of Cabin Related and Ground Operation Technologies Towards Flightpath 2050. In *Deutscher Luft- und Raumfahrtkongress 2013 (DLRK)*, Stuttgart, Germany, 2013.

[16] S. Marelli, G. Mattocks, and R. Merry. The role of computer simulation in reducing airplane turn time. *Boeing Aero Magazine*, (1), 1998.

[17] MIT. Airline Data Project, 2016. URL `http://web.mit.edu/airlinedata/www/default.html`.

[18] C. Schinwald and M. Hornung. Methodical Approach to Determining the Capacity Utilisation of Airports: the Development of the European Air Traffic System between 2008 and 2013. In *Deutscher Luft- und Raumfahrtkongress 2014 (DGLR)*, Augsburg, Germany, 2014.

[19] K. Andersson, F. Carr, E. Feron, and W. D. Hall. Analysis and Modeling of Ground Operations at Hub Airports. In *3rd USA/Europe Air Traffic Management R&D Seminar*, number June, pages 13–16, 2000. doi: 10.1109/JSTSP.2013.2237882.

[20] H. Balakrishnan, I. Deonandan, and I. Simaiakis. Opportunities for Reducing Surface Emissions through Airport Surface Movement Optimization. Technical Report ICAT-2008-07, MIT International Center for Air Transportation (ICAT), Cambridge, USA, 2008.

[21] Eurocontrol. CODA - Delays to Air Transport in Europe - Annual 2014. Technical report, 2014.

[22] C.-L. Wu and R. E. Caves. Modelling and optimization of aircraft turnaround time at an airport. *Transportation Planning and Technology*, 27(1):47–66, feb 2004. doi: 10.1080/0308106042000184454.

[23] I. Silverio, A. Juan, and P. Arias. A Simulation-Based Approach for Solving the Aircraft Turnaround Problem. In M. Fernández-Izquierdo, M. Muñoz-Torres, and R. León, editors, *Modeling and Simulation in Engineering, Economics, and Management SE - 18*, volume 145 of *Lecture Notes in Business Information Processing*, pages 163–170. Springer Berlin Heidelberg, 2013. ISBN 978-3-642-38278-9. doi: 10.1007/978-3-642-38279-6_18.

[24] Y. Suzuki. The relationship between on-time performance and airline market share: A new approach. *Transportation Research Part E: Logistics and Transportation Review*, 36(2):139–154, 2000. doi: 10.1016/S1366-5545(99)00026-5.

[25] S. AhmadBeygi, A. Cohn, and M. Lapp. Decreasing airline delay propagation by re-allocating scheduled slack. *IIE Transactions*, 42(7):478–489, apr 2010. doi: 10.1080/07408170903468605.

[26] M. Schmidt. The five minute turnaround - a reasonable goal? An overview of ongoing ground operations research. In *9th Asian Ground Handling International Conference*, Invited talk, Indonesia, 2016.

[27] M. Mirza. Economic Impact of Airplane turn-times. *Boeing Aero Magazine*, pages 15–19, 2008.

[28] D. Gillen and A. Lall. Competitive advantage of low-cost carriers: Some implications for airports. *Journal of Air Transport Management*, 10:41–50, 2004. doi: 10.1016/j.jairtraman.2003.10.009.

[29] A. M. Pilarski. *Why Can't We Make Money in Aviation?* Ashgate Publishing Ltd, Hampshire, England, 2007. ISBN 9780754649113.

[30] D. More and R. Sharma. The turnaround time of an aircraft: a competitive weapon for an airline company. *DECISION*, 41(4):489–497, 2014. doi: 10.1007/s40622-014-0062-0.

[31] International Air Transport Association (IATA). Airline Cost Performance. Technical report, 2006.

[32] E. Clayton and A. Hilz. Industry perspectives - 2015 Aviation Trends, 2015. URL `http://www.strategyand.pwc.com/perspectives/2015-aviation-trends`.

[33] T. I. Consortium. D3.6 Solutions Summary Report. Technical Report October, 2014.

[34] The 2050+ Airport Consortium. D4.1 - The Time-Efficient Airport Concept - An operational concept for 2050 and beyond. Technical report, 2013.

[35] The 2050+ Airport Consortium. D4-2 The Ultra-Green Airport Concept - An operational concept for 2050 and beyond. Technical report, 2013.

[36] The 2050+ Airport Consortium. D4-3 The Cost-Effective Airport Concept - An operational concept for 2050 and beyond. Technical report, 2013.

[37] M. Schmidt, P. Heinemann, and M. Hornung. Boarding and Turnaround Process Assessment of Single- and Twin-Aisle Aircraft. In *55th AIAA Aerospace Sciences Meeting*, AIAA SciTech Forum, Dallas, Texas, USA, 2017. American Institute of Aeronautics and Astronautics. doi: 10.2514/6.2017-1856.

[38] M. Schmidt, M. Engelmann, R. Rothfeld, and M. Hornung. Boarding Process Assessment of Novel Aircraft Cabin Concepts. In *30h International Congress of the Aeronautical Sciences - ICAS*, Daejoun, South Korea, 2016.

[39] J. Roskam. *Airplane Design - Part III: Layout Design of Cockpit, Fuselage, Wing and Empennage: Cutaways and Inboard Profiles.* Design Analysis & Research, Kansas, 1989.

[40] M. Schmidt, M. Engelmann, T. Brügge-Zobel, M. Hornung, and M. Glas. PAXelerate - An Open Source Passenger Flow Simulation Framework for Advanced Aircraft Cabin Layouts. In *54th AIAA Aerospace Sciences Meeting*, AIAA SciTech. American Institute of Aeronautics and Astronautics, San Diego, USA, jan 2016. doi: 10.2514/6.2016-1284.

[41] R. Callahan. Impact of the Next Two Aircraft Generations on Airport Design. In *AIAA 7th Annual Meeting and Technical Display*, Houston, Texas, 1970.

[42] R. W. K. Leung, J. W. Little, and D. C. H. Li. Getting Ready for the A380 Aircraft at Hong Kong International Airport. In *2007 FAA Worldwide Airport Technology Transfer Conference*, number April, Atlantic City, New Jersey, USA, 2007.

[43] M. Schmidt, A. Paul, M. Cole, and K. O. Plötner. Challenges for ground operations arising from aircraft concepts using alternative energy. *Journal of Air Transport Management*, 56(sep):107–117, sep 2016. doi: 10.1016/j.jairtraman.2016.04.023.

[44] D. Gaábor. Low-cost Airlines in Europe: Network Structures After the Enlargement of the European Union. *Geographica Pannonica*, 14(2):49–58, 2010.

[45] N. K. Taneja. *Designing Future-Oriented Airline Businesses.* Ashgate Publishing Ltd, Farnham, UK, 2014. ISBN 9781317152163.

[46] F. Dobruszkes, M. Givoni, and T. Vowles. Hello major airports, goodbye regional airports? Recent changes in European and US low-cost airline airport choice. *Journal of Air Transport Management*, 59:50–62, mar 2017. doi: 10.1016/j.jairtraman.2016.11.005.

[47] F. Dobruszkes. An analysis of European low-cost airlines and their networks. *Journal of Transport Geography*, 14:249–264, 2006. doi: 10.1016/j.jtrangeo.2005.08.005.

[48] S. D. Barrett. How do the demands for airport services differ between full-service carriers and low-cost carriers? *Journal of Air Transport Management*, 10:33–39, 2004. doi: 10.1016/j.jairtraman.2003.10.006.

[49] S. Calder. *No Frills – The Truth Behind the Low-Cost Revolution in the Skies.* Virgin Books, 2006. ISBN 978-0753510445.

[50] T. Lawton. *Cleared for Take-Off – Structure and Strategy in the Low Fare Airline Business*. Ashgate, Aldershot, 2002.

[51] P. Morrell. Airlines within airlines: An analysis of US network airline responses to Low Cost Carriers. *Journal of Air Transport Management*, 11(5):303–312, September 2005. doi: 10.1016/j.jairtraman.2005.07.002.

[52] G. Williams. Will Europe's charter carriers be replaced by „no-frills" scheduled airlines? *Journal of Air Transport Management*, 7(5):277–286, September 2001. doi: 10.1016/S0969-6997(01)00022-9.

[53] R. De Neufville. Low-Cost Airports for Low-Cost Airlines: Flexible Design to Manage the Risks. *Transportation Planning and Technology*, 31(January 2015):35–68, 2008. doi: 10.1080/03081060701835688.

[54] M. Schmidt, P. Nguyen, and M. Hornung. Novel Aircraft Ground Operation Concepts Based on Clustering of Interfaces. In *SAE International*, 2015-01-2401, Seattle, USA, sep 2015. doi: 10.4271/2015-01-2401.

[55] International Air Transport Association (IATA). Airport Handling Manual (AHM) - 34th Edition. Technical report, 2013.

[56] European Aviation Safety Agency (EASA). Certification Specifications for Large Aeroplanes CS-25, 2009.

[57] Federal Aviation Administration (FAA). Federal Aviation Regulations (FAR) Part 25 - Airworthiness Standards: Transport Category Airplanes, 2015.

[58] A. H. Midkiff, R. J. Hansman, and T. G. Reynolds. Air carrier flight operations. Technical Report ICAT-2004-03, MIT International Center for Air Transportation (ICAT), 2004.

[59] Airbus. A320 - Aircraft Characteristics Airport and Maintenance Planning. Technical report, 2015.

[60] H. Fricke and M. Schultz. Delay Impacts onto Turnaround Performance. In *USA/Europe Air Traffic Management Research and Development Seminar*, Napa, USA, 2009.

[61] C.-L. Wu. Monitoring Aircraft Turnaround Operations: Framework Development, Application and Implications for Airline Operations. *Transportation Planning and Technology*, 31(2):215–228, apr 2008. doi: 10.1080/03081060801948233.

[62] N. Easen. Business travel gets a female touch, 2013. URL `http://www.bbc.com/travel/blog/20130213-business-travel-gets-a-female-touch`.

[63] NEA. Survey on standard weights of passengers and baggage. Technical report, Zoetermeer, 2009.

[64] U.S. Department of Health and Human Services. Anthropometric Reference Data for Children and Adults: United States, 2007-2010. Technical Report 252, 2010.

[65] A. Strässle. Holländischer Weitblick, sep 2007. URL `http://www.nzz.ch/aktuell/startseite/hollaendischer-weitblick-1.549440#`.

[66] M. H. L. Van Den Briel, J. R. Villalobos, G. L. Hogg, T. Lindemann, and A. V. Mulé. America west airlines develops efficient boarding strategies. *Interfaces*, 35(3): 191–201, 2005. doi: 10.1287/inte.1050.0135.

[67] B. Yuan, J. Yin, and M. Wang. STAR: (Saving Time, Adding Revenues) Boarding/Deboarding Strategy. *UMAP Journal*, 28(3):371–384, 2007.

[68] H. S. Appel. *Analyse der Verzögerungen beim Boarding von Flugzeugen und Untersuchung möglicher Optimierungsansätze.* Dissertation, Rheinisch-Westfälischen Technischen Hochschule Aachen, 2014.

[69] M. Schultz, T. Kunze, and H. Fricke. Boarding on the critical path of the turnaround. In *Tenth USA/Europe Air Traffic Management Research and Development Seminar (ATM2013)*, Chicago, USA, 2013.

[70] European Comission. Comission Regulation (EC) No 859/2008. Technical Report July, 2008.

[71] D. Scholz, P. Krammer, and D. R. Sánchez. Schlussbericht FHprofUnd-Projekt "ALOHA" - Flugzeugentwurf für kostenoptimierten Bodenabfertigung. Technical report, Hamburg University of Applied Sciences, Hamburg, 2011.

[72] Deutsches Zentrums für Luft- und Raumfahrt (DLR). ASSET - D0.12 Project Final Report. Technical report, 2011.

[73] S. Zerkowitz and A. C. S. Sánchez. TITAN - Turnaround Integration in Trajectory and Network - The Book. Technical report, European Commission.

[74] R. M. Keown. E-cab - final activity report. Technical report, 2006.

[75] NLR. FANTASSY Project Homepage, 2014. URL `http://fantassy.nlr.nl/`.

[76] Bauhaus Luftfahrt e.V. Interdisciplinary cooperation in the research field of radical cabin architectures and novel ground handling processes, 2013.

[77] M. Stegmiller. *Detailed Design of a Multifunctional Aircraft Ground Handling Vehicle.* Semester thesis, Technische Universität München, 2014.

[78] M. Schmidt. Handling Innovation - Tomorrows Turn? *Ground Handling International*, December:42–43, 2015.

[79] D. C. Nyquist and K. L. McFadden. A study of the airline boarding problem. *Journal of Air Transport Management*, 14(4):197–204, 2008. doi: 10.1016/j.jairtraman.2008.04.004.

[80] F. Jaehn and S. Neumann. Airplane boarding. *European Journal of Operational Research*, 244(2):339–359, 2014. doi: 10.1016/j.ejor.2014.12.008.

[81] J. H. Steffen. Optimal boarding method for airline passengers. *Journal of Air Transport Management*, 14(3):146–150, 2008. doi: 10.1016/j.jairtraman.2008.03.003.

[82] J. H. Steffen and J. Hotchkiss. Experimental test of airplane boarding methods. *Journal of Air Transport Management*, 18(1):64–67, jan 2012. doi: 10.1016/j.jairtraman.2011.10.003.

[83] R. J. Milne and A. R. Kelly. A new method for boarding passengers onto an airplane. *Journal of Air Transport Management*, 34:93–100, 2014. doi: 10.1016/j.jairtraman.2013.08.006.

[84] H. Zeineddine. A dynamically optimized aircraft boarding strategy. *Journal of Air Transport Management*, 58:144–151, 2017. doi: 10.1016/j.jairtraman.2016.10.010.

[85] R. Cimler and K. Olševičová. Analysis Simulation of aircraft disembarking methods. In *Proceedings of 3rd World Conference on Information Technology (WCIT-2012)*, volume 03, pages 867–872, Barcelona, Spain, 2013.

[86] H. S. Appel. Einsetzbarkeit gezielter Aussteigevarianten beim Deboarding von Flugzeugen. In *Deutscher Luft- und Raumfahrtkongress 2010 (DLRK)*, Hamburg, Germany, 2010.

[87] Boeing. B737 ? Airplane Characteristics for Airport Planning. Technical report, 2013.

[88] AviationPros. Between Narrow and Wide-Body: Is There an Aircraft for the Niche Midsize Market?, 2016. URL `https://goo.gl/bjRQqS`.

[89] M. M. K. V. Sankrithi. Twin aisle small airplane, 2004.

[90] S. Engineering. Foldable Passenger Seat - SII Group - The Aida way. URL `http://www.sii-engineering.de/en/projects_passenger_seat`.

[91] M. Hertl. *Bewertung einer Klappsitzoption in Hinblick auf Bewegungsabläufe in der Fluggastkabine eines Verkehrsflugzeugs*. PhD thesis, Technische Universität Berlin, 2005.

[92] M. L. Designs. Side-Slip Seat, 2016. URL `http://www.airlineseats.biz`.

[93] A. T. Isikveren, A. Seitz, P. C. Vratny, C. Pornet, K. O. Plötner, and M. Hornung. Conceptual Studies of Universally-Electric Systems Architectures Suitable for Transport Aircraft. In *61. Deutscher Luft- und Raumfahrtkongress 2012 (DLRK)*, Berlin, Germany, 2012.

[94] M. Götz. *Engineering Concept Study of an Innovative Sideward Retractable Aircraft Seat.* Diploma thesis, Technische Universität München, 2014.

[95] Airbus. Airbus launches new pivoting overhead carry-on stowage bins for A320 Family with order from Delta Air Lines, 2014. URL `https://goo.gl/JAZGdK`.

[96] B. Mutzabaugh. First look: Boeing's new 'Space Bins' expand carry-on capacity, 2015. URL `http://www.usatoday.com/story/todayinthesky/2015/10/09/will-boeings-new-space-bins-help-ease-the-airline-carry-on-crunch/73577640/`.

[97] Bundesverband der Deutschen Luft- und Raumfahrtindustrie e.V. (BDLI). IMAGINE..., 2013. URL `http://bdli.de/index.php?option=com_content&view=article&id=2622`.

[98] F. L. Levy, G. L. Thompson, and J. D. Weist. The ABCs of the CRITICAL PATH Method. *Harvard Business Review*, 41(5):98–108, 1963.

[99] J. P. Braaksma and J. H. Shortreed. Improving airport gate usage with critical path. *Transportation Engineering Journal of ASCE*, 97(2):187–203, 1971.

[100] B. Page, N. Knaaka, and S. Kruse. A discrete event simulation framework for agent-based modelling of logistic systems. In *INFORMATIK 2007: Informatik trifft Logistik*, pages 397–404, 2007. URL `http://subs.emis.de/LNI/Proceedings/Proceedings109/gi-proc-109-072.pdf`.

[101] E. Bonabeau. Agent-based modeling: methods and techniques for simulating human systems. *PNAS*, 99(suppl. 3):7280–7287, 2002. doi: 10.1073/pnas.082080899.

[102] W. Ip, V. Cho, N. Chung, and G. Ho. A Multi Agent Based Model for Airport Service Planning. *International Journal of Engineering Business Management*, 2 (2):1, 2010. doi: 10.5772/9718.

[103] A. Vidosavljević and V. Tosić. Modeling of turnaround process using petri nets. In *14th Air Transport Research Society (ATRS) World Conference*, Porto, Portugal, 2010.

[104] P. G. Voulgarellis, M. A. Christodoulou, and Y. S. Boutalis. A MATLAB Based Simulation Language for Aircraft Ground Handling Operations at Hub Airports (SLAGOM). *Proceedings of the 2005 IEEE International Symposium on Mediterrean Conference on Control and Automation Intelligent Control 2005*, 2005. doi: 10.1109/.2005.1467037.

[105] G. Ioannidis, M. A. Christodoulou, and Y. S. Boutalis. A SIMULINK Based Simulation Language for Aircraft Simulation of Ground Handling Operations at Hub Airports (SSLA). *Proceedings of the 2005 IEEE International Symposium on Mediterrean Conference on Control and Automation Intelligent Control 2005*, 2005. doi: 10.1109/.2005.1467038.

[106] K. Andersson. *Potential Benefits of Information Sharing During the Arrival Process At Hub Airports*. Master thesis, Massachusetts Institute of Technology, 2000.

[107] C.-L. Wu and R. E. Caves. Modelling and simulation of aircraft turnaround operations at airports. *Transportation Planning and Technology*, 27(1):25–46, feb 2004. doi: 10.1080/0308106042000184445.

[108] M. M. Mota, N. D. Bock, G. Boosten, E. Jimenez, and J. Pinho. Simulation-based turnaround evaluation for lelystad airport. In *Air Transport Research Society World Conference*, 2015.

[109] A. Norin, T. A. Granberg, D. Yuan, and P. Värbrand. Airport logistics - A case study of the turn-around process. *Journal of Air Transport Management*, 20(0): 31–34, may 2012. doi: 10.1016/j.jairtraman.2011.10.008.

[110] R. Automation. Arena simulation software, 2016. URL `https://www.arenasimulation.com/`.

[111] Y. Tian, H. Liu, H. Feng, B. Wu, and G. Wu. Virtual Simulation-Based Evaluation of Ground Handling for Future Aircraft Concepts. *Journal of Aerospace Information Systems*, 10(5):218–228, may 2013. doi: 10.2514/1.49836.

[112] O. Crönertz. *Prozessorientierte Kalkulation von Flughafenleistungen: Schwerpunkt: Bodenabfertigungsdienste von Passagierflugzeugen*. Vdm Verlag Dr. Müller, 2008. ISBN 978-3836484602.

[113] Airport Research Center. CAST Ground Handling, 2015. URL `http://www.airport-consultants.com`.

[114] M. Bevilacqua, F. E. Ciarapica, G. Mazzuto, and C. Paciarotti. The impact of business growth in the operation activities: a case study of aircraft ground handling operations. *Production Planning & Control*, 26(7):564–587, may 2015. doi: 10.1080/09537287.2014.939234.

[115] ProSim. ProSimPlus - Steady-state simulation and optimization of processes. URL `http://www.prosim.net`.

[116] Lanner. WITNESS - predictive simulation software for modelling and application development. URL `http://www.lanner.com/technology/witness-simulation-software.html`.

[117] B. Oreschko, M. Schultz, J. Elflein, and H. Fricke. Significant Turnaround Process Variations due to Airport Characteristics. In *Air Transport & Operations Symposium 2010*, Delft, Netherlands, 2010.

[118] A. Schlegel. *Bodenabfertigungsprozesse im Luftverkehr: Eine statistische Analyse am Beispiel der Deutschen Lufthansa AG am Flughafen Frankfurt/Main.* 2010. ISBN 978-3-8349-8691-7. doi: 10.1007/978-3-8349-8691-7_2.

[119] D. R. Sanchez. *Analysis of Ground Handling Characteristics of Innovative Aircraft Configurations.* Master thesis, Hamburg University of Applied Science, 2009.

[120] E. Bachmat, D. Berend, L. Sapir, S. Skiena, and N. Stolyarov. Analysis of aeroplane boarding via spacetime geometry and random matrix theory. *Journal of Physics A: Mathematical and General*, 39(29):L453–L459, 2006. doi: 10.1088/0305-4470/39/29/L01.

[121] E. Bachmat, D. Berend, L. Sapir, S. Skiena, and N. Stolyarov. Analysis of Airplane Boarding Times. *Operations Research*, 57(2):499–513, 2009. doi: 10.1287/opre.1080.0630.

[122] M. H. L. V. D. Briel, J. R. Villalobos, and G. L. Hogg. The Aircraft Boarding Problem. In *Proceeding of the 12th Industrial Engineering Research Conference (IERC-2003)*, Portland, Oregon, 2003.

[123] M. Bazargan. A linear programming approach for aircraft boarding strategy. *European Journal of Operational Research*, 183(1):394–411, 2007. doi: 10.1016/j.ejor.2006.09.071.

[124] M. Soolaki, I. Mahdavi, N. Mahdavi-Amiri, R. Hassanzadeh, and A. Aghajani. A new linear programming approach and genetic algorithm for solving airline boarding problem. *Applied Mathematical Modelling*, 36(9):4060–4072, sep 2012. doi: 10.1016/j.apm.2011.11.030.

[125] H. Van Landeghem and a. Beuselinck. Reducing passenger boarding time in airplanes: A simulation based approach. *European Journal of Operational Research*, 142(2):294–308, oct 2002. doi: 10.1016/S0377-2217(01)00294-6.

[126] P. Ferrari and K. Nagel. Robustness of Efficient Passenger Boarding Strategies for Airplanes. *Transportation Research Record*, 1915(1):44–54, 2005. doi: 10.3141/1915-06.

[127] R. Livermore. *A multi-agent system approach to a sumulation study comparing the performance of aircraft boarding using pre-assigned seating and free-for-all strategies.* Master thesis, Open University, 2008.

[128] J. Audenaert, K. Verbeeck, and G. V. Berghe. Multi-agent based simulation for boarding. In *Proceedings of the 21st Benelux Conference on Artificial Intelligence*, 2009. URL http://wwwis.win.tue.nl/~bnaic/2009/papers/bnaic2009_paper_38.pdf.

[129] R. Cimler, E. Kautzká, K. Olševičová, and M. Gavalec. Agent-based model for comparison of aircraft boarding methods. *Proceedings of 30th International Conference Mathematical Methods in Economics Agent-based*, pages 73–78, 2012.

[130] U. Wilensky. NetLogo - a multi-agent programmable modeling environment, 2016. URL https://ccl.northwestern.edu/netlogo/.

[131] S.-J. Qiang, B. Jia, D.-F. Xie, and Z.-Y. Gao. Reducing airplane boarding time by accounting for passengers' individual properties: A simulation based on cellular automaton. *Journal of Air Transport Management*, 40(0):42–47, aug 2014. doi: 10.1016/j.jairtraman.2014.05.007.

[132] M. Schultz. *Entwicklung eines individuenbasierten Modells zur Abbildung des Bewegungsverhaltens von Passagieren im Flughafenterminal*. Dissertation, Technische Universität Dresden, 2010.

[133] A. Steiner and M. Philipp. Speeding up the airplane boarding process by using preboarding areas boarding areas. In *9th Swiss Transportation Conference*, Ascona, Switzerland, 2009.

[134] F. safety engineering group. AirExodus, 2015. URL http://fseg.gre.ac.uk/exodus.

[135] D. Z. für Luft-und Raumfahrt (DLR). Traffic Oriented Microscopic Simulator - TOMICS, 2011. URL http://www.dlr.de/fw/en/desktopdefault.aspx/tabid-5980/9752/read-19750.

[136] Airport Research Center. CAST Cabin, 2015. URL http://www.airport-consultants.com.

[137] T. Richter. *Simulationsmethodik zur Effizienz- und Komfortbewertung von Menschenflussprozessen in Verkehrsflugzeugen*. Dissertation, Technische Universität München, 2007.

[138] E. R. Winkler, J. French, G. E. Mattocks, and J. J. Konesky. Aircraft Passenger Flow System. Technical Report US 8,510,086 B1, 2013.

[139] Aircraft seat maps, flight shopping and flight information, 2017. URL https://www.seatguru.com/.

[140] C. Macal and M. North. Introductory Tutorial: Agent-Based Moedeling and Simulation. In *Proceedings of the 2014 Winter Simulation Conference*, pages 6–20, Savannah, USA, 2014. ISBN 9781479974863.

[141] Object Management Group (OMG). Meta Object Facility (MOF) - Core Specification. Technical Report April, 2014. URL `http://www.omg.org/spec/MOF/2.0/`.

[142] D. Steinberg, F. Budinsky, M. Paternostro, and E. Merks. *EMF: Eclipse Modeling Framework*. Addison-Wesley Professional, 2nd edition, 2008. ISBN 978-0321331885.

[143] E. Merks. Eclipse Modeling Framework - Interview with Ed Merks - JAXenter, 2010. URL `https://jaxenter.com/eclipse-modeling-framework-interview-with-ed-merks-100007.html`.

[144] T. H. Cormen, C. E. Leiserson, R. L. Rivest, and C. Stein. *Introduction to algorithms*. MIT Press, 3rd edition, 2009. ISBN 978-0-262-03384-8.

[145] Nuber, Mast, Junker, Heuer, Schmidt, and Richter. *Menschenmassen-Simulation - Allgemeines, Konzepte, Ansätze*. 2004.

[146] Y. Liu, W. Wang, H. Z. Huang, Y. Li, and Y. Yang. A new simulation model for assessing aircraft emergency evacuation considering passenger physical characteristics. *Reliability Engineering and System Safety*, 121:187–197, 2014. doi: 10.1016/j.ress.2013.09.001.

[147] Weidmann. Transporttechnik der Fußgänger. Technical Report 90, ETH Zurich, 1992.

[148] Engineering route planning algorithms. *Lecture Notes in Computer Science (including subseries Lecture Notes in Artificial Intelligence and Lecture Notes in Bioinformatics)*, 5515 LNCS:117–139, 2009. doi: 10.1007/978-3-642-02094-0_7.

[149] A. Patel. Stanford University - Game programming, 2010. URL `http://theory.stanford.edu/~amitp/GameProgramming/index.html`.

[150] P. Hart, N. Nilsson, and B. Raphael. A Formal Basis for the Heuristic Determination of Minimum Cost Paths. *IEEE Transactions on Systems Science and Cybernetics*, 4(2):100–107, 1968. doi: 10.1109/TSSC.1968.300136.

[151] E. Torenbeek. *Advanced Aircraft Design*. Wiley, 2013. ISBN 9781118568118.

[152] E. Torenbeek. *Synthesis of Subsonic Airplane Design*. Delft University Press, Delft, 1982. ISBN 978-94-017-3202-4.

[153] L. R. Jenkinson, P. Simpkin, and D. Rhodes. *Civil Jet Aircraft Design*. Arnold, Bodmin, Cornwall, 1999. ISBN 978-0340741528.

[154] A. Seitz. *Advanced Methods for Propulsion System Integration in Aircraft Conceptual Design*. Dissertation, Technische Universität München, 2012.

[155] H. C. Briggs. A Survey of Integrated Tools for Air Vehicle Design, Part I. In *56th AIAA/ASCE/AHS/ASC Structures, Structural Dynamics, and Materials Conference*, number January in AIAA SciTech, pages 1–13, Reston, Virginia, jan 2015. American Institute of Aeronautics and Astronautics. ISBN 978-1-62410-342-1. doi: doi:10.2514/6.2015-0802.

[156] Pacelab. Pacelab Aircraft Preliminary Design (APD) website, 2016. URL `https://www.pace.de/products/preliminary-design/pacelab-apd.html`.

[157] Raymer P. *Aircraft Design: A Conceptual Approach Fourth Edition*. AIAA eduction series, Reston, 4th edition, 2006. ISBN 978-1563478291.

[158] F. Dorbarth. *Luftfahrttechnisches Handbuch (LTH): Civil Jet Transport Aircraft - Statistical Mass Estimation*. Number MA 401 12-01. IASB, 2006.

[159] S. Weber. *Assessment of novel cabin layouts during the aircraft design process*. Semester thesis, Technische Universität München, 2015.

[160] T. Horstmeier and F. D. Haan. Influence of ground handling on turn round time of new large aircraft. *Aircraft Engineering and Aerospace Technology*, 73(3):266–270, 2001.

[161] R. Curran, S. Raghunathan, and M. Price. Review of aerospace engineering cost modelling: The genetic causal approach. *Progress in Aerospace Sciences*, 40(8): 487–534, nov 2004. doi: 10.1016/j.paerosci.2004.10.001.

[162] P. Wesseler. *Determination of aircraft life cycle cost during conceptual design phase*. Diploma thesis, Technische Universität München, 2011.

[163] K. O. Plötner, M. Cole, M. Hornung, A. T. Isikveren, P. Wesseler, and C. Essling. Influence of Aircraft Parameters on Aircraft Market Price. In *61st Deutscher Luft- und Raumfahrtkongress (DLRK)*, Berlin, Germany, 2012.

[164] A. T. Isikveren. Identifying Economically Optimal Flight Techniques of Transport Aircraft. *Journal of Aircraft*, 39(4):528–544, jul 2002. doi: 10.2514/2.2982.

[165] AEA. Operating Economy of AEA Airlines 2007. Technical Report December 2007, 2007.

[166] Transport Studies Group. Aircraft Crewing - Marginal Delay Costs. Technical Report October, University of Westminster, London, 2008.

[167] International Air Transport Association. Airport & Air Navigation Charges Manual. Technical Report 22, Montreal, 2008.

[168] O. C. Rupp. *Vorhersage von Instandhaltungskosten bei der Auslegung ziviler Strahltriebwerke*. Dissertation, Technische Universität München, 2000.

[169] K. Khan and G. Houston. Design Optimization using Life Cycle Cost Analysis for Low Operating Costs. In *Bombardier Aerospace Downsview*, number October, Ontario, 2000. URL `http://oai.dtic.mil/oai/oai?verb=getRecord&metadataPrefix=html&identifier=ADP010423`.

[170] Air Transport Association of America. ATA Specification 100 - Specification for Manufacturers' Technical Data. Technical report, Revision No. 37, 1999.

[171] K. O. Plötner, P. Wesseler, and P. Phleps. Identification of key aircraft and operational parameters affecting airport charges. *International Journal of Air Transport Management*, 2(1/2):91–115, 2013.

[172] International Civil Aviation Organization (ICAO). Engine Exhaust Emissions Databank, Doc 9646- AN/943. Technical report, 2014.

[173] K. O. Plötner, P. Wesseler, and P. Phleps. Identification of Key Aircraft Parameters Related to Airport Charge Quantification. In *15th Air Transport Research Society (ATRS) World Conference*, Sydney, Australia, 2011.

[174] Airbus. A330 - Aircraft Characteristics Airport and Maintenance Planning. Technical report, 2014.

[175] K. Risse, K. Schäfer, F. Schültke, and E. Stumpf. Central Reference Aircraft data System (CeRAS) for research community. *CEAS Aeronautical Journal*, 7(1):121–133, 2016. doi: 10.1007/s13272-015-0177-9.

[176] FRED - Economic Research. Gross Domestic Product: Implicit Price Deflator, 2017. URL `https://fred.stlouisfed.org/series/GDPDEF/`.

[177] X-Rates. Monthly average conversion rates, 2017. URL `http://www.x-rates.com/average/?from=USD&to=EUR&amount=1&year=2016`.

[178] M. D. Byrne. How many times should a stochastic model be run? An approach based on confidence intervals. pages 445–450, Ottawa, Canada, 2013.

[179] International Civil Aviation Organization (ICAO). Aerodrome Standards - Aerodrome Design and Operations. Technical Report July, 1999.

[180] B. Mutzabaugh. First look: Boeing's new 'Space Bins' expand carry-on capacity, 2015. URL `http://www.usatoday.com/story/todayinthesky/2015/10/09/will-boeings-new-space-bins-help-ease-the-airline-carry-on-crunch/73577640/`.

[181] A. James. Peoples Choice. *Aircraft Interiors International*, pages 46–58, 2009.

[182] B. Nagel, D. Böhnke, V. Gollnick, P. Schmollgruber, A. Rizzi, G. La Rocca, and J. J. Alonso. Communication in Aircraft Design: Can We Establish a Common Language? In *28th International Congress of the Aeronautical Sciences*, 2012. ISBN 9781622767540.

[183] X. Cui and H. Shi. A*-based Pathfinding in Modern Computer Games. *International Journal of Computer Science and Network Security*, 11(1):125–130, 2011.

[184] M. Schmidt and P. Heinemann. Improving the Boarding Performance of Regional Aircraft. In *17th AIAA Aviation Technology, Integration, and Operations Conference*, Denver, Colorado, 2017. American Institute of Aeronautics and Astronautics. doi: 10.2514/6.2017-3424.

A. Model input data

A.1. Passenger egress and ingress simulation

The process modeling of the passenger egress and ingress simulation uses empirical data for the passengers anthropometrics (see Table A.1) and the hand luggage stowing process (see Table A.2).

Table A.1.: Mean values for passengers anthropometrics.

Mean Value [m]	Male	Female
Width	0.47	0.41
Depth	0.30	0.27

Table A.2.: Input values for hand luggage stowing.

Luggage Type	Mean Stow Time [s]	Volume [m^3]	Bulkiness [%]	Walking Speed Factor [-]
Small HL	10	0.01	15	0.95
Medium HL	15	0.02	30	0.90
Big HL	20	0.04	60	0.75

A.2. Turnaround equipment positioning and removal times

The positioning and removal times of the ground handling equipment are determined based on empirical data summarized in Table A.3.

Table A.3.: Summary of position and removal times based on [114, 119].

	Positioning			Removal		
Process	min [s]	mean [s]	max [s]	min [s]	mean [s]	max [s]
Boarding bridge/stairs	108	120	198	60	78	96
Fuel truck	42	54	72	60	72	84
Cargo equipment	108	120	198	60	78	96
Catering truck	51	63	72	57	69	78
Potable/waste water truck	39	48	57	27	36	51
Ground power unit	54	60	66	54	60	66
Towing truck	216	240	264	189	210	231

B. Direct operating cost

The used input values for the performed DOC analysis and absolute cost shares for the validation cases are summarized in the following. The stated cost values are inflationary adjusted and represent 2016 cost levels.

B.1. Input values for operating economics

The calculation of DOC is highly dependent on the chosen input parameters. Here, the baseline input parameters for the DOC model based on Wesseler [162] are listed in Table B.1 and the specific unit cost rates for turnaround cost estimation based on the findings of Crönertz [112] are summarized in Table B.2. Each performed cost analysis is based on those general input values.

Table B.1.: Input values for operating economics (based on model by Wesseler [162]).

Parameter	Unit	Value
Flight crew operations	-	short haul
World region	-	global
Flight type	-	international
Aircraft price range	-	mean (case 6)
Depreciation period	y	20
Interest period	y	20
Interest rate	% p.a.	4.00
Aircraft insurance rate	% p.a.	0.20
Fuel price	USD/gal	2.00
Unit rate eurocontrol	€	66.57
Labor rate (maintenance)	USD	52.00
Flight and cabin crew region	-	global

Table B.2.: The specific unit cost rates are based on the findings of Crönertz [112].

Category	Description	Cost [€/min]
Labor	Supervisor	0.65
	Worker	0.65
	Service	0.75
	Bus driver	0.50
Ground Support Equipment	Air starter	0.60
	Dolly (bulk cargo)	0.02
	Dolly (ULD)	0.04
	Tractor	0.02
	Bulk cargo laoder	0.15
	Towing truck (90-350 t MTOW)	1.96
	Towing truck (350 t MTOW and above)	1.03
	Potable water truck	0.26
	Waste water truck	0.32
	Pre-conditioned air (PCA)	5.75
	Ground power unit (GPU)	0.17
	High loader (medium)	0.26
	High loader (small)	0.38
	ULD transporter	0.30
	Bus (20 passengers)	0.53
	Bus (60 passengers)	0.49
	Bus (100 passengers)	0.61
	Stairs (small)	0.26
	Stairs (medium)	0.40
	Stairs (large)	0.91
Material	Cleaning fluid	0.13
	Potable water	0.05
	Power	0.17

B.2. Direct operating cost of an A320neo and an A330-300

The absolute cost shares for the DOC estimation of the validation cases covering the A320neo and A330-300 on an 3,000 nm off-design mission are summarized in Table B.3.

Table B.3.: Absolute cost shares for A320neo and A330-300

Cost share	Cost per Trip [USD]	
	A320neo	A330-300
Fuel	9,829	22,758
Ground handling	293	455
Airport	1,421	3,416
Navigation	2,897	5,547
Direct maintenance	2,419	4,871
Crew	4,650	7,933
Cash Operating Cost	21,273	44,634
Depreciation	4,509	5,050
Interest	2,994	4,205
Insurance	37	55
Cost of Ownership	7,539	9,310
Additional Operating Cost	547	1,513
Direct Operating Costs	29,359	55,456